Neural circuits underlying CO_2 behavior in *Drosophila melanogaster*

Lasse Björn Bräcker

Dissertation der Fakultät für Biologie

der Ludwigs-Maximilians-Universität München

München, 2014

Diese Dissertation wurde angefertigt

unter der Leitung von Dr. Ilona Grundwald Kadow

am Max Planck Institut für Neurobiologie

Erstgutachter: Professor Dr. Alexander Borst

Zweitgutachter: Professor Dr. Nicolas Gompel

Tag der Abgabe: 10.08.2013

Tag der mündlichen Prüfung: 30.06.2014

Eidesstattliche Versicherung

Hiermit, erkläre ich an Eides statt, dass ich die vorliegende Dissertation selbständig und ohne unerlaubte Hilfe angefertigt habe. Ich habe mich dabei keiner anderen als der von mir ausdrücklich bezeichneten Hilfen und Quellen bedient.

Ich erkläre hiermit an Eides statt, dass ich mich nicht anderweitig ohne Erfolg einer Doktorprüfung unterzogen habe. Die Dissertation wurde in ihrer jetzigen oder ähnlichen Form bei keiner anderen Hochschule eingereicht und hat noch keinen sonstigen Prüfungszwecken gedient.

München, 10.08.2013

_____

Lasse Björn Bräcker

Die vorliegende Arbeit wurde zwischen September 2009 und August 2013 am Max Planck Institut für Neurobiologie unter Leitung von Dr. Ilona Grunwald Kadow durchgeführt.

Table of content

Index of figures

Index of tables

Abbreviations

AL	antennal lobe
ANOVA	analysis of variance
biVPN	bilateral V-glomerulus projection neuron
DGRC	Drosophila genomics resource center
dSO	*Drosophila* stress odor
FRT	flippase recognition target
GFP	green fluorescent protein
iACT	inner antennocerebral tract
imACT	inner medial antennocerebral tract
IR	ionotropic receptor
KC	Kenyon cell
LH	lateral horn
LN	local interneuron
mACT	medial antennocerebral tract
MB	mushroom body
MBEN	mushroom body extrinsic neuron
NPF	neuropeptide F
oACT	outer antennocerebral tract
OBP	odor binding protein
OR	olfactory receptor
ORCO	olfactory receptor co-receptor
ORN	olfactory receptor neuron
PA-GFP	photoactivatable GFP
PAM	protocerebral anterior medial cluster

PI	performance index
PN	projection neuron
PPL	protocerebral posterior lateral cluster
ROI	region of interest
SOG	suboesophagial ganglion
UAS	upstream activation sequence
VPN	V-glomerulus projection neuron

Summary

Animals use a wide variety of sensory cues to orientate themselves in their environment. They use olfactory cues for locating food sources, finding and selecting suitable mating partners or to avoid danger. CO_2 is such an olfactory cue and several different species can detect elevated levels of this ubiquitous gas. *Drosophila melanogaster* reacts with a strong avoidance behavior when confronted with a CO_2 stimulus. This is surprising since the natural habitat of this fly includes several sources of CO_2 that should be appetitive, such as rotting fruit parts. Thus, CO_2 avoidance behavior is likely to undergo modification to better suit the survival of this animal.

Indeed, I was able to show that in the context of starvation, flies overcome their CO_2 aversion in favor of approaching the food related vinegar odor when presented with a choice between air and CO_2 plus vinegar in a T-maze assay. This modification of avoidance was not observed when replacing CO_2 with 3-octanol, also an aversive odor, in this experiment.

CO_2 is perceived by the fly through olfactory sensory neurons on the antenna, which express two CO_2 co-receptors: Gr21a and Gr63a. These neurons project their axons to the antennal lobe in the brain. The antennal lobe is the first olfactory processing center in the insect brain and is comprised of spherical structures called glomeruli. Within each glomerulus, olfactory receptor neurons that express the same odor receptor converge and synapse with projection neurons. In the case of CO_2, this is the ventral most glomerulus (V-glomerulus). Only one projection neuron that carries CO_2

information has been described so far. It connects the V-glomerulus to the lateral horn, a higher processing center in the brain.

Together with the expansive genetic toolkit which is available for *Drosophila*, the easily reproducible CO_2 avoidance behavior is an ideal model for studying innate olfactory behavior and the underlying neural circuits. A large scale behavioral screen was conducted to find novel components of the CO_2 neural circuit. I used a selection of 1024 GAL4 driver lines to block random subsets of neurons via expression of Shibire^{ts1}. Shibire^{ts1} blocks neuronal transmission at 32°C but has no effect at 25°C. Flies which expressed this effector were tested for CO_2, vinegar and CO_2 plus vinegar behavior at high temperature. I selected 107 lines with abnormal behavior in at least one of the paradigms for a secondary screen. In this secondary screen, I quantified the behavior of experimental flies and compared their performance to control groups. Several of the lines analyzed this way are promising candidates for future research on novel CO_2 pathway components.

In parallel to the large scale approach, I tested a set of GAL4 lines with known expression patterns. These lines covered different parts of the mushroom body. The mushroom body is a higher brain center for olfactory processing in the fly brain. Kenyon cells are the major intrinsic neuron type of this structure. Projection neurons synapse with Kenyon cells to provide them with olfactory input from the antennal lobe. In addition to this input, mushroom bodies receive input from a wide variety of intrinsic and extrinsic neurons. Previous studies showed their role in olfactory learning as well as processing starvation signals related to olfactory learning. Based on these findings, the mushroom body is a suitable candidate neuropil for processing and modifying CO_2

avoidance behavior in different contexts. I blocked different Kenyon cell subsets by employing Shibire^{ts1} as an effector. Blocking the mushroom body in fed flies had no effect on CO_2 avoidance. In the context of starvation however, I found that blocking the whole mushroom body or just the α'/β' subset impairs CO_2 avoidance. A starvation time of at least 24 hours was required for shifting CO_2 avoidance processing from mushroom body independent to dependent, while a starvation time of just 12 hours had no effect.

Calcium imaging of the mushroom body employing GCaMP5.0 as a genetically encoded calcium sensor proved that Kenyon cells react to stimulation with CO_2. This was found across all tested Kenyon cell subsets, although α/β and γ populations showed the smallest fluorescence signals.

Encouraged by this finding, I searched for a neuron that could deliver the CO_2 signal to the mushroom body. A novel type of projection neuron, termed biVPN, was described based on the results of this search. Its anatomy is atypical compared to other projection neurons. The cell bodies of biVPNs are located lateral to the suboesophagial ganglion. Each biVPN innervates both V-glomeruli and sends one projection to the ipsi- and one to the contralateral side of the brain. These projections bifurcate and innervate both the lateral horn as well as the mushroom body calyx. Blocking neuronal output of the biVPN abolished CO_2 avoidance in 12 hours starved flies but not in fed flies. Imaging neuronal activity of these projection neurons demonstrated that they respond to CO_2 stimulation in a concentration dependent manner.

Having shown that the requirement of the mushroom body as well as the corresponding projection neuron depends on starvation, I searched for circuit components that integrate this starvation signal during CO_2 avoidance behavior. Dopamine has been implicated in learning and memory related hunger signaling (Krashes et al. 2009). Thus, I manipulated the dopaminergic system in behaving animals. Blocking dopaminergic neurons via TH-GAL4 and Shibire^{ts1} increased CO_2 avoidance exclusively in starved flies. Consistent with this finding, activating dopaminergic neurons via dTRPA1 decreased CO_2 avoidance exclusively in fed flies. Imaging experiments further demonstrated that application of dopamine before CO_2 stimulation reduced the CO_2 response of the mushroom body. No effect of this treatment was detected in already starved flies.

Taken together, the data presented in this thesis show that CO_2 avoidance is processed by two separate circuits and modified based on the context of other external and internal signals. The biVPN and the mushroom body are redundant for CO_2 avoidance under fed conditions but become required under starved conditions. The mushroom body does most likely also integrate the vinegar signal in a context with both CO_2 and vinegar present and thus enables the fly to overcome its avoidance reaction by lowering the aversive CO_2 input. I demonstrated in this thesis, that innate avoidance is modified based on the current needs of the animal and that behavioral decisions related to an olfactory cue are formed by an elaborate multi-pathway neural circuit.

Zusammenfassung

Tiere nutzen eine Vielzahl sensorischer Signale um ihre Umgebung zu erfassen. Sie benutzen olfaktorische Signale um Futterquellen zu orten, Geschlechtspartner zu finden und um Gefahren zu vermeiden. CO_2 ist ein solches olfaktorisches Signal und verschiedene Spezies können erhöhte Konzentrationen dieses Gases wahrnehmen. *Drosophila melanogaster* reagiert auf CO_2 Stimuli mit einer ausgeprägten Fluchtreaktion. Dies ist überraschend, da der natürliche Lebensraum verschiedene Quellen von CO_2 aufweist, wie zum Beispiel verrottende Pflanzenteile, welche eigentlich attraktiv sein sollten. Aus diesem Grunde ist es wahrscheinlich, dass die Reaktion auf CO_2 modifiziert wird, um bessere Überlebenschancen durch angepasstes Verhalten zu ermöglichen.

In der hier vorliegenden Arbeit konnte ich zeigen, dass Fliegen im Kontext von Hunger ihre CO_2 Aversion überwinden können und sich dem futterbezogenen Duft von Essig annähern, wenn sie vor die Wahl zwischen Luft oder CO_2 plus Essig in einem Verhaltensexperiment gestellt werden. Diese Modifikation der Aversion konnte nicht beobachtet werden wenn CO_2 im selben Experiment durch 3-Octanol, einem anderen aversiven Duft, ersetzt wurde.

CO_2 wird von der Fliege durch olfaktorische Sinneszellen auf der Antenne detektiert, welche die zwei CO_2 Korezeptoren Gr21a und Gr63a exprimieren. Diese Neuronen schicken ihre Axone zum Antennallobus im Gehirn. Der Antennallobus ist das erste olfaktorische Verarbeitungszentrum im Insektengehirn und besteht aus sphärischen Strukturen, die Glomeruli

genannt werden. Innerhalb jedes Glomerulus treffen die Axone aller olfaktorischen Sinneszellen zusammen, welche den gleichen Duftrezeptor exprimieren um dann mit Projektionsneuronen Synapsen zu bilden. Im Falle von CO_2 ist es der am weitesten ventral gelegene Glomerulus (V-Glomerulus). Bis zu diesem Zeitpunkt wurde nur ein Projektionsneuron beschrieben, welches CO_2 Information erhält. Es verbindet den V-Glomerulus mit dem lateralen Horn, welches ein höheres Verarbeitungszentrum im Hirn ist.

Zusammen mit umfangreichen genetischen Werkzeugen ist das leicht zu reproduzierende CO_2 Fluchtverhalten von *Drosophila melanogaster* ein ideales Modell um angeborenes olfaktorisches Verhalten und die zugrundeliegenden neuralen Netzwerke zu studieren. Ein groß angelegter Verhaltensscreen wurde durchgeführt um neue Komponenten des neuronalen CO_2 Netzwerks zu identifizieren. Ich benutzte eine Auswahl von 1024 GAL4 Treiber Linien um zufällige Gruppen von Neuronen mit Hilfe der Expression von Shibire^{ts1} zu blockieren. Shibire^{ts1} blockiert die neuronale Übertragungen bei 32°C, während es bei 25°C keinen Effekt auslöst. Fliegen, die diesen Effektor exprimierten, wurden auf ihr CO_2, Essig und CO_2 plus Essig Verhalten getestet. Ich suchte 107 Linien mit abnormalen Verhalten in mindestens einem der Tests aus, um sie in einem zweiten Durchgang erneut zu testen. In diesem zweiten Durchgang quantifizierte ich das Verhalten der experimentellen Fliegen und verglich es mit dem von Kontrollgruppen. Mehrere der getesteten Linien sind vielversprechende Kandidaten für zukünftige Forschungen zu Komponenten des neuralen CO_2 Netzwerks.

Parallel zu den oben beschriebenen Experimenten habe ich eine Auswahl von GAL4 Linien mit bereits bekanntem Expressionsmuster getestet. Diese Linien deckten unterschiedliche Teile des Pilzkörpers ab. Der Pilzkörper ist ein höheres Hirnzentrum für olfaktorische Verarbeitung im Fliegengehirn. Kenyonzellen sind der vorrangige intrinsische Neuronentyp dieser Struktur. Projektionsneurone bilden Synapsen mit Kenyonzellen und verbinden diese so mit olfaktorischen Signalen aus dem Antennallobus. Zusätzlich zu diesen Signalen erhalten Kenyonzellen Informationen von einer Vielzahl intrinsischer und extrinsischer Neurone. Sowohl ihre Rolle im olfaktorischen Lernen als auch in der Verarbeitung von lernrelevanten Hungersignalen wurde in früheren Studien gezeigt. Basierend auf diesen Entdeckungen ist der Pilzkörper ein geeignetes Hirnzentrum zur Verarbeitung und Modifizierung von CO_2 Fluchtverhalten in verschiedenen Kontexten. Ich blockierte verschiedene Untergruppen der Kenyonzellen durch den Effektor Shibire^{ts1}. Das Blockieren des Pilzkörpers in gefütterten Fliegen hatte keine Auswirkung auf das CO_2 Verhalten. Im Kontext von Hunger jedoch wurde das CO_2 Verhalten nach Blockieren des gesamten Pilzkörpers oder der α'/β' Untergruppe beeinträchtigt. Eine Hungerzeit von mindestens 24 Stunden war nötig um die Verarbeitung des CO_2 Verhaltens abhängig vom Pilzkörper zu machen. Eine Hungerzeit von nur 12 Stunden hatte keinen Effekt.

Calcium imaging des Pilzkörpers unter Verwendung des genetisch kodierten Calcium Sensors GCaMP5.0 zeigte, das Kenyonzellen auf Stimulation mit CO_2 reagieren. Dies wurde für alle getesteten Untergruppen der Kenyonzellen beobachtet, obwohl die α/β und γ Populationen die kleinsten Fluoreszenzsignale zeigten.

Als nächstes suchte ich nach einem Neuron, welches die CO_2 Information an den Pilzkörper weiterleitet. Ein neuer Typ von Projektionsneuron, welcher biVPN getauft wurde, konnte als Resultat dieser Suche beschrieben werden. Die Anatomie des biVPNs ist atypisch. Die Zellkörper befinden sich lateral zum suboesophagialen Ganglion. Jedes biVPN innerviert beide V-Glomeruli und schickt jeweils einen Neuriten in die ipsi- und die contralaterale Hirnhälfte. Diese Neurite teilen sich und innervieren sowohl das laterale Horn als auch den Calyx des Pilzkörpers. Das Blockieren des biVPN führte zu einer vollständigen Reduktion der CO_2 Aversion von Fliegen die seit 12 Stunden vor dem Experiment hungerten, aber hatte keinen Effekt bei gesättigten Fliegen. Durch Imaging der neuronalen Aktivität dieser Projektionsneurone konnte zudem gezeigt werden, dass sie auf Stimulation mit CO_2 konzentrationsabhängig antworten.

Nachdem ich gezeigt hatte, dass sowohl die Erforderlichkeit des Pilzkörpers als auch des zugehörigen Projektionsneurons von Hunger abhängt, suchte ich nach Komponenten des neuralen Netzwerks welche dieses Hungersignal während des CO_2 Verhaltens integrieren. Die Rolle von Dopamin als Hungersignal in Zusammenhang mit Lernen und Gedächtnis wurde bereits in früheren Studien gezeigt. Deshalb manipulierte ich das dopaminerge System der Fliegen während des Tests. Die Inaktivierung von dopaminergen Neuronen via TH-GAL4 und Shibire^{ts1} steigerte die CO_2 Aversion ausschließlich in gehungerten Fliegen. Die Aktivierung von dopaminergen Neuronen durch dTRPA1 reduzierte die CO_2 Fluchtreaktion ausschließlich in gesättigten Fliegen. Somit stehen die Ergebnisse von Inaktivierung und Aktivierung dieser Neurone im Einklang. Imaging Experimente konnten

weiterhin zeigen, dass die Applikation von Dopamin vor einer Stimulation mit CO_2 die Reaktion der Pilzkörperneurone verringerte. Diese Behandlung hatte keinen Effekt in bereits gehungerten Fliegen.

Zusammengefasst zeigen die Daten, welche in dieser Dissertation präsentiert werden, dass das CO_2 Fluchtverhalten durch äußere und innere Stimuli modifiziert wird. CO_2 Fluchtverhalten, welches eine angeborene olfaktorische Verhaltensweise ist, wird durch zwei separate neurale Netzwerke verarbeitet. Zunehmender Hunger aktiviert den biVPN und Pilzkörper abhängigen Netzwerkteil, welcher bei Sättigung redundant ist. Der Pilzkörper integriert sehr wahrscheinlich auch das Signal des Essigs und ermöglicht so der Fliege ihre CO_2 Aversion durch eine Reduktion des CO_2 Signals zu überwinden. Ich konnte in dieser Dissertation demonstrieren, dass selbst angeborene Fluchtreaktionen modifiziert werden können. Diese Modifikation hängt von den gegenwärtigen Bedürfnissen des Tieres ab. Entscheidungen zur Reaktion auf ein olfaktorisches Signal werden von einem hochentwickelten neuronalen Netzwerk getroffen, welches aus multiplen Pfaden aufgebaut ist.

Publications and contributions

The results presented in this thesis have been published in the following articles:

Lasse B. Bräcker*, K.P. Siju*, Nélia Varela, Yoshinori Aso, Mo Zhang, Irina Hein, Maria Luísa Vasconcelos, Ilona C. Grunwald Kadow. Essential Role of the Mushroom Body in Context-Dependent CO_2 Avoidance in *Drosophila*. *Current Biology*, Volume 23, Issue 13, 8 July 2013, Pages 1228-1234, ISSN 0960-9822.

* equal contribution

K.P. Siju*, **Lasse B. Bräcker***, Ilona C. Grunwald Kadow. Neural mechanisms of context-dependent modification of CO_2 avoidance behavior in fruit flies. *Fly*, Volume 8, Issue 2, published online 4 February 2014.

* equal contribution

Specifically, the content of the following figures of the results and discussion section were published in peer reviewed journals:

Figure 4.1, 4.4, 4.5, 4.6, 4.7, 4.8, 4.9, 4.10, 4.11, 4.12 and 4.13 were published in Bräcker et al. 2013.

Figure 4.15, 5.1 and the raw data analyzed in figure 4.16 were published in Siju, Bräcker, & Grunwald Kadow 2014.

Figures 4.2, 4.3 and tables 4.1, 4.2 and 4.3 were not previously published. This applies to all data regarding the screen of the NP-GAL4 library.

The following section lists all persons who contributed to this thesis. Names of persons who contributed experimental data are highlighted.

The primary screen of the NP-GAL4 library was conducted in collaboration with the labs of Hiromu Tanimoto (Max Planck institute of neurobiology, Martinsried) and Matthieu Louis (CRG, Barcelona). Specifically, the preparatory workload was shared with Christine Damrau and Verena Kurz.

Yukiko Yamada conducted parts of the secondary screening of the NP driver library (parts of the vinegar attraction and CO_2 aversion experiments), which are listed in table 4.1 and 4.2.

Siju K. Purayil conducted all of the imaging experiments presented in this thesis as well as large parts of the histological analysis. The results of these experiments are shown in figure 4.5 (A), 4.10, 4.11, 4.12 (F), 4.13, 4.15 (A) and 4.16.

Neuronal tracing via photoactivatable GFP was performed by **Nélia Varela**, in the lab of Maria Luísa Vasconcelos (Instituto Gulbenkian de Ciência, Oeiras). The results of these experiments are shown in figure 4.12 (A-E).

Yoshinori Aso in the lab of Gerald Rubin generated two of the transgenic fly lines used in this thesis.

Experiments performed by the remaining authors of Bräcker et al. 2013 were not incorporated in this thesis.

1 Introduction

To orientate themselves in their environment, animals and humans use a wide variety of different cues. These sensory signals have to be processed and put into context to generate appropriate behaviors. One of the oldest senses is chemoreception. Even single cell organisms possess the ability to detect different molecules in their surroundings. This feature translates to almost every cell in multicellular organisms. More sophisticated chemosensory organs are derived from this basic property. These are either used for near field detection of chemicals via diffusion (gustation) or long range detection via air or water streams (olfaction). Olfaction has evolved to be generally more sensitive and specific compared to gustation (Wehner & Gering 1995).

The sense of smell is used by animals to gather various different cues: locating food sources, mating partners or avoiding danger. Thus, olfactory cues have to be processed based on the context of additional external and internal signals. For instance, women become more sensitive and more attracted to male body odors around the time of ovulation (Navarrete-Palacios, Hudson, Reyes-Guerrero, & Guevara-Guzmán 2003). Also a change in the metabolic state of an animal influences how certain odors are perceived and processed (Gruber et al. 2013; Moss & Dethier 1983; Rolls 2011; Root, Ko, Jafari, & Wang 2011; Schloegl et al. 2011; Siju, Hill, Hansson, & Ignell 2010; Y. Wang, Pu, & Shen 2013). In judging a potential food source, starved animals are more likely than fed animals to suppress fear and aversion of potential danger and its associated odor cues (Lin et al. 2010;

Rolls 2007). Taken together, olfactory behavior and the underlying neuronal circuit is a great model to investigate how animals make choices based on context.

1.1 The olfactory system of *Drosophila*

The olfactory system of *Drosophila* has been studied to a great extent in the past. Olfactory receptor neurons (ORNs), which perceive odorants in *Drosophila*, generally express olfactory receptors (ORs) or ionotropic receptors (IRs) for odor detection (Benton, Vannice, Gomez-Diaz, & Vosshall 2009; Clyne et al. 1999). ORs determine the response profile of the neuron and thus which odors it responds to (Hallem & Carlson 2006). All ORs function together with a co-receptor: ORCO (olfactory receptor co-receptor, previously known as Or83b in *Drosophila melanogaster*) (Benton, Sachse, Michnick, & Vosshall 2006; Larsson et al. 2004; Neuhaus et al. 2005) (Figure 1.1). While ORs are specific to the neuron type, ORCO is generally expressed together with one of the other ORs. IRs are less well understood. It has been shown that at least two IRs function as co-receptors in combination with others (Abuin et al. 2011).

Olfactory receptor neurons are housed in hair-like structures called sensilla, which are located on the two main olfactory appendages of the fly: the antenna and the maxillary palp (Figure 1.1). Together with support cells at the base, each sensillum houses three to four sensory neurons which express different receptor combinations. These cells create a specific haemolymph environment. Airborne molecules can enter this haemolymph through pores

on the sensillum. While not fully understood, for some odors it has been shown that specific odor binding proteins (OBPs) bind to the odor molecule and facilitate receptor binding (Xu, Atkinson, Jones, & Smith 2005). Sensilla are categorized by shape which can either be basiconic, trichoid or coeloconic. The different types of sensilla can be found in specific regions on the antenna and maxillary palp (Figure 1.1). ORNs housed in the same type of sensillum innervate neighboring regions in the antennal lobe (AL), which is the primary olfactory center in the fly brain.

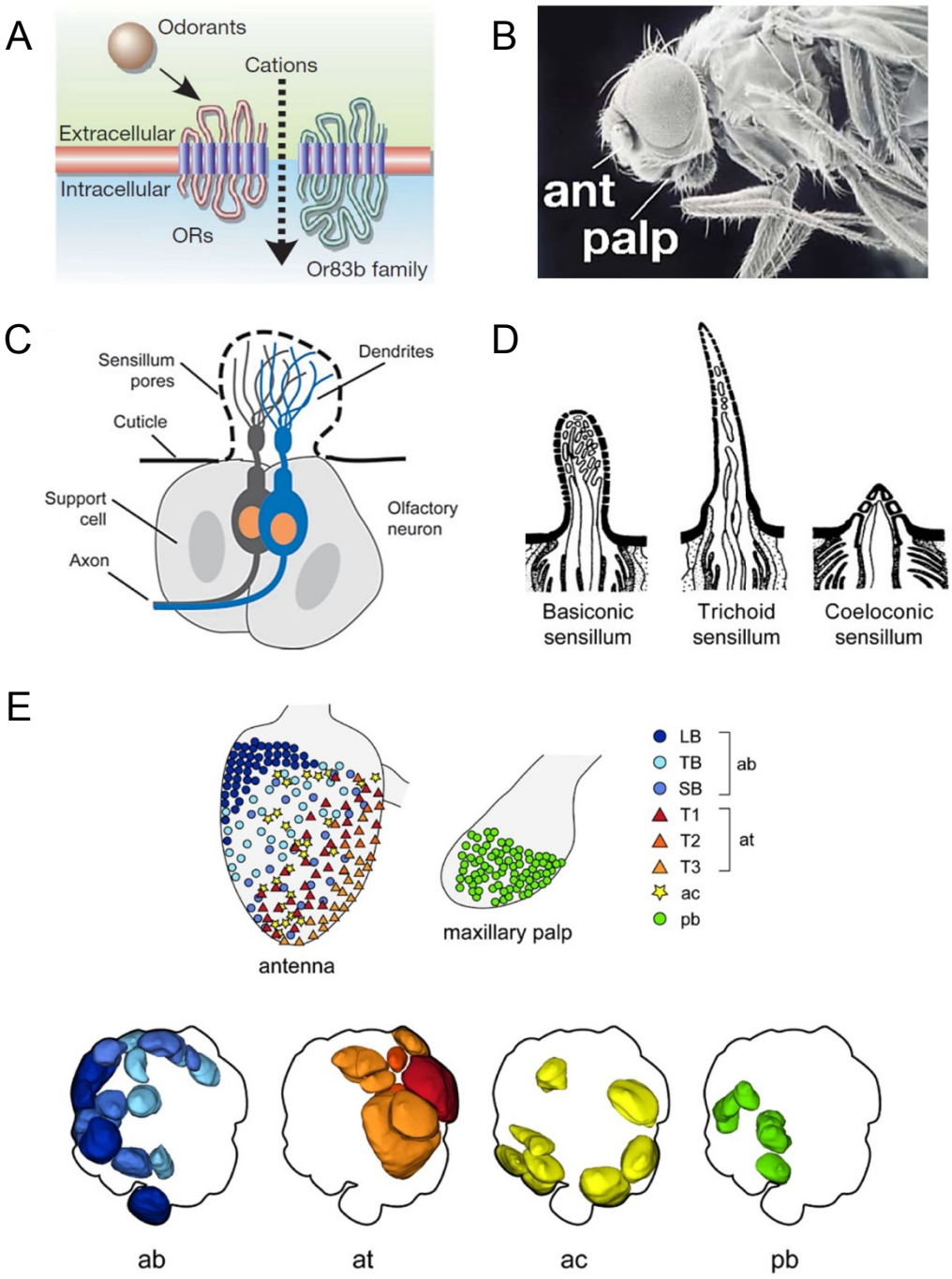

Figure 1.1: Odor detection in *Drosophila*

(A) Structure of the ligand gated OR/Or83b channel complex. Figure adapted from Sato et al. 2008. **(B)** Scanning electron micrograph of a fruit fly. ant, antenna; palp, maxillary palp. Figure adapted from Smith 2007. **(C)** Anatomy of a typical sensillum housing two ORNs (black and blue). Figure adapted from Vosshall & Stocker 2007. **(D)** Different types of sensilla based on morphology. Figure adapted from Stocker 1994. **(E)** Distribution of different sensilla types on the maxillary palp and the antenna. ORNs within each sensillum target correspondent glomeruli with the same color. Glomeruli are colored according to sensillum type for the corresponding ORN class. LB, large basiconic; TB, thin basiconic; SB, small basiconic. Figure adapted from Couto et al. 2005.

ORNs extend their axons into the brain via the antennal nerve. They terminate first in the ipsilateral AL, a paired neuropil in the anterior part of the fly brain, and then send one projection across the brain midline to the contralateral AL. ALs consist of a multitude of spherical structures called glomeruli (Tanaka, Endo, & Ito 2012). All ORNs that express the same receptor combination converge in the same glomerulus, where they synapse onto projection neurons (PNs) (Couto, Alenius, & Dickson 2005). This connectivity principle is conserved across individuals and leads to the formation of an olfactory map within the AL (Figure 1.2). Any given odor will elicit a certain pattern of glomerular activity in the AL based on the ORN type it activates. The third major neuron type which innervates the ALs are local interneurons (LNs) (Figure 1.2). These can be inhibitory or excitatory and are either innervating a few selected glomeruli or nearly all glomeruli of each AL (Chou et al. 2010; Das et al. 2011). LNs provide another level of processing for olfactory signals.

PNs are postsynaptic to ORNs and pick up the processed signals from the glomeruli to carry them to higher brain centers. PNs can be categorized based on several characteristics. Their innervation in the AL can either be confined to a single glomerulus (uniglomerular PN) or cover several glomeruli (multiglomerular PN) (Tanaka et al. 2012).

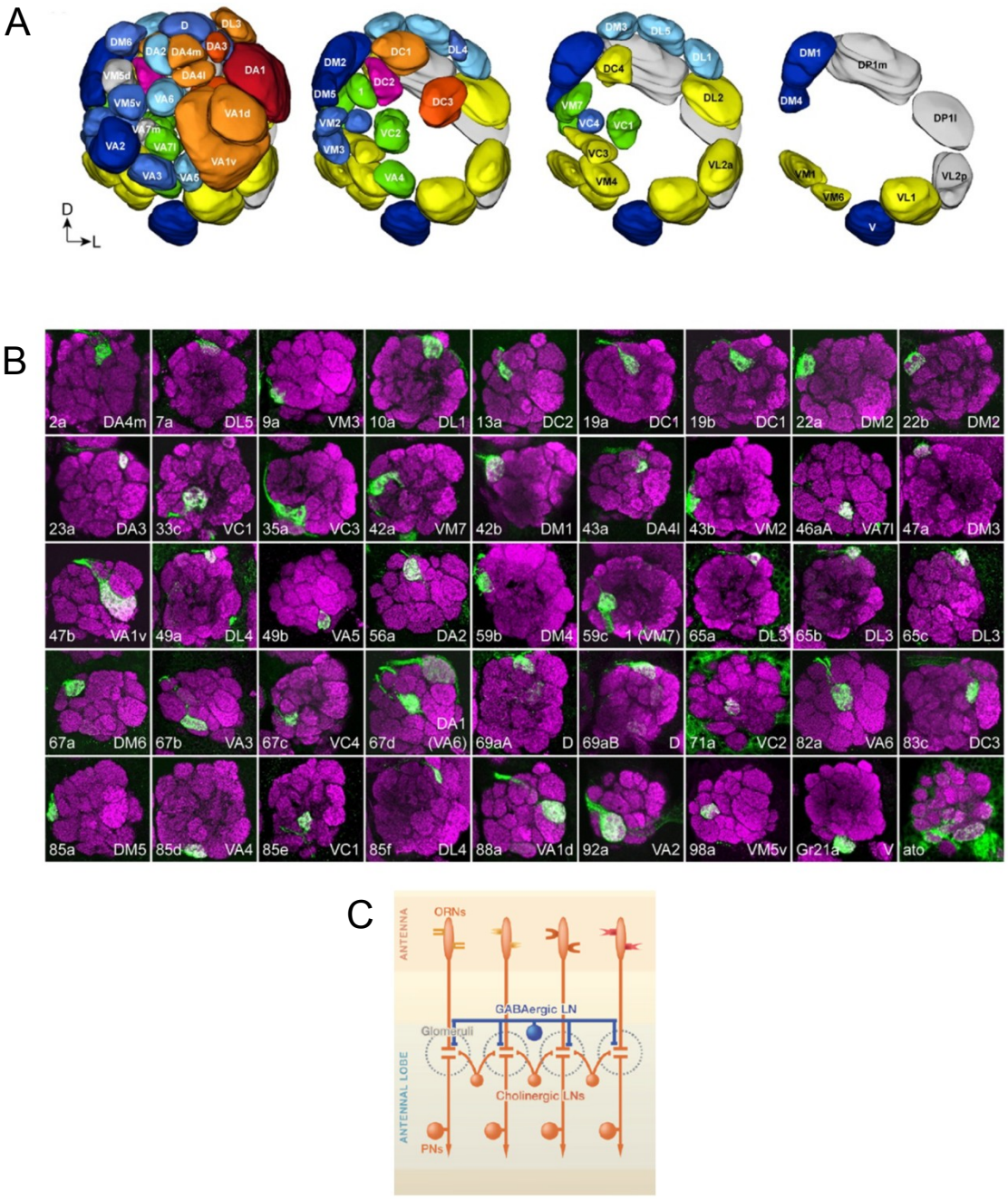

Figure 1.2: Wiring of the antennal lobe

(A) 3D reconstruction of the antennal lobe, showing the positions of 49 glomeruli. The view is anterior, with the labeled glomeruli removed in each successive panel to reveal the underlying glomeruli. Figure adapted from Couto et al. 2005. **(B)** Targeting glomeruli of different ORN classes in the AL. Innervation is visualized by expressing mCD8-GFP either under control of the respective GAL4 line or directly as a fusion construct with the respective OR promoter. Figure adapted from Couto et al. 2005. **(C)** Wiring diagram of the AL. Each glomerulus consists of sensory neuron and projection neuron synapses. These receive modulatory input from LNs which connect them with other glomeruli. Figure adapted from Su et al. 2009.

The axons of PNs run via several tracts through the brain and terminate in higher brain areas. Antennocerebral tracts formed this way are categorized based on their anatomy (Figure 1.3). They can generally travel via the inner, medial or outer antennocerebral tract (iACT, mACT and oACT respectively) (Tanaka, Tanimoto, & Ito 2008). Finally, PNs differ in their area of termination. Typically, they innervate the mushroom body and the lateral horn or just the lateral horn.

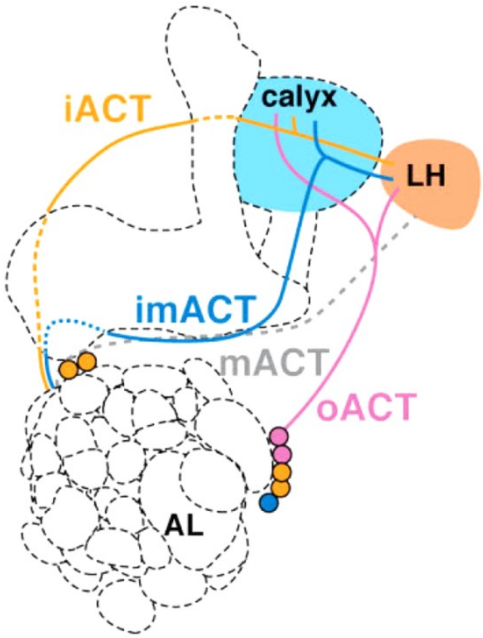

Figure 1.3: Projection neuron tracts

PNs can be classified based on their projection path via different tracts: the inner, outer, medial or inner medial antennocerebral tracts (iACT, oACT, mACT, imACT respectively). AL, antennal lobe; LH, lateral horn. Figure adapted from Tanaka et al. 2008.

1.2 CO_2 perception and related behaviors

CO_2 is a cue that is used as an indicator for various things by different animals (Guerenstein & Hildebrand 2008). Increased levels of this ubiquitous gas can be actively smelled by many insects, nematodes (Hallem & Sternberg 2008) and mammals such as mice (Y. Y. Wang, Chang, & Liman 2010). Nocturnal moth use CO_2 emitted by flowers to locate them and feed on their nectar (Goyret, Markwell, & Raguso 2008). Bees sample CO_2 levels in their hives. In case the level of CO_2 becomes too high for their larvae to develop optimally, groups of worker bees gather at the entrance and fan fresh air into the hive until CO_2 levels are lower again (Guerenstein & Hildebrand 2008). Mosquitoes and other blood feeding insects sense the CO_2 exhaled from their mammalian hosts. For these insects, CO_2 serves as a near field navigational cue that is sensed together with host odors as well as body heat (Bowen 1991).

In *Drosophila melanogaster*, CO_2 concentrations higher than 0.02% above atmospheric level trigger a strong avoidance reaction (Faucher, Forstreuter, Hilker, & De Bruyne 2006; Suh et al. 2004). When tested in a T-maze (Tully & Quinn 1985), nearly all flies rapidly avoid the side with the CO_2 and flee to the air side. This strong innate response can be easily reproduced under a wide range of conditions, and has thus become a model for innate olfactory behavior in several studies.

While bearing some unique features, the neural circuit underlying CO_2 perception in *Drosophila* has been shown to follow in general the connectivity scheme of insect olfactory systems. Taking advantage of the large genetic toolkit available in *Drosophila*, it has been shown that CO_2 perception depends on two co-receptors expressed on the antenna in the third neuron of

basiconic sensilla (termed ab1c) (Figure 1.4). These two receptors are Gr21a and Gr63a. Single sensillum recordings proved that neurons which express these receptors respond to CO_2, even when these receptors are expressed

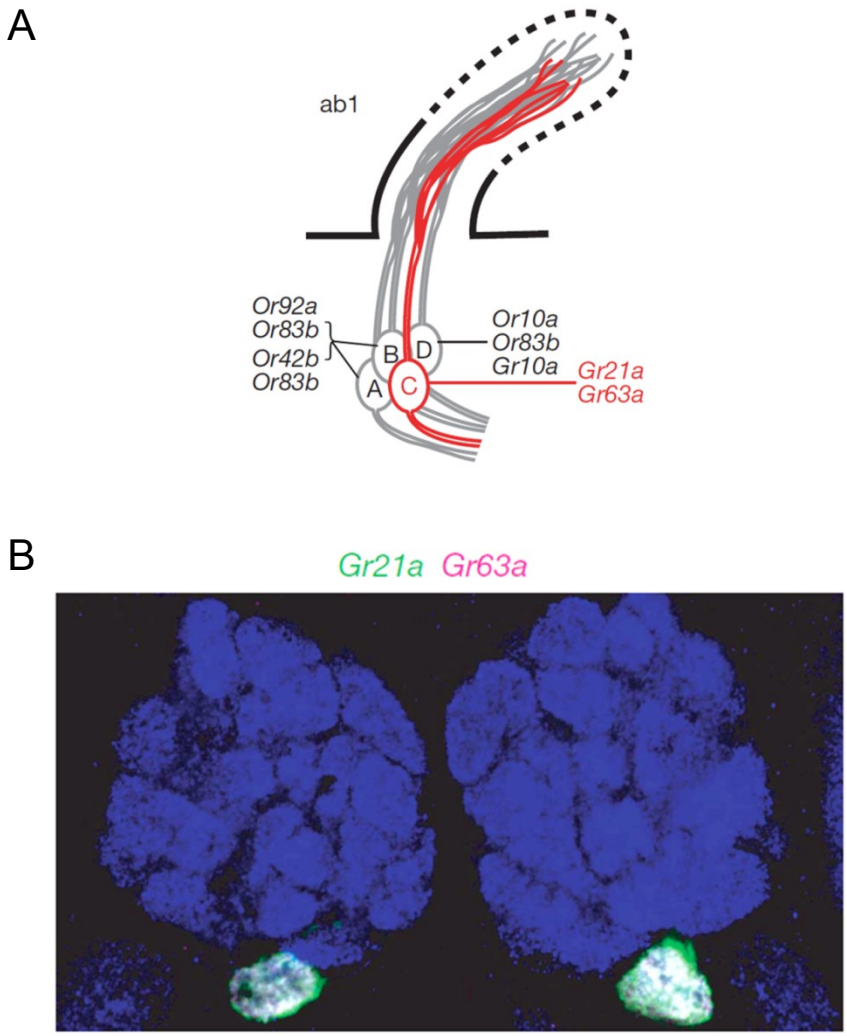

Figure 1.4: CO_2 sensing neurons in *Drosophila*

(A) The ab1c sensillum houses CO_2 responsive ORNs. These express Gr21a/Gr63a. Other expressed receptor pairs are indicated. **(B)** ab1c neurons target the V-glomerulus. Gr21a positive axons are visualized by Gr21a-GAL4 driven CD8-GFP expression. Gr63a positive axons are visualized by sytRFP expression directly under control of the Gr63a promoter. Figure adapted from Jones et al. 2007.

ectopically in a different type of sensillum (Jones, Cayirlioglu, Kadow, & Vosshall 2007).

Contrary to other olfactory receptors expressed on the antenna, CO_2 receptors belong to the gustatory receptor family. While their signaling mechanism remains largely unknown, a role of the G-protein $G\alpha_q$ has been implicated (Yao & Carlson 2010). The anatomy of the CO_2 circuit past the level of sensory neurons remains largely unknown in *Drosophila*. CO_2 sensitive neurons innervate the ventral most glomerulus (termed V) of the AL (Figure 1.4), which is not activated by any other odor. Only one PN type has been described which innervates this glomerulus (Sachse et al. 2007). It connects CO_2 sensory neuron information to the LH.

Gr21a and Gr63a are sufficient to convey CO_2 sensitivity in an ORN, when expressed ectopically in an otherwise Gr21a/Gr63a negative ORN (Jones et al. 2007). Output from Gr21a/Gr63a positive sensory neurons is both necessary and sufficient to trigger CO_2 avoidance in *Drosophila* (Suh et al. 2004, 2007). This has been demonstrated through artificial silencing or activation of these sensory neurons in behaving animals.

The ecological significance of the CO_2 avoidance reaction has not been fully determined yet. One study investigating stress response behaviors showed that CO_2 is the major component of *Drosophila* stress odor (dSO) (Suh et al. 2004). Similar to other animals such as mice, flies emit dSO after prolonged stress such as physical shaking. This odor is aversive for naïve flies that did not experience the stress themselves. However, CO_2 is not the only

component of dSO, since blocking Gr63a/Gr21a positive neurons did not completely abolish avoidance of dSO.

CO_2 is produced by rotting fruits and plant parts which are the natural food source for *Drosophila*. Thus, a CO_2 avoidance reaction seems counter intuitive for survival. A study dealing with this question searched for mechanisms to modify CO_2 behavior. Indeed, a chemical compound was found which can suppress firing of sensory neurons (Turner & Ray 2009). This suppression is based on direct inhibition of the CO_2 receptors. However, the odors described in this study can only be found in low concentrations in food fruits. Their interaction with CO_2 perception is thus likely to be only one of several mechanisms to help flies navigate CO_2 rich environments.

Another study focusing on behavior showed, that the presence of a low concentration of CO_2 does not alter approach of a food related odor source in starved flies (Faucher et al. 2006). This finding indicates a possible interaction of other odors with CO_2 behavior.

1.3 The mushroom body

As mentioned before, the mushroom body (MB) is one of the two higher brain centers that mainly receive olfactory input. The mushroom body of *Drosophila* is a paired structure in the dorsal protocerebrum. Kenyon cells (KCs) are the major intrinsic neuron type of the MB (Figure 1.5). These neurons have their cell bodies located in a large cluster posterior to the calyx. The calyx is the region of input for KCs. In the calyx, KCs synapse with PN boutons by forming dendritic claws (Kremer et al. 2010). Claws from several KCs around one PN

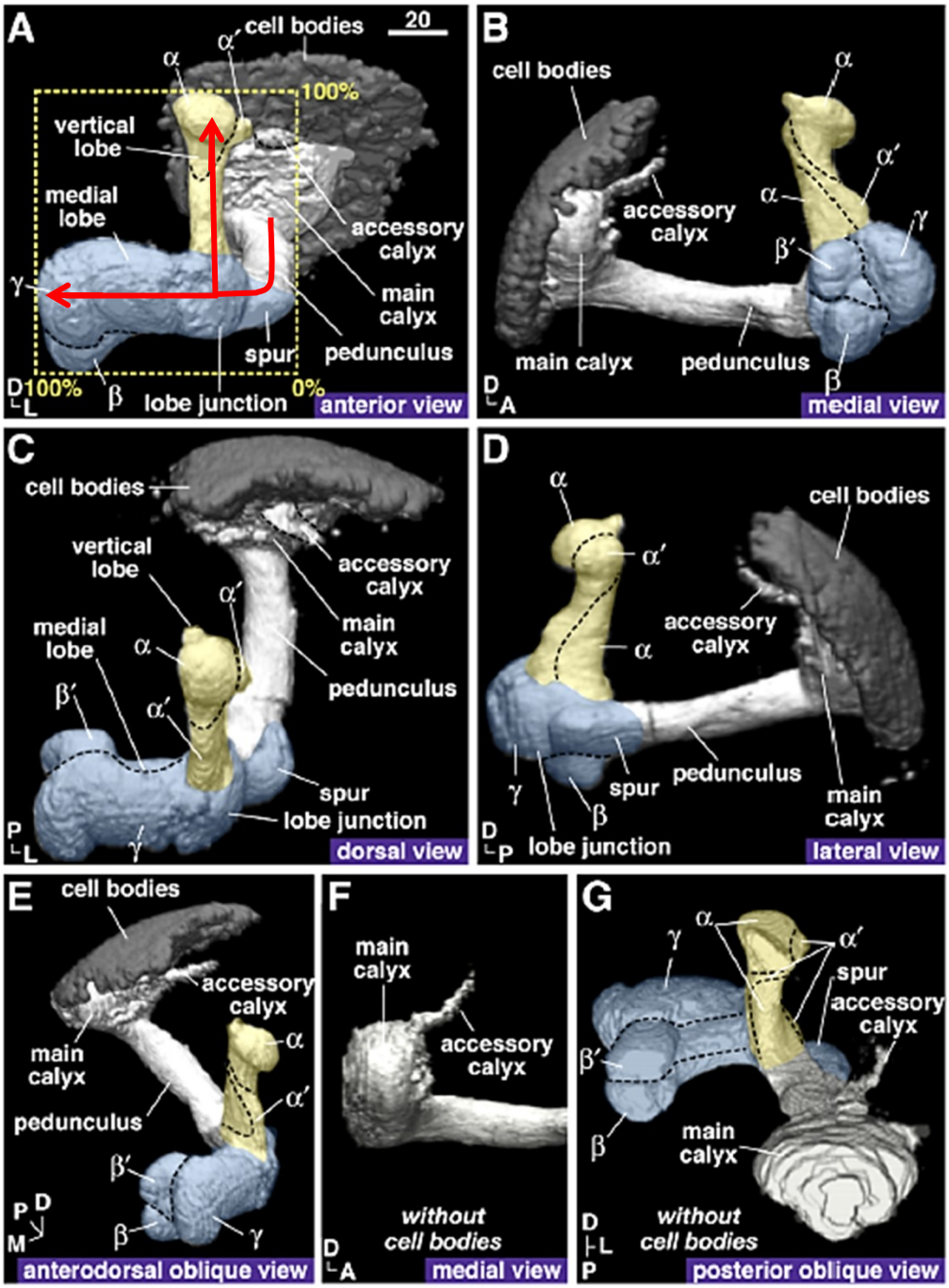

Figure 1.5: The mushroom body of *Drosophila*

3D reconstruction of the mushroom body. **(A-G)** different viewing angles of the mushroom body as indicated. The vertical lobe is marked in yellow and the horizontal lobe is marked in blue. In **A**, the general projection path of a single KC is superimposed in red. Figure adapted from Tanaka et al. 2008.

bouton form a microglomerulus. Each KC shows random connectivity with several PNs, leading to a code sparsening of the olfactory map carried by the PNs (Murthy, Fiete, & Laurent 2008). KCs project their axons anteriorly in a

large bundle called the peduncle. This bundle eventually bifurcates to form a horizontal and a vertical lobe. The population of KCs can be subdivided into three subpopulations based on anatomical and genetic characteristics: α/β, α'/β' and γ (Aso et al. 2009). The Vertical lobe consists of two subdivisions: the α subdivision (formed by axons from α/β KCs) and the α' subdivision (formed by axons from α'/β' KCs). The horizontal lobe is made up of three subdivisions: the β subdivision (formed by axons from α/β KCs), the β' subdivision (formed by axons from α'/β' KCs) and the γ subdivision (formed by axons from γ KCs). Apart from PNs, KCs synapse with a multitude of extrinsic neurons (mushroom body extrinsic neurons, MBENs), both pre- and postsynaptically (Tanaka et al. 2008). These confer different signals onto the MB or serve as output neurons to KCs (Krashes et al. 2009; Mao & Davis 2009a; Qin et al. 2012; Séjourné et al. 2011). MB lobes can be further segmented based on the innervation pattern of MBENs, which give rise to concise compartments that are either organized in a linear fashion along the lobe or in layers.

The MBs of *Drosophila* as well as other insects, such as bees, have been studied extensively in the past for their role in olfactory behaviors. These studies mostly focused on olfactory learning and memory. The essential role of the MB in olfactory learning was first shown by structural mutants and chemical ablation of the MB, which resulted in a defect of both appetitive and aversive olfactory memory (Heisenberg et al. 1985; Belle & Heisenberg 1994). Further studies showed that different subdivisions of the MB take over different roles in the formation and retrieval of olfactory memory. For example,

both memory types require output of α/β KCs for memory retrieval but not for formation and consolidation (Krashes, Keene, Leung, Armstrong, & Waddell 2007). To form this memory, MBENs signal reinforcement as well as other components such as hunger in the case of appetitive memory onto the MB (Krashes et al. 2009). These properties make it a structure that can integrate various different sensory modalities as well as internal signals. Apart from associative memories, various other behaviors have been linked to the MB. The MB and its different KC subsets have been studied in the context of many different behaviors including visual context generalization (L. Liu, Wolf, Ernst, & Heisenberg 1999), courtship conditioning (McBride et al. 1999), sleep (Joiner, Crocker, White, & Sehgal 2006), and visual choice behavior (Tang & Guo 2001).

The MB is thought to be dispensable for innate odor processing. This was demonstrated most profoundly in experiments with flies that lacked MBs. Two mutants that either have an abnormal MB structure (*mushroom body deranged*, *mbd*) or are devoid of KCs (*mushroom body miniature*, *mbm*) showed normal osmotropotaxis towards food related odors and normal avoidance of aversive odors (Heisenberg et al. 1985). Similarly, chemical ablation of the MBs through hydroxyurea treatment during development did not alter odor avoidance (Belle & Heisenberg 1994). Thus, flies that have no functioning MBs are not anosmic and display normal olfactory avoidance and attraction behavior. While innate olfactory behavior was not affected, all of the aforementioned MB impairments abolished olfactory learning. This finding is in line with the results of several studies, that suggest a role for the MB in

associative memories of odors (Qiu & Davis 1993; Hitier et al. 1998; Zars et al. 2000; Josh Dubnau et al. 2001; Fiala 2007).

Taken together, two important conclusions can be deduced from the aforementioned characteristics of the MB: First, the MB receives mainly olfactory input and is indispensable for olfactory learning and memory. Thus, it is possible that other olfactory behaviors might also require the MB as a processing center. Second, the MB seems to be dispensable for innate olfactory avoidance and attraction. Thus, a MB independent pathway for olfactory information processing must exist in the fly brain.

1.4 The lateral horn

Significantly less is known about the function of the lateral horn (LH) as a higher brain center in the fly. The LH of each hemisphere is located at the most lateral protrusion of the protocerebrum (Figure 1.6). At least one input source for this structure is of olfactory nature, which is provided through PNs. While some data suggests that the LH has an internal structure composed of a dorsal and a ventral area (Jefferis et al. 2007), it is not as well characterized as the MB. Studies in locusts demonstrated that a multitude of different neuron types converge within the LH, and thus it might serve multiple purposes such as multimodal and bilateral integration (Gupta & Stopfer 2012). For example, the innate attraction of *Drosophila* to ammines has been traced to PNs that project to a specific area within the LH which is segregated from the area in which PNs of aversive odors terminate (Min, Ai, Shin, & Suh

2013). Currently, it is being thought of as a center for innate olfactory behavior.

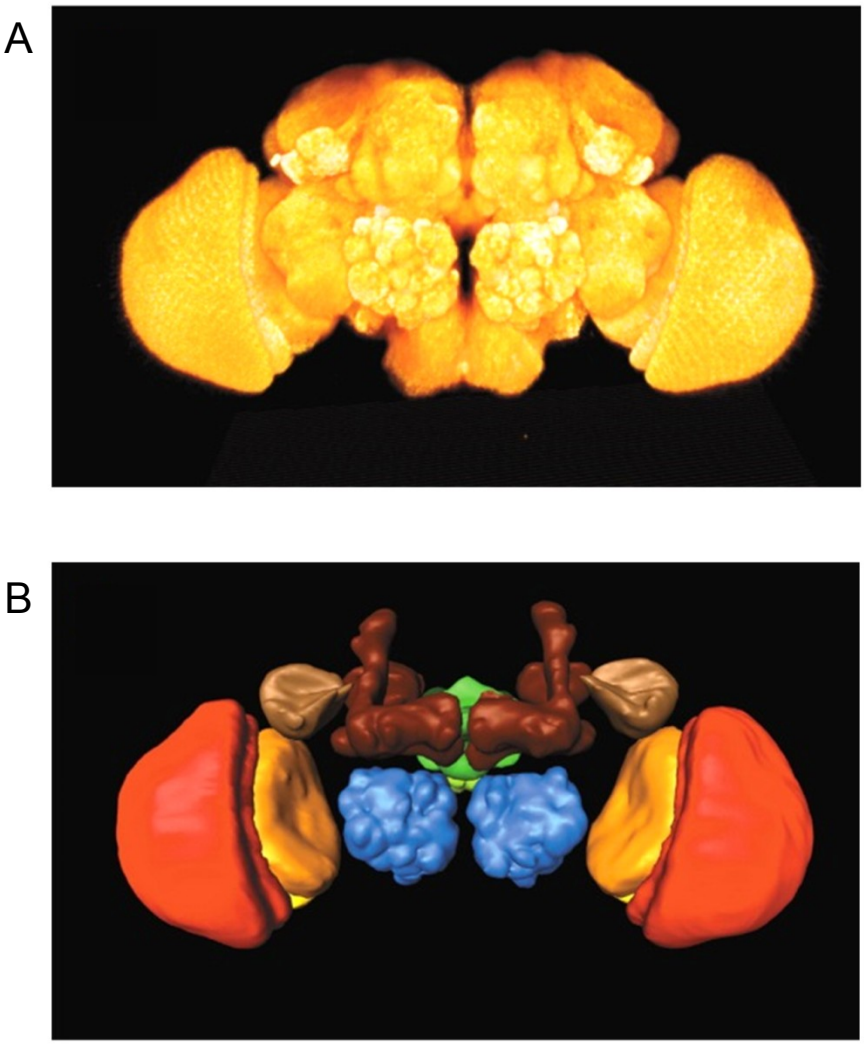

Figure 1.6: Processing centers of the *Drosophila* brain

(A) Overview of the *Drosophila* brain, visualized through anti neuropil staining. **(B)** 3D reconstruction of different processing centers within the brain. blue, antennal lobe; red, medulla; orange, lobula; yellow, lobula plate; beige, lateral horn; brown, mushroom body; green, central complex. Figure adapted from Rein, Zöckler, Mader, Grübel, & Heisenberg 2002.

1.5 The neurobiology of decision making

The brain can be understood as a structure that detects certain aspects of the outer world, and then analyses them to produce an appropriate behavior. The sensory data needs to undergo different steps of processing to assure that it can be interpreted properly, such as gain control or filtering. Apart from this basic processing, the brain also needs to perform another important task: decision making. Decisions need to be made in order to achieve the two ultimate goals of every animal: survival and reproduction. The needs of an animal possess an intrinsic hierarchy which is based on evolutionary logic. For example, self-preservation by escaping a predator should take higher priority than mating, because only a surviving animal is able to mate again in the future. Thus, the animal needs to evaluate the benefit of each action and then choose the appropriate one based on its current situation. This valuation of benefits integrates the needs of the animal into each action and thus gives the action and the outcome of the action a specific value.

Value based decision making can be best understood and studied inside a framework, which divides the process into several distinct computations the animal has to perform (reviewed in Rangel et al. 2008). First, the animal needs to form a representation of its current situation. This includes information about the internal state, such as hunger or the fertilization state of a female, as well as the external state. The external state includes all sensory input of the environment and the stimuli that can be derived from that input. Based on this information, the representation of a decision problem provides the animal with a range of possible actions to perform. The second computation of the decision process is to assign a specific value to each

action. A high value means that a particular action is beneficial for the animal, because it leads to the achievement of one of the major evolutionary goals described above. Once the value of each action has been determined, the animal can choose the most beneficial action and execute it. After the primary decision making process is finished, the animal has to perform a fourth computation: an evaluation of the outcome of the action. This evaluation is vital to a meaningful decision process, because it is needed to update the previous representation. In case the action did not change the previous representation, a new decision process has to be initiated. Even if this is the case, the animal can use the action to outcome relationship to modify future decisions by storing it as a memory. All three previous decision making computations can thus be improved over time.

One goal of neurobiology is to understand how these computations are performed in the brain, and what the corresponding neural substrates are. Building a representation of the inside and outside world is probably the best understood step of the decision process. This is especially true for the model organism *Drosophila melanogaster*. Neuroscientists were able to demonstrate how sensory systems employ various different strategies to generate a representation of the outside world in the brain of the fruit fly. Odors are represented by a specific glomerular activity pattern within the AL, that is generated by extensive interglomerular processing (for review see Su et al. 2009 and Masse et al. 2009). Visual stimuli are processed in a series of layers within the optic lobes, which extract more and more complicated features from the primary sensory input and represent them in the activity of specific cell types, such as the directional tuned activity of T4 and T5 interneurons (Maisak

et al. 2013). Apart from sensory systems that detect the outside world, other sensory systems are known in *Drosophila*, which form a representation of the inner state of the fly. Neurosecretory cells in the brain measure and regulate the internal energy level of the fly through secretion of either insulin like peptides or the adipokinetic hormone (for review see Leopold & Norbert Perrimon 2007). Hunger related signaling is then relayed onto various other neural circuits, for example the AL, through a system of multiple neuropeptides such as NPF or sNPF (for a review see Nässel & Winther 2010). Interestingly, more direct sensory systems to measure the internal state exist in the fly brain. They evaluate nutrient levels in the haemolymph by expression of the fructose receptor Gr43a and then utilize this information to convey positive or negative valence in a conditioning paradigm (Miyamoto, Slone, Song, & Amrein 2012). These cells might thus be a first a first step in a neural circuit that is used to assign value to food uptake.

1.6 Valuation systems in decision making behavior

Based on the representation generated from internal and external sensory sources, the animal has to assign specific values to each possible action in a decision process. Different valuation systems that have been proposed for this function are described below (reviewed in Rangel et al. 2008).

The Pavlovian system provides values for specific actions based on innate standards. These standards are derived from evolutionary experience and thus represent a behavioral repertoire that ensures fitness. Such a hardwired system can encode only a limited set of actions. These can for example

consist of an aversive stimulus and the corresponding escape reaction. The CO_2 avoidance behavior of *Drosophila* has very likely a high priority compared to other actions, because of such a Pavlovian valuation system. One particular characteristic of this system is that innate values can be transferred to stimuli that do not trigger a specific action on their own. Classical conditioning can thus transfer the positive value of imminent food intake to the neutral stimulus of the sound of a bell. The alternative to a value based decision making system is a simple perceptual based one. In a perception based system, sensory stimuli form a representation of sensory space, which is then computed by simple processing steps, such as addition or subtraction of two signals, into a choice probability (Sugrue, Corrado, & Newsome 2005). However, a Pavlovian value system might incorporate perception based decision making. During evolution, values assigned to certain actions, such as the reaction to important environmental stimuli, might have become hardcoded in the form of stimuli dependent computations. Within a network that performs such a task, synaptic weights and other adaptable processing factors might represent the valuation of a stimulus.

Another valuation system is based on learning through trial and error. It can thus be called habitual. As described above, decision making includes an evaluation of the outcome of each action. Information acquired this way, can then be used to predict the value of an action in a similar situation in the future. A relatively constant environment that provides such similar situations is thus crucial for the success of this valuation system. A habitual system can lead to a series of decisions with no beneficial outcome, and is thus slow in finding the optimal solution to a particular problem. Most importantly,

decisions based on this value system do not adapt the choice of action in a novel situation, but rather form a decision based on a previously experienced problem, which might not be very similar at all. Thus, values assigned in this system rely on generalization.

Finally, a third system uses a goal directed approach and computes the value of each action based on how beneficial the outcome is to solve the current problem. Compared to the habitual and the Pavlovian systems, which assign always the same value to a particular action within the same situation, the goal directed valuation system adapts the value if the outcome is not beneficial anymore. While the previous two systems can make a decision based on a single stimulus, the goal oriented system takes into account the complete representation generated at that point in time, with both the internal and external state of the animal as well as the available set of actions. As soon as one of these factors differs, the outcome of a particular action might not be desirable anymore and thus its value is diminished. A goal oriented value assignment is the most adaptable system, but is limited by the amount of possible outcomes that can be stored at that point in time. Also, it is limited by the predictability of possible outcomes. Assigning a value through the Pavlovian system might be more successful in such a situation, because of the immense time frame evolution had to find a more optimal response.

The valuation systems described above are neither separated nor exclusively responsible for the decision making process in an animal. Especially the goal driven system partially relies on the other two systems.

Drosophila provides a promising model organism for investigating how these systems are realized within a neural circuit. Previous studies with different behavioral paradigms showed, that all three valuation systems are used by the fly to form decisions. Strong innate reactions of *Drosophila* towards certain stimuli, for example phototaxis, have been exploited to study both the genetical as well as the neural basis of behavior (Benzer 1967; Gong et al. 2010; Zhu, Nern, Zipursky, & Frye 2009). Another example is CO_2 avoidance behavior, which is thought to be a hardwired behavioral response (Suh et al. 2007). Thus, any decision involving it is most likely conducted via a Pavlovian valuation system. Decisions which are based on a habitual valuation system can also be experimentally investigated in *Drosophila*. This has been demonstrated by the fruit flies capability to solve different operant conditioning tasks (Heisenberg et al. 1985; Sitaraman et al. 2008). Finally, experiments on oviposition behavior provide an example for a possible goal oriented way of making decisions. These experiments reveal that female flies prefer acetic acid rich food media as an oviposition site, but avoid it otherwise (Joseph, Devineni, King, & Heberlein 2009). Thus, these experiments expose the fly to a stimulus that has conflicting valence based on context. Their preference to place eggs on acetic acid rich food demonstrates, that they assign a more positive value to positioning on this food than to avoiding it, because they connect it to the value of the outcome of finding a good oviposition site for their offspring. Similarly, if this outcome is not connected to the action of positioning on acetic food, they value the action of avoidance higher. These results show that flies might be capable of making goal directed decisions. However, it remains unknown how this process is realized within the brain.

The only evidence provided by the aforementioned study is, that the perception of acetic acid in positioning and oviposition is performed by separate sensory systems. Furthermore, the requirements of higher brain centers for the avoidance and attraction behavior seem to differ. Taken together, *Drosophila* is an ideal model organism to study which valuating systems are necessary for a specific decision making process and which neuronal circuits contribute to this computational process.

1.7 Aims of this thesis

Knowledge about the processing of innate olfactory behavior is limited. CO_2 avoidance has been used as a model system to study this topic, but the neural underpinnings have not been characterized beyond the level of sensory neurons and one previously implicated PN remained without further characterization in behavioral experiments. In particular, the requirement of higher brain centers remains unknown. Furthermore, it has not been fully explained how the fly copes with higher background CO_2 levels generated by their natural habitat such as rotten fruit. It is unknown whether CO_2 processing can be altered based on context. Thus, one goal of this thesis was to explore and map unknown parts of the CO_2 olfactory circuit, because it can serve as a model circuit to gain insight into how neural circuits generate behavior. With its sensory level rather well explored, I focused on the function of higher processing centers in this circuit and the related avoidance behavior.

Furthermore, exploring the CO_2 circuit and its interaction with the processing of other stimuli can serve as an example to understand decision making

processes in a more specific way. As mentioned previously, the fly might be capable of employing all three proposed valuation systems. It will be interesting to test which valuation systems are used by the fly to make decisions in different contexts, and which neural circuits underlie these computations. Studying a similar decision process under different contexts might also reveal novel insight into how a representation of the inner and outer states of the animal influences the process of valuation. Taken together, investigating these aspects was another goal of this thesis.

I addressed these questions by two different strategies: First, I conducted a large scale screen of a driver line library to facilitate an unbiased discovery of novel circuit components. I expressed a protein to block neuronal transmission transiently in 1024 different driver lines, each covering a random subset of neurons. I paired this method with three different behavioral paradigms that where based on the classical T-maze assay. I tested flies for their avoidance of CO_2, their approach to vinegar and their reaction to a combination of both CO_2 and vinegar versus air. To address the influence of different inner states, I tested flies under starved and fed conditions.

This unbiased approach was complemented with a small scale screen of driver lines that expressed in known neuronal assembles. Again I used a genetically expressed effector to silence these neurons and test flies for their avoidance of CO_2 and their ability to integrate the CO_2 response into a context containing a food related odor. Specifically, I tested the requirement of the mushroom bodies for innate CO_2 avoidance. Furthermore, imaging experiments were conducted to test for a response of the mushroom body during CO_2 stimulation.

In order to further map the circuit, I searched for novel projection neurons that carry CO_2 information to higher brain centers utilizing various techniques.

Finally, to elucidate the connection between hunger, food odors and CO_2, I searched for a neurotransmitter that alters CO_2 avoidance in this context. Therefore I tested the dopaminergic system both in behavior and physiology.

2 Materials

2.1 Buffers and antibodies

Table 2.1: Buffers used for histology

Name	Ingredients
Phosphate buffered saline PBS (1x)	137mM Na_2HPO_4 1.5mM KH_2PO_4 137mM NaCl 2.7mM KCl adjusted to pH 7.2 in H_2O
Phosphate buffered saline plus 0.5% Triton PBT (1x)	0.5% Triton X-100 in PBS
Phosphate buffer lysine (200ml) PBL (1x)	1) dissolve 3.6g lysine 2) add 0.1M Na_2HPO_4 until pH reaches 7.4 3) add 0.1M NaH_2PO_4 until volume reaches 200ml 4) filter sterilize 5) store at 4°C for up to 3 months
Periodate-Lysine-Paraformaldehyde PLP (4%)	4% paraformaldehyde in PBL
Blocking solution	10% donkey serum in PBT

Table 2.2: Buffers used for calcium imaging

Name	Ingredients
Drosophila Ringer solution	182mM KCl 46mM NaCl 3mM $CaCl_2$ 10mM Tris-Cl adjusted to pH 7.2 in H_2O
Dopamine stimulation solution	1M dopamine hydrochloride in Drosophila Ringer solution

Table 2.3: Antibodies

Antibody	Type	Source
anti-discs large (mouse, 1:200)	primary	Hybridoma Bank (USA)
anti-GFP (rabbit, 1:1000)	primary	Clonetech (USA)
anti-mouse-Cy5 (goat, 1:200)	secondary	Dianova (Germany)
anti-rabbit-488 (goat, 1:200)	secondary	Dianova (Germany)

2.2 Chemicals and odors

Table 2.4: Chemicals

Chemical	Source
Agarose (high electroend.)	Biomol (Germany)
Donkey serum	Sigma-Aldrich (USA)
Dopamine hydrochloride	Sigma-Aldrich (USA)
Paraformaldehyde (16%)	Electron Microscopy Sciences (USA)
Tris base	Merk (Germany)
Triton-X	Roth (Germany)

Table 2.5: Odors

Odors	Source
Balsamico vinegar	Alnatura (Germany)
3-octanol	Sigma-Aldrich (USA)
Paraffine oil	Sigma-Aldrich (USA)
Carbondioxide (pressured)	Westfalen (Germany)
Air (pressured)	Westfalen (Germany)

2.3 Consumables and equipment

Table 2.6: Consumables

Consumable	Purpose	Source
Facial tissue	starvation bottles	SCA (Sweden)
Qualitative filter paper 415	starvation bottles	VWR (Germany)
Drosophila vial (15ml, PS)	stimulus tubes	VWR (Germany)
Parafilm	stimulus tubes	Pechiney Plastic Packaging (USA)
Microscope slides (76 x 26mm)	mounting	Menzel Gläser (Germany)
Microscope cover glass (24 x 24mm)	mounting	Menzel Gläser (Germany)
Vectashield H-1000 fluorescence medium	mounting	Vectalabs (USA)

Table 2.7: Equipment

Equipment	Purpose	Source
DM6000FS fluorescence microscope	calcium imaging	Leica Microsystems (Germany)
DFC 360 FX fluorescence camera	calcium imaging	Leica Microsystems (Germany)
Custom made CO_2 and odor stimulus device	calcium imaging	Smartec (Germany)
Blade holder	calcium imaging	Fine Science Tools (Germany)
Razor blade No. 35010.20	calcium imaging	Martor Solingen (Germany)
Plastic foil	calcium imaging	Cigarette packaging
Protemp II dental glue	calcium imaging	3M ESPE (Germany)
FV-1000 confocal microscope	histology	Olympus (Japan)
Dumont #55 forceps	histology	Fine Science Tools (Germany)
GM70 portable CO_2 meter	stimulus tubes	Vaisala (Finland)
Mass flow controller MC-500	stimulus tubes	Natec Sensors (Germany)
Custom made climate box with humidity controller and heat plate	behavior	Max Planck Institute for Neurobiology workshop (Germany)
Custom made T-maze	behavior	Max Planck Institute for Neurobiology workshop (Germany)

2.4 Fly stocks

The following fly stocks were used as a basis for all crosses in this thesis. The final genotypes were generated by the indicated crosses.

Table 2.8: Fly stocks

Referred to as	Genotype	Insertion site	Source
w^-	w^{1118}	X	Bloomington stock center
MB186B-GAL4	*P{52H09-p65ADZp}attP40/CyO;P{34A03-ZpGdbd}attP2/TM6b*	II,III	Gerald Rubin
MB010B-GAL4	*P{13F02-p65ADZp}attP40/CyO;P{52H09-ZpGdbd}attP2/TM6b*	II,III	Gerald Rubin
R67B04-GAL4	w^{1118}*;P{GMR67B04-GAL4}attP2*	III	Bloomington stock center
MB247-GAL4	*w*;P{w[+m*]=Mef2-GAL4.247}3*	III	Bloomington stock center
OK107-GAL4	*w*;P{GawB}ey*^{OK107}	IV	Bloomington stock center
D52H-GAL4	*w*,P{dnc-GAL4.D52H}*	X	Hiromu Tanimoto
biVPN-GAL4	w^{1118}*; P{GMR53A05-GAL4}attP2*	III	Bloomington stock center
UAS-shi^{ts1}	*w*,P{UAS-shits1.K};P{UAS-shits1.K},P{UAS-shits1.K}*	X, III	Hiromu Tanimoto
UAS-dTRPA1	*w*;P{UAS-TrpA1.K}attP2/TM6B,Tb*^{1}	III	Bloomington stock center
UAS-mCD8-GFP	*w*,P{UAS-mCD8::GFP.L};P{UAS-mCD8::GFP.L}/CyO;P{UAS-mCD8::GFP.L}*	X, II, III	Hiromu Tanimoto
UAS-GCaMP5	*w*; P{20XUAS-IVS-GCaMP5G}attP40*	II	Bloomington stock center
heatshock flip	*w*,y*,hsflp;UAS>CD2,y+>CD8GFP/CyO;TM2/TM6b*	X,II	Laboratory stock
Nsyb-GAL4	*w-; UAS-SPA/CyO; Nsyb-GAL4/TM6b*	II, III	Maria Luísa Vasconcelos
UAS-C3PA-GFP	*w-; UAS-c3PA/CyO; UAS-C3PA/TM6b*	II, III	Maria Luísa Vasconcelos
MB247DsRed	*w-; MB247DsRed/CyO; UAS-C3PA/TM6b*	II, III	Maria Luísa Vasconcelos

2.5 Fly food

Table 2.9: *Drosophila melanogaster* medium

Ingredients	Amount
Agar	585g
Corn flour	5kg
Yeast	925g
Soy flour	500g
Molasses	4kg
Propionic acid	315ml
Nipagin	125g
Ethanol (20%)	1l
Phosphatidic acid (10%)	500ml
water	up to 50l total volume

2.6 Climate box

The following custom made climate box (Max Planck Institute for neurobiology workshop) was used for all experiments to generate either the 25°C or the 32°C temperature conditions. In principle, a heating plate at the bottom generated warm air which was circulated by two fans through the box and a pipe system. Through the pipe system, the air passed a container in which an ultrasound fog generator produced water vapor. Both the heating plate and fog generator were activated by a control box that regulated the temperature and the humidity in the desired tolerance range.

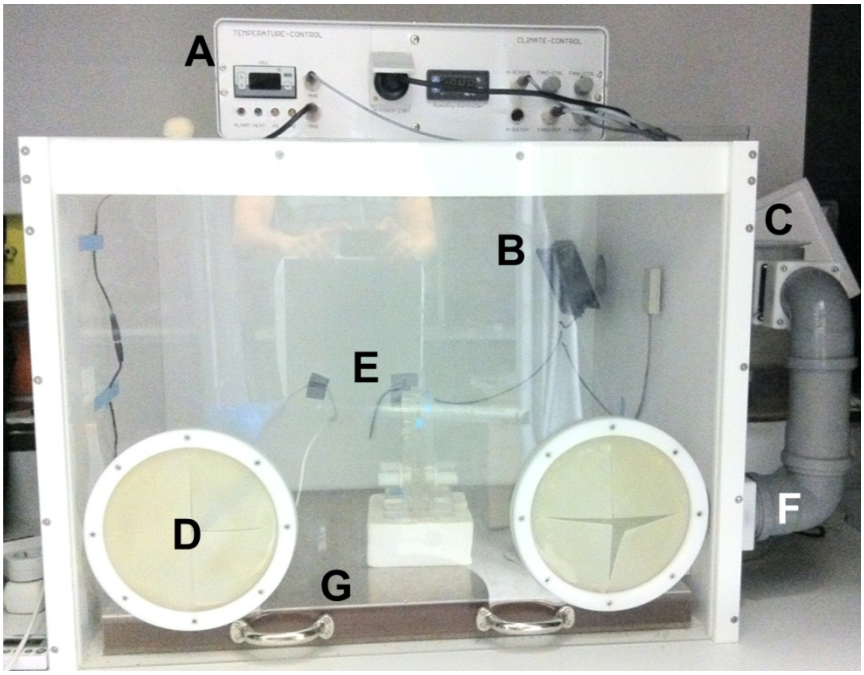

Figure 2.1: Climate box

This climate box was used to create high temperature environments for heat sensitive experiments such as blocking neurons via Shibire^{ts1}. A, regulation unit; B, inner fan; C, ultrasound fog generator; D, manual entry for experimenter; E, humidity and temperature sensor; F, air circulation pipes; G, heating plate.

3 Methods

3.1 Fly rearing and starvation

For behavioral experiments, flies were reared on standard cornmeal medium at 18°C and 60% relative humidity. After eclosion, flies were transferred to 25°C and used for experiments at the age of 6-8 days. For experiments that required starvation, flies were transferred 42 hours prior to the experiment into bottles that contained tissue paper and a supply of 7,5 ml of water but no access to food.

3.2 Survival experiments

To determine the starvation resistance of different lines, up to 40 flies of the respective genotype were placed in small vials. These vials only contained 1% agarose prepared with tap water as a form of water supply. At the indicated time points, female flies were counted and a survival curve was generated by dividing the number of surviving females by the total number of females in the respective tube.

3.3 T-maze behavior experiments

Animals were tested in groups of ~60 in a standard non-aspirated T-maze (Suh et al. 2004; Tully & Quinn 1985). To create a stimulus, testing tubes (15ml) with a controlled CO_2 atmosphere (0.1%) were prepared by mixing compressed air (Westfalen Gas) and pure CO_2 (Westfalen Gas) through mass

flow controllers (Natec sensors) and containing this atmosphere within the tube by sealing it with three layers of parafilm (Pechiney Plastic Packaging). The CO_2 concentration within the tubes was controlled by using a CO_2 detector device (Vaisala). Vinegar (balsamico vinegar, Alnatura Germany) was diluted 1:10 in water. For 3-octanol experiments, 3-octanol was diluted in paraffin oil. 40 µl of these solutions were added on to a paper strip within the respective tube.

Before each experiment, experimental and control fly groups were transferred into incubation vials. Groups were then shifted to high temperature conditions (32°C, 60% relative humidity) or low temperature conditions (25°C, 60% relative humidity) respectively within two separate climate boxes. After 20 minutes of incubation (90 seconds for dTRPA1 related experiments), they were transferred into the T-maze elevator. To start the test, flies were transferred via the elevator to the choice point (Figure 3.1). Here, they were given 60 seconds time to decide between the two tubes that were connected to the T-maze: one filled with CO_2 or other odors and one with just air. To minimize interference with other stimuli, these tests were carried out in complete darkness and silence.

After the test, flies were counted and the performance index (PI) was calculated by subtracting the number of flies on the air side from the number of flies on the odor side and normalizing this result to the total number of flies. The means of different groups were compared by one-way analysis of variance (ANOVA) to determine whether they behave significantly different. This testing procedure compares the variance between means to the variance within the samples. Two means are termed significantly different if the

variance between the different means is higher than the variance within the different samples. To control the familywise error rate and thus avoid false positive results when multiple statistical comparisons were made, all tests were subjected to a Bonferroni correction. Doing so adjusts the probability threshold (below which two groups are accepted as significantly different) by dividing it by the total amount of comparisons made. Statistical analysis was performed using GraphPad Prism software.

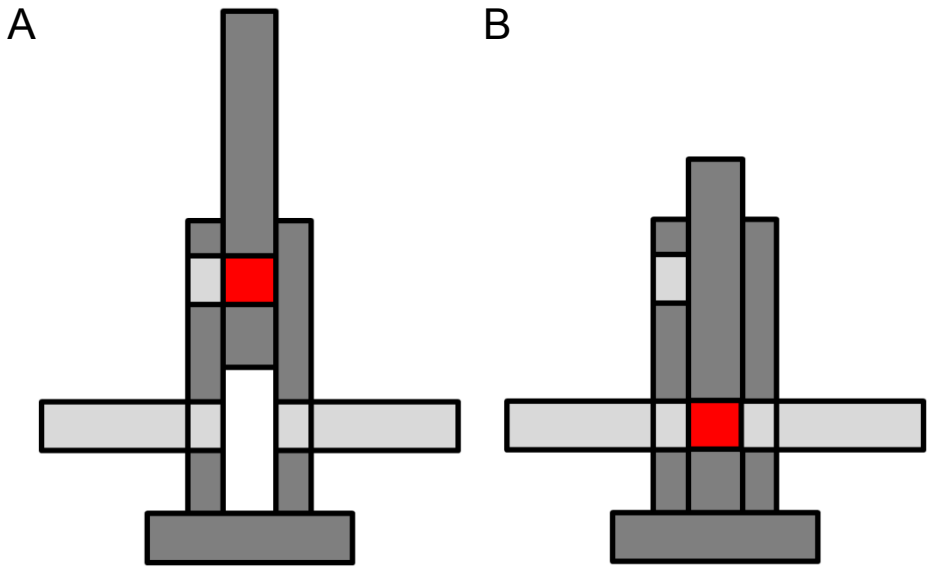

Figure 3.1: T-maze assay

Schematic diagram of the non-aspirated T-maze assay. The assay consists of two fixed parts with a sliding part in the middle. **(A)** Loading position of the T-maze. Flies are transferred into the elevator in the middle part (red) by tapping. **(B)** Test position of the T-maze. Flies are transferred in the elevator to the choice point (red). Two tubes with different stimuli are attached on both sides of the choice point. The test is ended by sliding the middle part with the elevator up again to trap the flies in the respective stimulus tubes.

3.4 Calcium Imaging

For calcium imaging experiments, all flies expressed the calcium indicator GCaMP5.0 (Akerboom et al. 2012). To image the MB, *in vivo* preparations of flies were prepared based on a method previously described (Fiala & Spall 2003). Flies were anesthetized on ice and then restrained in a piece of a pipette tip. Afterwards, the dorsal part of the head was gently pushed against a piece of thin plastic foil, which was fixed to a metal preparation folder. The preparation holder was a rectangular 2 mm thick aluminum piece with a hole at the end were the foil could be glued to. Through the hole, the top of the foil was exposed for further preparation. The head was firmly fixated using inert dental glue, but leaving all olfactory appendages free for stimulation. After the fly was fixed in such a way, a small window was cut into the plastic foil and a similar window in the cuticula. This preparation was covered with *Drosophila* Ringer solution and then placed under the microscope. For imaging of the biVPN, a modified protocol was used in which the mouth parts of the fly were removed so that the head could be imaged from the ventral side.

The *in vivo* preparations were imaged using a Leica DM6000FS fluorescent microscope equipped with a 40X water immersion objective and a Leica DFC360 FX fluorescent camera. All images were acquired with the Leica LAS AF E6000 image acquisition suite. Images were acquired for 30 s at a rate of 20 frames per second with 4 x 4 binning mode. During all measurements the exposure time was kept constant at 20 ms. In all experiments, the stimulus was applied at 5 s after the start of each measurement.

A continuous and humidified airstream (2000 ml/min) was delivered to the fly throughout the experiment via an 8 mm diameter glass tube positioned 10 mm away from the preparation. A custom-made odor delivery system (Smartec, Martinsried), consisting of mass flow controllers (MFC) and solenoid valves, was used for delivering a continuous airstream and stimuli in all experiments. For CO_2 stimulation, a precise amount of pure CO_2 was flown into the main airstream to attain the desired CO_2 concentrations (0.05%, 0.1%, 0.5%, 1%, 5% and 10%) at the delivery end. In the same way, pure air was flown to the main airstream for air stimulation. Stimuli were delivered in all experiments for 500 ms and during stimulations the continuous airstream flow in the delivery tube was maintained at 2000 ml/min. To measure the fluorescent intensity change at the MB, the region of interest was delineated by hand and the resulting time trace was used for further analysis. For the biVPN cell body and V-glomerulus imaging, standard sized regions of interest (ROI) were used to measure the fluorescence across all flies. To calculate the normalized change in the relative fluorescence intensity, we used the following formula: $\Delta F/F = 100(Fn-F0)/F0$, where Fn is the *n*th frame after stimulation and F0 is the averaged basal fluorescence of 15 frames before stimulation. For all experiments, we used the peak maxima of the response peak for calculation of the signal strength. The pseudo colored images were generated in MATLAB using a custom written program. All analysis and statistical tests were done using Excel and GraphPad Prism software, respectively.

For bath application experiments with dopamine, the first calcium response to 1% CO_2 was measured as described above. Then, 5 µl of 1 M dopamine hydrochloride (Sigma) dissolved in imaging saline were added to 500 µl of

imaging bath to attain a final dopamine concentration of 10 mM. 5 min after adding the dopamine to the bath, the calcium response to 1% CO_2 was measured again. The same procedure was repeated for control experiments, but instead of dopamine, 5 µl of imaging saline were added. Data analysis was done as described above.

3.4 Histology

Adult fly brains were dissected, fixed and stained using standard protocols. Flies were anesthetized with CO_2, washed in 100% ice cold ethanol and then transferred into ice cold phosphate buffered saline (PBS). Fly brains were individually dissected in room temperature PBS and then transferred into PLP buffer containing 4% paraformaldehyde for fixation. Fixation took place overnight at 4°C temperature and was stopped by washing the brains three times in 0,5% PBT for 15 minutes each wash. After washing, brains were incubated for 2 hours at room temperature in blocking solution. Brains were then incubated in primary antibody diluted in blocking solution for 4 hours at room temperature, which was followed by three washing cycles for 15 minutes in PBS at room temperature. Afterwards, brains were incubated for 2 hours at room temperature in secondary antibody diluted in blocking solution under exclusion of light. As a final step, brains were washed three times for 15 minutes each in PBS and then mounted in Vectashield (Vectalabs). Microscopy was performed at an Olympus FV-1000 confocal microscope. Images were processed using ImageJ and Photoshop.

Anti-discs large antibody (1:200, Hybridoma bank) was generally used as a primary antibody to visualize the neuropil. Anti-GFP antibody (1:1000, Clontech) was used as a primary antibody to increase the intensity of the GFP signal. As secondary antibodies, anti-mouse-Cy5 (1:200, Dianova) and anti-rabbit-488 (1:200, Dianova) were used.

3.5 Tracing

For all photoactivation experiments an Ultima two-photon laser scanning microscope (Prairie Technologies) equipped with galvos driving two Coherent Chameleon XR lasers was used. All images were acquired with an Olympus BX61 microscope equipped with a 40x0.8 NA objective. Images were obtained at 1.5 µm steps with a 512x512 resolution. These images were then used in the AMIRA software where we obtained the three-dimensional reconstruction of brain structures by using the segmentation editor and reconstructed the neuronal pathway with the filament editor. Maximum projection images were acquired with ImageJ. For the photoactivation experiments, flies were generated that carried Nsyb-GAL4 or biVPN-GAL4 and two copies of UAS-C3PA-GFP (Patterson & Lippincott-Schwartz 2002). Whenever the MB needed to be labeled, MB247-GAL4 line was used to drive expression of DsRed (Riemensperger, Völler, Stock, Buchner, & Fiala 2005). Photoactivation was carried out on adult flies with 12 hours post-eclosion. First, the V-glomerulus was identified at 925 nm (at this wavelength photoconversion is ineffective) and a z-series of the whole brain was made. Then the Prairie View software was used to determine the photoactivation power needed to photoactivate each V-glomerulus or cell body. Due to

orientation variations of each brain, the power needed depended greatly on the depth of the target. The necessary power level was determined through a single z-series starting at a low level and enhancing it until photoconversion took place. A region of interest around the V-glomerulus was defined afterwards and a z-series of the whole V-glomerulus at 1 µm step was scanned. This z-series was never more than 10 slices. A photoactivation mask volume was set by drawing a two-dimensional mask on each section of this z-series. For cell body photoactivation, no z-series or mask was necessary. To achieve photoconversion, 90 cycles of exposure at 710 nm laser light (a wavelength that more efficiently photoconverts the fluorophore) with a “rest” period of 30 s were applied. The “rest” period allowed diffusion of the photoconverted fluorophore into the neural processes and minimized photodamage. Finally, the initial z-series of the whole brain was repeated.

3.6 GAL4-UAS / split-GAL4

The GAL4/UAS system is a two-component expression system designed to spatially and temporally control expression of transgenes such as proteins (Brand & Perrimon 1993). Derived from yeast, the GAL4 protein is a transcription factor that binds with high specificity to the upstream activation sequence (UAS), where it triggers transcription (Figure 3.2). GAL4 expression is restricted spatially and temporally within the organism by bringing it under control of an endogenous enhancer element or by fusing it to an engineered promoter sequence. This specific expression pattern is transferred to the expression of any transgene downstream of a UAS-sequence. In this work, I used both engineered enhancers (such as R67B04-GAL4) and endogenous

ones (such as OK107-GAL4) to control expression. Transgenes expressed this way served various different purposes: manipulation of neuronal circuits in behaving animals (such as Shibire^{ts1}), imaging of neuronal function (GCaMP5.0), describing neuronal anatomy (GFP) and visualizing putative connectivity (PA-GFP).

To further enhance the restrictiveness of expression patterns, two lines used in this thesis were generated utilizing the split-GAL4 method (Luan, Peabody, Vinson, & White 2006). It builds upon the same principle as the basic GAL4/UAS system. Split-GAL4 uses two GAL4 constructs, each expressing one half of the GAL4 protein under control of an individual promoter element (Figure 3.2). The full active GAL4 protein can only be reconstituted in cells that express both GAL4 parts. Thus, this method creates an intersection of both expression patterns. This intersection is a very specific expression pattern that is created from two broader ones. Split-GAL4 lines can be combined with any UAS-line.

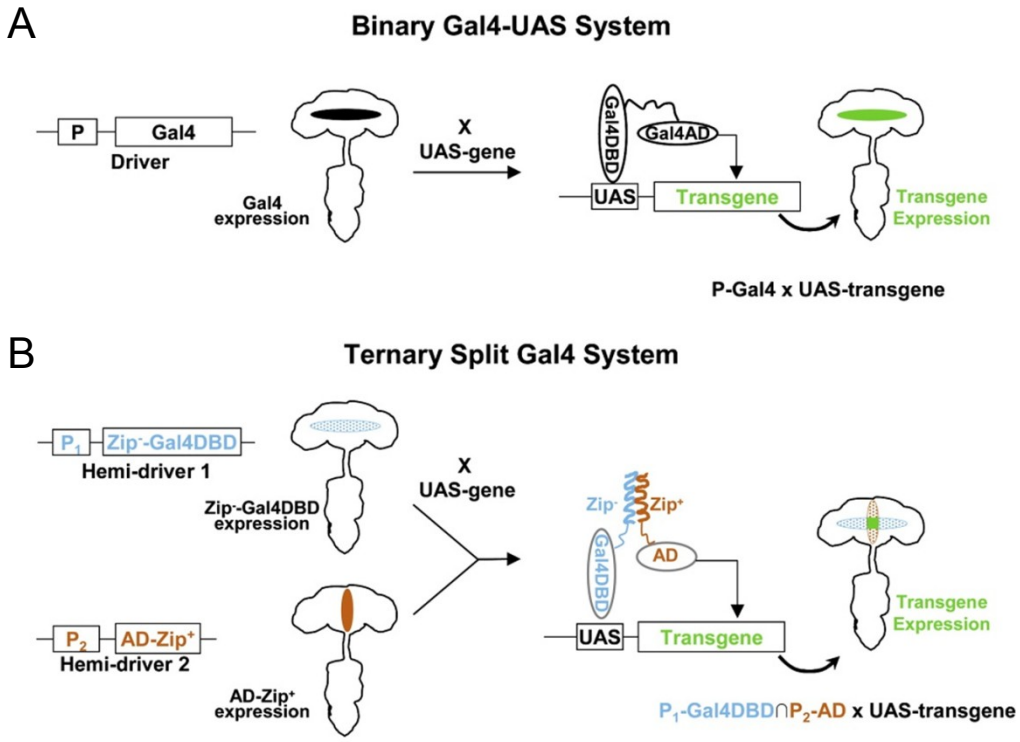

Figure 3.2 The GAL4 and the split-GAL4 expression system

The GAL4 expression system allows for transgene expression in a spatially defined way. The expression pattern of the GAL4 transcription factor is controlled by a promoter element (P). In cells with an active promoter element, GAL4 binds to the UAS sequence with its DNA-binding domain (GAL4DBD) and thus activating transcription through its activation domain (AD). (B) The split-GAL4 system utilizes the two GAL4 domains as separate proteins. Both halves are expressed under control of two different effectors. An active GAL4 protein can only be reconstituted with the help of two leucine zippers (Zip) in cells that express both halves. Figure adapted from Luan et al. 2006.

3.7 Generating heat shock flip clones

To generate heat shock flip clones, flies from the biVPN-GAL4 line were crossed with flies of the *w-,y-,hsflp;UAS>CD2,y+>CD8GFP/CyO;TM2/TM6b* fly line. This construct carries two flippase recognition target (FRT) sites. In presence of a flippase, mitotic recombination events are induced. When successful, they lead to excision of the sequence separating the UAS sequence and the GFP transgene (Bohm et al. 2010). When the event happened in a GAL4 positive cell, all daughter cells of this cell will express GFP.

Expression of the flippase was induced through a heat shock promoter. Since recombination is based on mitosis events, clones can be restricted to specific neuron types based on their time of birth during development. Taken together, this method allows restriction of an otherwise broad expression pattern for in depth analysis.

Once the larvae of the desired genotype emerged in the culture tubes, they were heat shocked for 30 to 45 minutes at 37° C in a water bath. This treatment triggered flippase expression. Adult flies that emerged after the heat shock treatment were dissected, stained, and visualized as described above. Three-dimensional reconstructions of neurons were made using IMARIS software.

4 Results

Drosophila's strong innate avoidance of CO_2 is surprising, since CO_2 is abundant in the natural habitat of the fruit fly. Rotting fruits and other plant parts, which represent food sources for *Drosophila*, emit this gas. While possible mechanisms to counter this avoidance and permit the fly to approach these food sources have been suggested (Turner & Ray 2009), I wanted to explore whether CO_2 behavior can be modified based on context. I thus exposed flies to a choice between air on one side of a T-maze and a combination of CO_2 plus vinegar on the other. Vinegar is a food related odor and flies are attracted to it when starved. Before the experiment, I subjected the flies to one of two different treatments. One group was kept on food until testing (fed group), while a second group was food deprived for 42 hour before testing (starved group). Flies that were fed before the experiment avoided the mixture of CO_2 and vinegar to the same degree as CO_2 alone (Figure 4.1). Under starved conditions however, flies overcame this aversion and approached the mixture. The reaction to CO_2 alone was not changed in starved flies compared to that of fed flies. Thus, CO_2 avoidance can be modified based on the inner state of the fly and in the presence of other stimuli. Since fed flies fully avoided the side that contained CO_2 and vinegar, the reduction observed under starved conditions cannot be attributed to an interaction of vinegar odor with CO_2 sensing neurons on the peripheral level. A modification of olfactory avoidance behavior might not be restricted to CO_2 but could be a general feature of odor processing. To answer this question, I

replaced CO_2 with a different aversive odor. I chose 3-octanol for this purpose. 3-octanol triggers, at the concentration used in the experiment (1:10 diluted in paraffin oil), a similar avoidance reaction as CO_2 (Figure 4.1). In contrast to CO_2, starved flies did not overcome their avoidance of 3-octanol when it was combined with vinegar. This result further suggests that dedicated parts of the CO_2 circuitry are able to perform the task of integrating context dependent signals into CO_2 behavior. Furthermore, these experiments demonstrate that the avoidance of CO_2 is more flexible than previously thought. It might even be possible that this form of processing is a special characteristic of CO_2 processing, because 3-octanol avoidance was not modified at the concentration tested.

To explore the neural circuits underpinning CO_2 behavior and how they control and modify CO_2 behavior, I employed two strategies:

1. A large scale screen of an enhancer trap collection for behavioral deficits after blocking random sets of neurons.

2. Screening a selected set of GAL4 lines with known expression patterns.

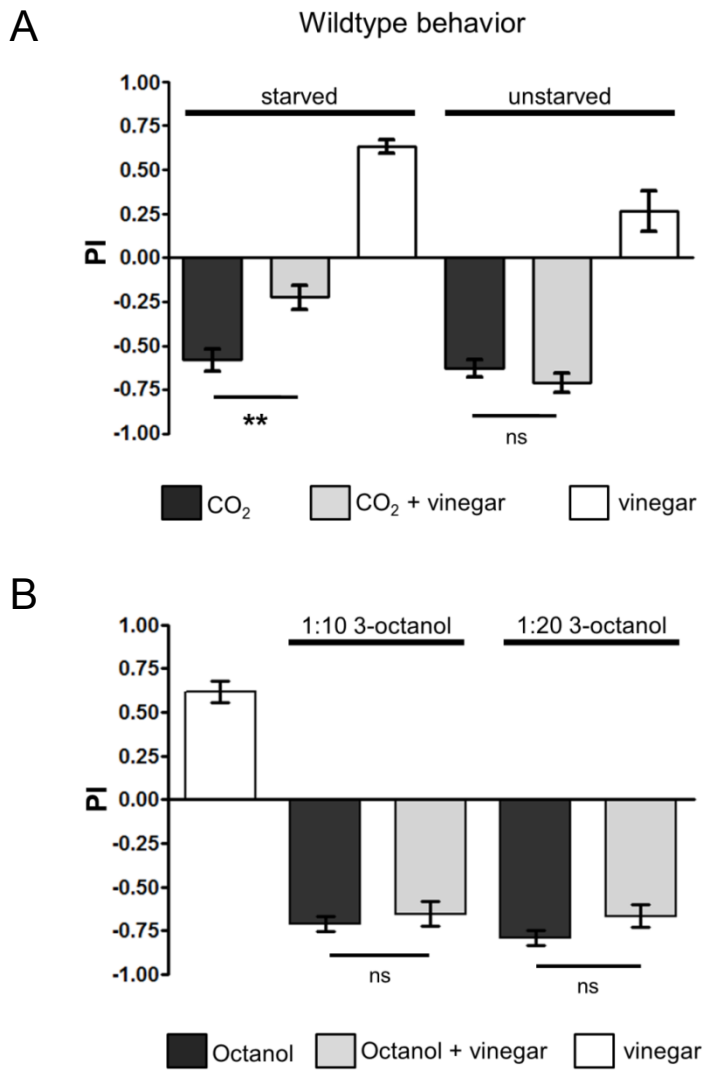

Figure 4.1: Starved flies can overcome their CO_2 avoidance behavior

(A) Behavior of wild-type flies towards CO_2, vinegar, and CO_2 plus vinegar in a T-maze assay. Wild-type flies were either starved 42 hours prior to experiments (starved) or kept on food (fed). Error bars represent SEM (n = 9). **p < 0.01; ns, p > 0.05 (ANOVA, Bonferroni's multiple comparison test). **(B)** Behavior of wild-type flies towards different concentrations of 3-octanol, vinegar, and 3-octanol plus vinegar in a T-maze assay. Wild-type flies were starved 42 hours prior to experiments. Error bars represent SEM (n = 9). ns, p > 0.05 (ANOVA, Bonferroni's multiple comparison test). Figure adapted from Bräcker et al. 2013 with permission.

4.1 Screening a large GAL4-line collection for behavioral defects

A large scale behavioral screen of driver lines which were not selected for specific expression patterns, represents an unbiased way to explore CO_2 behavior related neural circuits. Randomly selected driver lines might cover neurons that were not previously connected to CO_2 related or other olfactory behaviors. For this purpose, the NP collection of enhancer trap GAL4 lines was chosen. This large collection of stocks was generated by a consortium of different labs and institutions based in Japan (Hayashi et al. 2002). The collection is now freely available through the Kyoto DGRC stock center (http://kyotofly.kit.jp/cgi-bin/stocks/index.cgi). All lines have been mapped for their locus of insertion as well as partially characterized for expression at embryonic and larval stages. To facilitate throughput, both the selection of lines to test as well as the experimental protocol were adjusted to facilitate tests on a large number of lines in a reasonable amount of time. The selection process thus excluded lines that did not carry their insertion either on the second or third chromosome. By excluding these lines, a general crossing procedure could be set up in which virgins of the effector line were collected in large numbers and mixed with only few males of the respective NP line. Furthermore, lines that carried balancer chromosomes were discarded in order to avoid a complicated post experimental selection process.

I chose Shibire^{ts1} as an effector and expressed it via the GAL4/UAS system. The *shibire* gene is a dynamin allele, which translates to a protein that changes conformation at higher temperatures (32°C used here) (Kitamoto 2001). This change blocks synaptic vesicle recycling at chemical synapses because dynamin is required for newly formed vesicles to dissociate from the

cell membrane. The synapse becomes silent since no new vesicles can be loaded with neurotransmitter. Shibire^{ts} induced silencing is fully reversible and neurons act like wild type cells at permissive temperature. The temperatures used in these experiments are 32°C for restrictive and 25°C for permissive conditions. Experimental flies were generated by crossing NP-GAL4 males to UAS-*shibire*^{ts1} virgin females.

I tested three different choice behaviors in a T-maze under restrictive conditions: CO_2 avoidance, vinegar attraction and the reaction to a combination of vinegar and CO_2. All odors were tested versus air. I carried out one test per line and condition. During the test, I observed the behavior of the flies and took note of the results.

After shifting them to restrictive temperature, experimental flies often showed paralysis, which was likely caused by expression of Shibire^{ts} in motor neurons. 135 lines displayed this seizure like behavior. A large number of lines also showed severe movement defects which either lead to hyperactivity or defect walking behavior. This was the case for 122 lines. I excluded both groups from all of the statistics listed below.

From all 1024 lines, I found 203 lines with abnormal avoidance of CO_2 (Figure 4.2). All of these abnormal avoidance behaviors could be grouped into five phenotypes. The normal avoidance behavior of *Drosophila* is a very strong avoidance reaction. I found 10 lines that showed attraction, although this attraction was not very pronounced. Most of the lines I found to be defective in CO_2 avoidance showed an equal distribution in the T-maze and this phenotype was classified as no avoidance (99 lines). Furthermore, I observed

milder defects in CO_2 avoidance. 44 lines displayed reduced avoidance and 17 lines displayed increased movement to the CO_2 side. While wild type flies tended to stay on the air side of the T-maze throughout the one minute testing time, the latter category of lines frequently entered the CO_2 containing arm of the T-maze (termed shuttling behavior). Finally, I grouped 29 lines of the 203 lines with a defect in CO_2 behavior into one category of defects which could not be described by any of those phenotypes previously mentioned. This included behavioral defects such as increased time before an avoidance reaction was displayed.

A similar discrimination based upon severity of defect was made for all lines that showed an abnormal behavior in the CO_2 plus vinegar combinatorial paradigm. From all lines tested, 221 showed a defective behavior when tested for their reaction to CO_2 and vinegar in one arm of the T-maze versus air in the other (Figure 4.2). Normal flies overcome the aversion of CO_2 and approach the vinegar. Thus, the observed behavior consists of two phases: one aversion and one approach phase with a delayed onset. After one minute of testing, this results in an equal distribution of flies on both sides of the T-maze. 51 lines showed no aversion in this two component behavior and thus most flies were present in the CO_2 and vinegar containing arm of the T-maze. A comparable amount of lines (41) showed a milder version of this phenotype which resulted in a just slightly increased number of lies on the odor side. For 66 lines, I found the opposite of a reduced aversion. These lines showed no attraction phase and generally avoided the CO_2 and vinegar side to a great extent. A similar phenotype was observable in 44 lines which had a reduced but still detectable attraction behavior. Finally, I found 21 lines that did not fall

in line with the behaviors described above. These lines displayed such phenotypes as increased shuttling behavior or an increased decision time.

To further analyze hits obtained in the primary screen, a follow up screen was designed. With this secondary analysis, I aimed to solidify the evidence for abnormal behaviors by repeating the tests from the initial screen. Of the 1024 lines I tested, 423 lines showed an abnormal behavior in one or more parameters (Figure 4.2). For a secondary analysis, all lines that also showed abnormal movement were eliminated and a final pool of 307 lines was selected. As a first step of this secondary analysis, I scored the expression patterns of these lines for coverage of brain regions and overall density of expression. This was made possible due to collaboration with the lab of Kei Ito, which generously provided an expression database covering most of these GAL4 lines. The database consisted of images of GFP expression patterns which were scanned under a confocal microscope in selected sections. After evaluation and scoring of the provided images, I decided to group all lines into three categories: broad expressing lines, which cover a large amount of cells in multiple regions of the fly brain (98 lines); medium expressing lines which cover a larger amount of cells located in one or two brain regions (76 lines); and sparse expressing lines that only cover few cell types which are located in one or two brain regions (107 lines).

I selected all 107 lines with the most restricted expression pattern for further behavioral analysis. In these experiments, I increased the sampling per line to at least four repeats and quantified the results by counting flies on both sides of the T-maze. Experimental parameters remained the same as in the primary screen. All GAL4 lines were crossed to UAS-*shibire*^{ts1} and then tested under

fed conditions for CO_2 and under starved conditions for vinegar and CO_2 plus vinegar related behavior in a T-maze. The distribution of flies was quantified after each test and the resulting performance index (PI) was put into relationship to that of the respective wild type control (UAS-*shibire*^{ts1} flies crossed to *w*^{1118} flies), which was tested on the same day. Positive delta scores indicated an increase in attraction to the odor side while negative delta values resulted from an increased aversion of the odor side. The data set that was acquired in the secondary screen shows that performances were distributed over a wide range of PIs (Table 4.1 - 4.3). While some lines are confirmed to be abnormal in their behavior, others turn out to be false positive hits from the primary screen. These experiments were carried out in collaboration with Yukiko Yamada.

Future work will have to concentrate on the confirmed lines. Further characterization of their behavior in these three paradigms is a priority. Additional experiments will have to be performed to rule out that any secondary defects influence the performance in a T-maze such as motor or activity defects. These could influence the ability of the flies to successfully avoid or approach an odor. As a consequence of this, lines could show a large deviation in the respective PI without the blocked neurons actually playing a role in olfactory behavior. In addition to this behavioral analysis, an in depth anatomical analysis on positive hits should be performed. Utilizing GFP as a reporter, an analysis of expression patterns might reveal novel neuronal pathways which might play a role in these odor guided behaviors. Furthermore, an anatomical analysis of motor centers such as the thoracic ganglion will be necessary to rule out any motility defects.

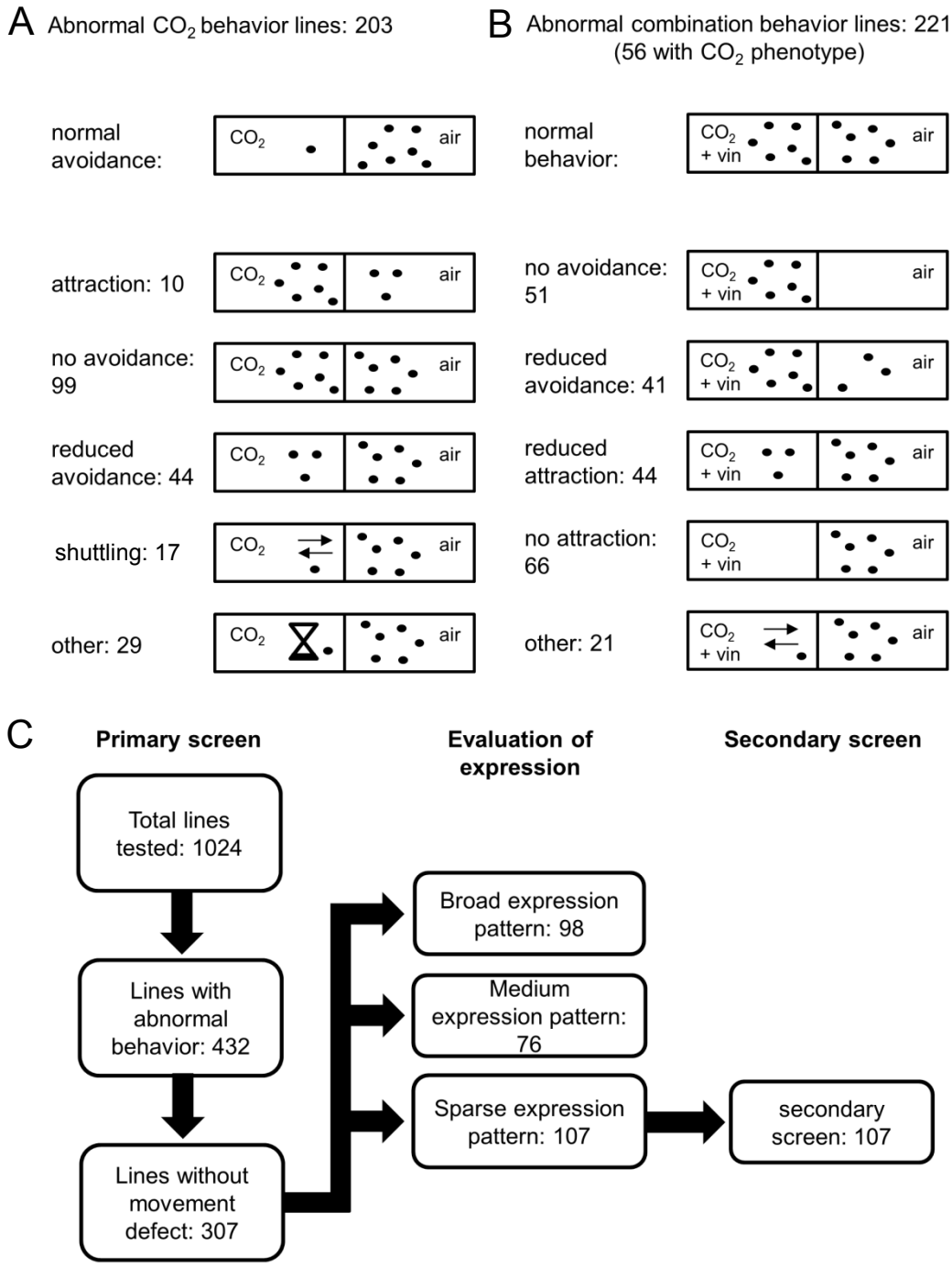

Figure 4.2: Primary screen overview

(A,B) Results obained for CO_2 avoidance behavior and CO_2 plus vinegar behavior in the primary behavioral screen. Boxes symbolize the two sites of the T-maze wich contain the indicated stimuli. Points in the boxes symbolize the distribution of flies wich can be observed for the respective phenotype. **(C)** Overview of the large behavioral screen conducted for this thesis. Numbers indicate the amount of lines with the respective phenotype after blocking random subsets of neurons and observing different behaviors.

As an example for particularly promising candidate lines, I analyzed the expression patterns of a group of lines which share a similar locus of insertion. These are NP1159, NP1171 and NP6336. All of these lines have their P-element inserted into the *escargot* (*esg*) locus. *esg* encodes a transcription factor and recent work has implicated a role in the development of the CO_2 circuitry (Hartl et al. 2011). In particular, it has been shown that its expression is regulated by mir-279 and the absence of this micro-RNA causes an abnormal development of the CO_2 sensory system in *Drosophila*. Thus, the neurons that express these GAL4 constructs might hold a special connection to the CO_2 circuit. Indeed, these lines showed a phenotype in the secondary screen when tested for CO_2 or CO_2 plus vinegar behavior. Their expression patterns were analyzed through confocal microscopy of anti-GFP immunostained fly brains (Figure 4.3). These expression patterns consistently cover a particular neuron type. It innervates the AL and projects dorsally into the ipsilateral protocerebrum area which is located posterior to the vertical lobe of the MB. Several neurons of this type exist in both brain hemispheres and their cell bodies are located lateral to the AL. Reconstructing the processes of both clusters reveals a neuronal anatomy (Figure 4.3) that strongly resembles temperature sensing dTRPA1 positive neurons (Shih & Chiang 2011). Future studies analyzing these lines as well as the other hits contained in this data set might reveal novel insights into the circuitry that underlies CO_2 behavior in *Drosophila*.

Table 4.1: Secondary screen results for CO_2 avoidance behavior

Genotype	control PI-line PI
NP1530	0.86
NP0534	0.54
NP1159	0.53
NP6219	0.49
NP0187	0.47
NP1376	0.46
NP6317	0.42
NP3375	0.41
NP3518	0.41
NP0205	0.39
NP0026	0.39
NP2425	0.35
NP0778	0.34
NP2583	0.30
NP0895	0.29
NP3015	0.28
NP5167	0.27
NP1114	0.27
NP6256	0.26
NP1283	0.22
NP1530	0.22
NP0681	0.21
NP3175	0.20
NP0804	0.19
NP3460	0.15
NP5197	0.14
NP0118	0.14
NP2783	0.13
NP1376	0.10
NP6677	0.09
NP2018	0.09
NP5274	0.08
NP0697	0.07
NP3016	0.07
NP5284	0.07
NP0341	0.06
NP1214	0.06
NP2144	0.06
NP1326	0.05
NP2762	0.05
NP0174	0.05
NP0200	0.05
NP3291	0.05
NP2160	0.05
NP0132	0.04
NP2392	0.04
NP6262	0.04
NP1204	0.03
NP6680	0.03
NP7352	0.03
NP7349	0.03
NP1189	0.02
NP0784	0.02
NP6206	0.02

Genotype	control PI-line PI
NP5270	0.02
NP1245	0.02
NP2332	0.01
NP2776	0.01
NP2589	0.01
NP5269	0.01
NP2375	0.01
NP0396	0.01
NP5209	0.00
CS	0.00
NP0201	0.00
NP2510	0.00
NP3305	0.00
NP0702	0.00
NP0668	0.00
NP2288	-0.01
NP0662	-0.01
NP3337	-0.01
NP5216	-0.01
NP6336	-0.01
NP1240	-0.02
NP1337	-0.02
NP2777	-0.02
NP2075	-0.02
NP3182	-0.02
NP3040	-0.03
NP2400	-0.03
NP1121	-0.03
NP5180	-0.03
NP6235	-0.03
NP2303	-0.03
NP7060	-0.03
NP7322	-0.03
NP6678	-0.03
NP2414	-0.03
NP1258	-0.03
NP2424	-0.03
NP1171	-0.04
NP0791	-0.04
NP2291	-0.05
NP2155	-0.06
NP1613	-0.06
NP3244	-0.06
NP2009	-0.06
NP6366	-0.06
NP2178	-0.07
NP2292	-0.07
NP2146	-0.07
NP1580	-0.09
NP2535	-0.12
NP5133	-0.12
NP1212	-0.17
NP0171	-0.22
NP1106	-0.22

Performance indices (PIs) of all secondary screen lines tested for CO_2 avoidance behavior. Neurons covered by their expression patterns were blocked via Shibire^{ts1}. Numbers represent the delta PI obtained by subtracting the line PI from the respective control PI measured on the same day. ($n \geq 4$).

Table 4.2: Secondary screen results for vinegar attraction behavior

Genotype	control PI-line PI
NP6206	-0.32
NP0118	-0.28
NP0529	-0.22
NP6262	-0.22
NP6336	-0.22
NP2375	-0.19
NP6219	-0.19
NP6292	-0.17
NP3337	-0.17
NP6258	-0.14
NP5209	-0.14
NP6256	-0.14
NP1240	-0.13
NP5197	-0.12
NP7322	-0.11
NP5274	-0.11
NP0396	-0.10
NP6366	-0.10
NP0200	-0.09
NP5270	-0.09
NP2291	-0.08
NP7349	-0.08
NP0205	-0.07
NP5284	-0.06
NP7352	-0.05
NP1530	-0.05
NP2303	-0.05
NP6677	-0.04
NP5167	-0.04
NP3460	-0.03
NP2777	-0.03
NP3015	-0.03
NP3040	-0.03
NP0662	-0.02
NP1245	-0.02
NP7060	-0.02
NP2535	-0.01
NP0804	-0.01
NP2400	-0.01
NP2425	-0.01
NP2589	-0.01
NP0702	-0.01
NP0174	-0.01
NP2178	-0.01
NP0201	-0.01
NP5216	0.00
NP1337	0.00
NP1580	0.00
NP0668	0.01
NP2783	0.01
NP1106	0.01
NP2144	0.01
NP0681	0.02
NP0341	0.02
NP2288	0.02
NP2155	0.02
NP0026	0.02
NP0187	0.03
NP3182	0.03
NP1212	0.04
NP0171	0.04
NP0132	0.04
NP6680	0.04
NP0778	0.04
NP2392	0.04
NP2160	0.04
NP6317	0.05
NP3518	0.05
NP2018	0.05
NP0791	0.05
NP2510	0.06
NP6678	0.07
NP2075	0.07
NP2776	0.07
NP1283	0.07
NP2146	0.07
NP5133	0.07
NP3175	0.07
NP1171	0.08
NP1613	0.08
NP1326	0.09
NP1204	0.09
NP0784	0.09
NP5269	0.10
NP3375	0.10
NP1376	0.10
NP1159	0.11
NP1214	0.11
NP0697	0.11
NP1189	0.11
NP2009	0.11
NP1258	0.14
NP3291	0.15
NP2414	0.15
NP0534	0.15
NP1114	0.16
NP2332	0.18
NP5180	0.19
NP2583	0.19
NP2424	0.20
NP3305	0.20
NP1121	0.22
NP2292	0.23
NP3016	0.24
NP0895	0.24
NP3244	0.30

Performance indices (PIs) of all secondary screen lines tested for vinegar attraction behavior. Neurons covered by their expression patterns were blocked via Shibire^{ts1}. Numbers represent the delta PI obtained by subtracting the line PI from the respective control PI measured on the same day. ($n \geq 4$).

Table 4.3: Secondary screen results for CO_2 plus vinegar behavior

Genotype	control PI-line PI
NP2332	-0.62
NP2292	-0.60
NP5216	-0.56
NP0200	-0.52
NP6262	-0.50
NP3182	-0.37
NP7322	-0.31
NP3016	-0.30
NP6258	-0.29
NP2783	-0.26
NP6680	-0.24
NP6292	-0.19
NP6206	-0.18
NP2392	-0.17
NP3291	-0.17
NP3337	-0.15
NP0261	-0.11
NP5167	-0.07
NP5284	-0.04
NP0702	-0.04
NP6678	-0.04
NP2291	-0.04
NP6256	-0.03
NP3460	-0.02
NP5274	-0.02
NP2776	-0.01
NP1258	0.00
NP0804	0.00
NP6677	0.01
NP0697	0.01
NP1189	0.02
NP0132	0.03
NP5209	0.03
NP3518	0.03
NP1613	0.04
NP2144	0.04
NP3040	0.08
NP1214	0.08
NP5270	0.11
NP3175	0.11
NP0778	0.12
NP6292	0.12
NP5133	0.12
NP2018	0.14
NP1212	0.14
NP0171	0.15
NP3040	0.15
NP1376	0.15
NP3375	0.16
NP1283	0.17
NP2303	0.19
NP5180	0.20
NP2583	0.22

Genotype	control PI-line PI
NP5197	0.22
NP2400	0.22
NP2160	0.22
NP2535	0.24
NP3244	0.24
NP0791	0.25
NP1530	0.25
NP0534	0.26
NP0681	0.27
NP6336	0.28
NP2009	0.28
NP0026	0.29
NP1337	0.29
NP2510	0.29
NP1204	0.30
NP7349	0.31
NP1159	0.31
NP6219	0.33
NP0341	0.33
NP0205	0.34
NP1171	0.35
NP0187	0.35
NP1114	0.35
NP1106	0.36
NP0174	0.36
NP2589	0.36
NP2762	0.37
NP3015	0.38
NP7352	0.40
NP5269	0.40
NP1121	0.41
NP2375	0.41
NP2424	0.41
NP7060	0.42
NP0895	0.42
NP0662	0.42
NP2414	0.43
NP2425	0.43
NP3305	0.44
NP1245	0.44
NP6317	0.45
NP0784	0.47
NP2146	0.47
NP2075	0.48
NP2777	0.49
NP0668	0.49
NP0118	0.50
NP1326	0.51
NP2155	0.52
NP1240	0.54
NP2288	0.57
NP0396	0.60
NP1580	0.62

Performance indices (PIs) of all secondary screen lines tested for CO_2 plus vinegar behavior. Neurons covered by their expression patterns were blocked via Shibire^{ts1}. Numbers represent the delta PI obtained by subtracting the line PI from the respective control PI measured on the same day. ($n \geq 4$).

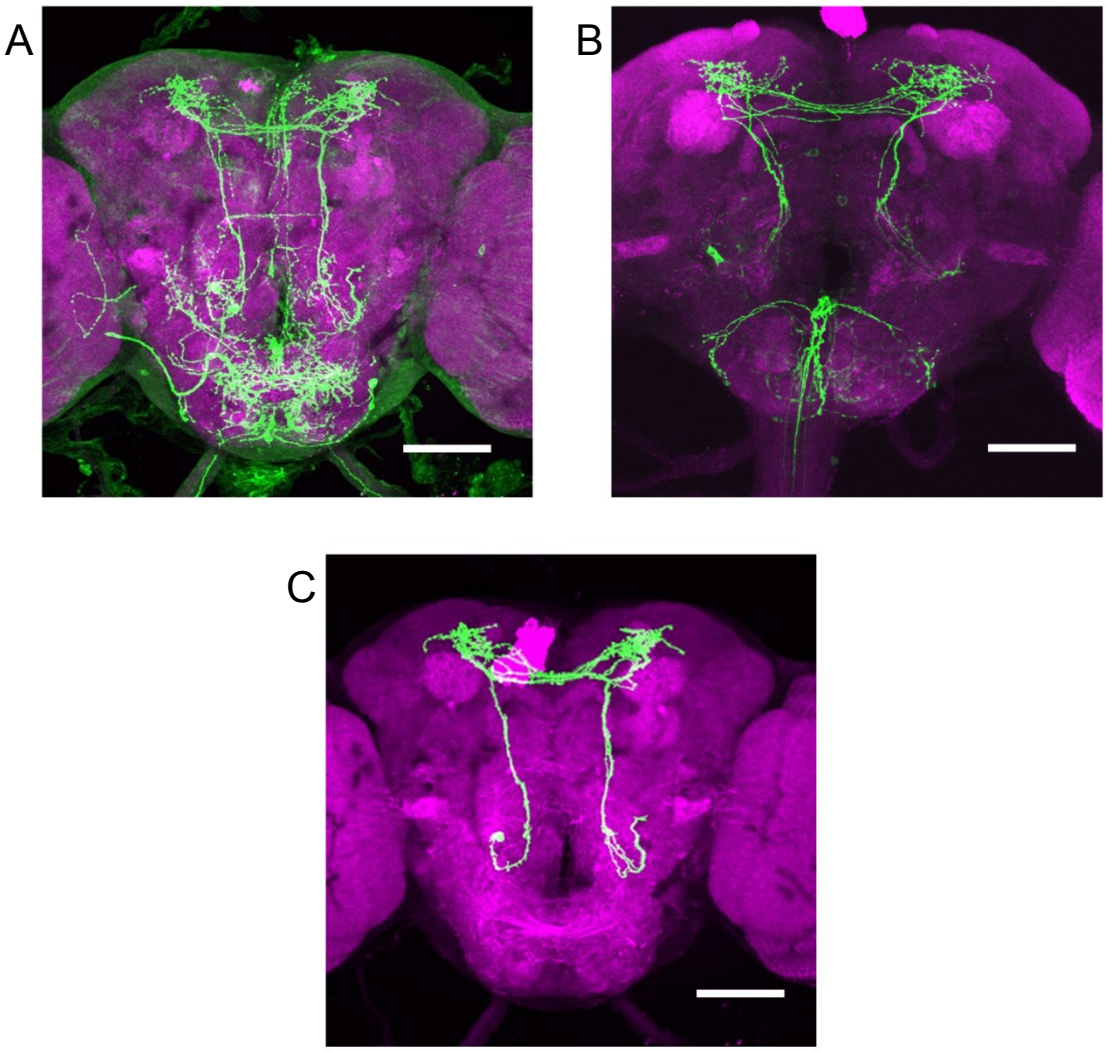

Figure 4.3: Expression pattern of two candidate lines

(A) Expression pattern of NP1159-GAL4 visualized by anti mCD8-GFP immunostaining. The neuropil was labeled by anti-discs large immunostaining. **(B)** Expression pattern of NP1171-GAL4 visualized by anti mCD8-GFP immunostaining. The neuropile was labelled by anti-discs large immunostaining. **(C)** Reconstruction of candidate neurons covered by NP1159-GAL4. The reconstruction is based on the staining seen in (A) using the simple neurite tracer plugin for Image J. Scale bars represent 50μm.

4.2 The mushroom body is essential for CO_2 avoidance behavior

In addition to the large scale screen described above, I tested a selection of candidate lines with known expression patterns that cover different parts of the MB. This higher brain center receives olfactory input via projection neurons, as well as a multitude of other inputs via extrinsic neurons from other brain areas. The role it plays in olfactory learning and memory in the fly is well documented and thus the MB is also a suitable candidate site for modifying innate olfactory behaviors such as CO_2 avoidance.

I thus investigated this possibility by transiently blocking the output of all Kenyon cells (KCs) or KC subsets and measuring the impact on CO_2 behavior. Similarly to the large scale screen described above, I utilized expression of Shibire^{ts} to impair synaptic transmission upon shifting the animals to 32°C. Preparatory experiments showed that differences in the genetic background and differences between generations of the same genotype lead to variances in starvation resistance (Figure 4.4). As a consequence of this observation, I always used flies of the same genotype and generation as controls. These control flies were tested at permissive temperature (25°C) and the resulting PI was used as a reference for the behavior of flies tested at restrictive temperature.

For manipulation of the MB, I chose to utilize two split-GAL4 lines as well as four GAL4 lines that were used in previous studies revolving around characterization of the MB (Aso et al. 2009; Jenett et al. 2012). The split-GAL4 lines were generously provided by Gerald Rubin and Yoshinori Aso, who engineered and characterized them.

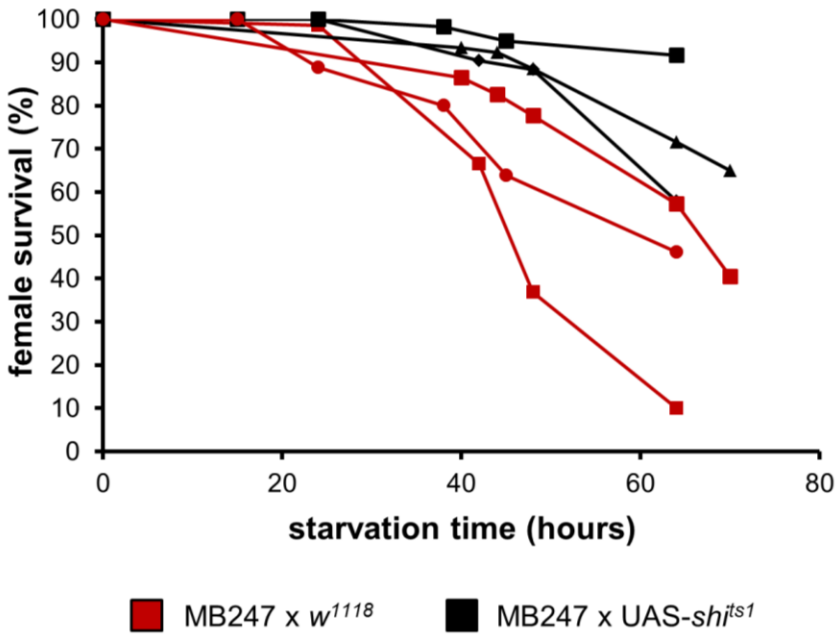

Figure 4.4: Starvation resistances vary greatly between genotypes and between different generations of the same genotype

Each curve represents the survival rate of females from one cross of the respective genotype. Flies were kept on 1% agarose without nutrition. Red curves, MB247-GAL4 x w^{1118}; black curves MB247-GAL4 x UAS-shi^{ts1}. (n=4). Figure adapted from Bräcker et al. 2013 with permission.

Blocking the MB in fed flies did not result in any behavioral change compared to control flies (Figure 4.5). Starved flies however showed a significant impairment in CO_2 avoidance upon blocking all KCs via MB010B or only α'/β' KCs via MB186B. Blocking the α/β subset of KCs via R67B04 did not result in a reduction of avoidance, neither in fed or in starved flies. The result that MB function is required for innate CO_2 avoidance in a starvation-dependent manner was surprising, since previous studies implicated the MBs function mainly in learning and memory but not innate olfactory behavior. In addition to these driver lines, I employed three lines that have been described in previous MB related studies: OK107-GAL4 which covers all KCs, MB247-GAL4 which covers α/β and γ and D52H-GAL4 which also covers α/β and γ (Aso et al.

2009). The results obtained from these lines corroborate the previous experiment. I observed a strong impairment of CO_2 avoidance when all KCs were blocked in starved flies via OK107-GAL4, while blocking KC subsets α/β and γ via MB247-GAL4 and D52H-GAL4 did not show any effect (Figure 4.5).

To test whether this dependency on the MB translates to the processing of other odors, I again utilized 3-octanol as a substitute for CO_2. Blocking KC output did not influence the ability to avoid 3-octanol after prolonged starvation consistently when comparing all tested lines (Figure 4.6). This result is surprising and indicates that the recruitment of the MB under starved conditions might be a feature that is specific to CO_2 related odor processing.

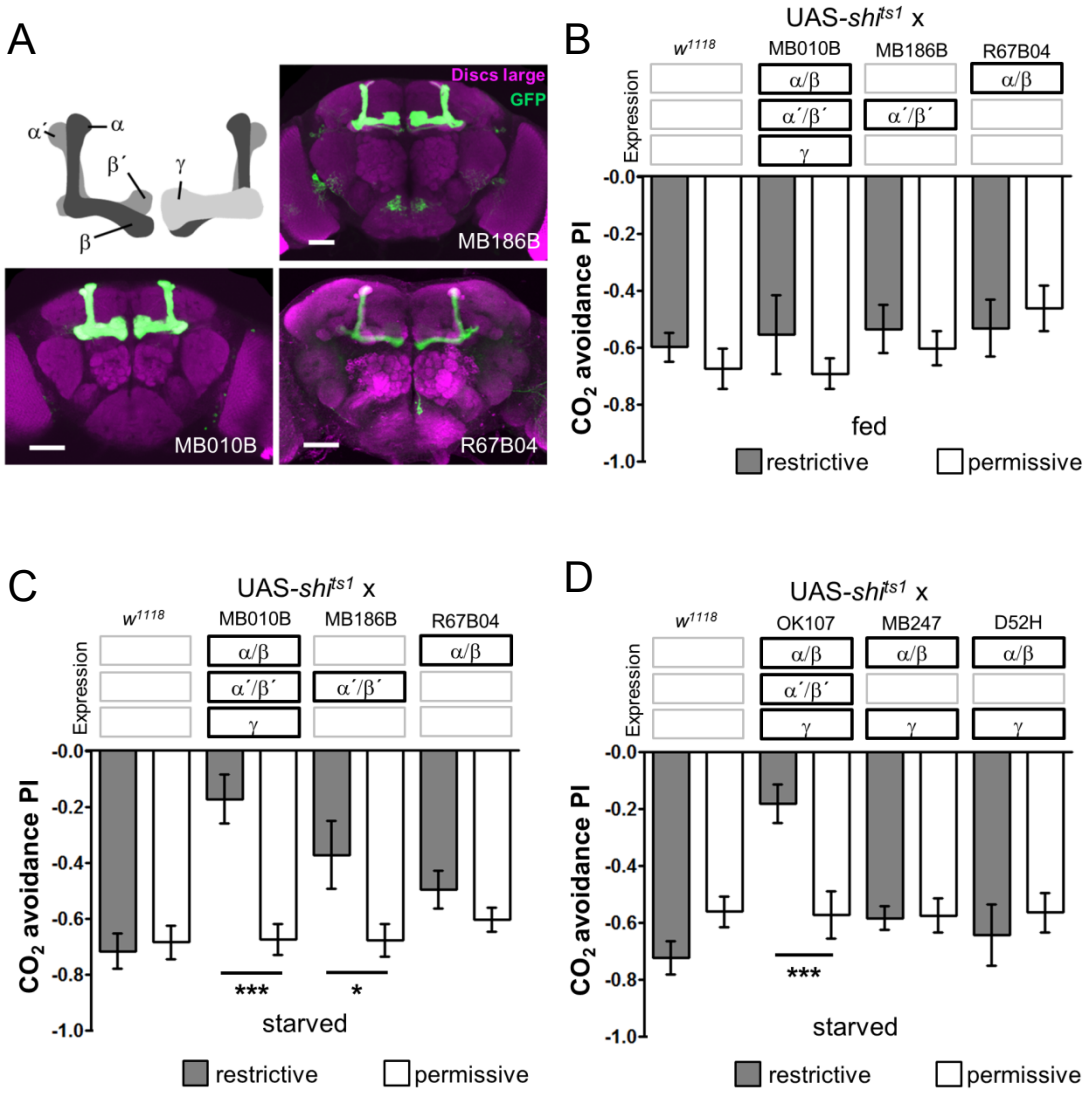

Figure 4.5: CO_2 avoidance requires the mushroom body when flies are starved

(A) Expression patterns of three different GAL4 drivers lines that were used in this study but have not been described in detail before. Each line targets different subsets of Kenyon cells (KC): MB010B is expressed in all KCs, MB186B is expressed in the α'/β' subset and R67B04 is expressed in the α/β subset. Expression patterns were visualized by mCD8-GFP expression as well as anti-GFP and anti-discs large immunostaining. Scale bars represent 50 μm. **(B-D)** CO_2 avoidance of flies that carried different GAL4 drivers as well as UAS-*shi*^{ts1}. OK107 is expressed in all KCs and MB247 and D52H are expressed in the α/β and γ subset. Mushroom body output was blocked by shifting flies to 32°C (restrictive) and CO_2 avoidance was compared to the behavior of flies tested at 25°C (permissive). Animals were either starved 42 hours prior to experiments (starved) or kept on food (fed). Error bars represent SEM (n = 8 or 9). *p < 0.05, ***p < 0.001 (ANOVA, Bonferroni's multiple comparison test). Figure adapted from Bräcker et al. 2013 with permission.

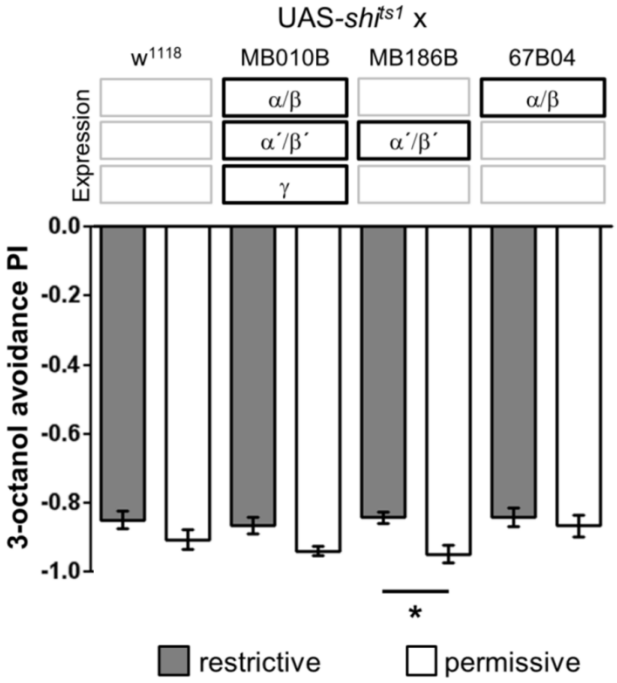

Figure 4.6: Blocking the mushroom body does not impair 3-octanol avoidance

3-octanol avoidance of three different MB specific driver lines crossed to UAS-*shi*^{ts1}. Mushroom body output was blocked by shifting flies to 32°C (restrictive) and comparing the behavior to that of flies tested at 25°C (permissive). Flies were starved for 42 hours prior to the experiment. Error bars indicate s.e.m. (*n*=8). * p<0.05 (ANOVA, Bonferroni's multiple comparison test). Figure adapted from Bräcker et al. 2013 with permission.

Starvation affects an animal in multiple ways and triggers physiological and behavioral changes. Since these changes are based on the length of starvation time and thus gradual, I tested two additional starvation regimes: 12 and 24 hours of starvation. Blocking all KCs via MB010B directed expression of Shibire^{ts1} did not affect behavior after 12 hours of starvation (Figure 4.7). 24 hours of starvation treatment caused the same genotype to display a significantly reduced CO_2 avoidance. Thus two circuits which are necessary

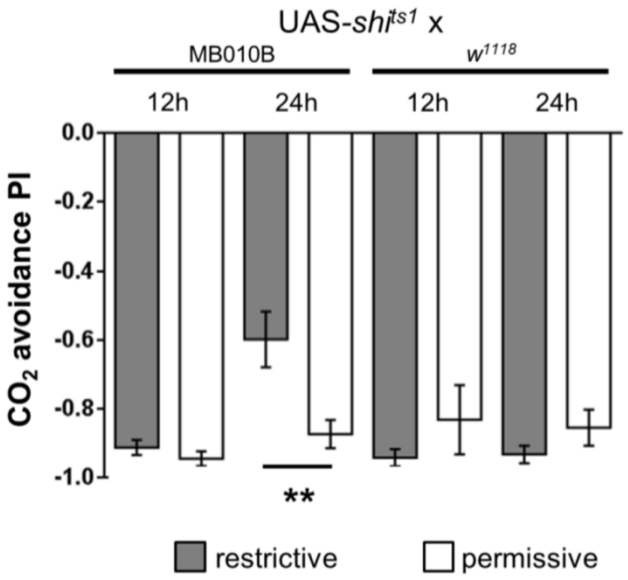

Figure 4.7: The role of the mushroom body in CO_2 avoidance depends on starvation time

CO_2 avoidance of flies expressing UAS-*shi*^{ts1} under control of a GAL4 driver which covers all Kenyon cell subsets. Flies were either starved 12 hours (12h) or 24 hours (24h) before the experiments. CO_2 avoidance is impaired after 24 hours of starvation but not after 12. Error bars indicate s.e.m. (*n*=9). **p<0.005 (ANOVA, Bonferroni's multiple comparison test). Figure adapted from Bräcker et al. 2013 with permission.

for CO_2 avoidance behavior exist in the fly brain: one MB independent pathway that is utilized under fed conditions and one MB dependent pathway that is utilized under starved conditions. The switch between both depends on starvation time and is thus gradual with a partial redundancy.

Behavioral performance is influenced by a multitude of factors. Thus, effects caused by the genetic background can lead to a false interpretation of data. Such effects arise from P-element insertion into the locus of genes which are necessary for behavior or general healthiness of the flies. I conducted an experiment in which the driver lines MB010B and MB186B were crossed with flies of the *w*^{1118} background. The offspring of these crosses showed a normal

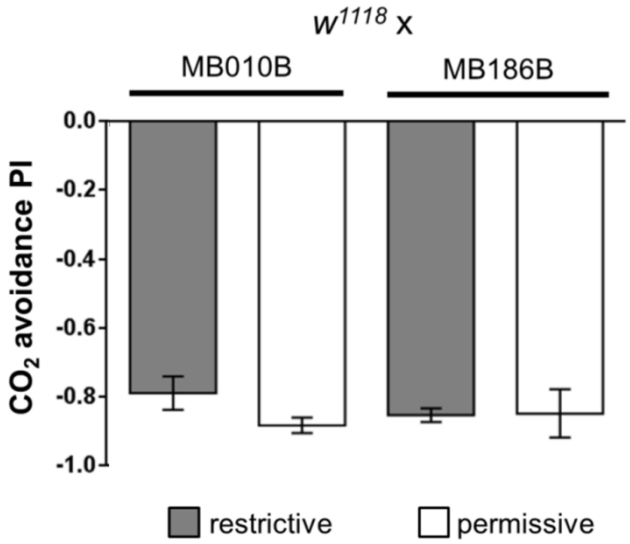

Figure 4.8: CO_2 avoidance is not influenced by genetic background

CO_2 avoidance of control flies that carried the respective GAL4 construct in a w^{1118} background. Flies were tested after 42 hours of starvation. Error bars indicate s.e.m. (*n*=8). (ANOVA, Bonferroni's multiple comparison test). Figure adapted from Bräcker et al. 2013 with permission.

CO_2 avoidance when tested after 42 hours of starvation (Figure 4.8). Together with the results from offspring of the effector line crossed to w^{1118} background, there is no evidence for an influence of genetic background on CO_2 avoidance.

Based on the observation that the modification of CO_2 aversion in the context of vinegar odor also requires a period of food deprivation, I asked whether the aforementioned MB dependent CO_2 processing pathway is also the substrate for integrating these two stimuli. I thus blocked the MB in fed and starved flies and quantified their reaction to a combination of CO_2 plus vinegar tested versus air. Blocking the MB had no impact on the behavior of starved flies which overcame CO_2 avoidance to the same degree as control flies which were tested at permissive temperature (Figure 4.9). However, fed flies with

impaired MB output showed a significantly increased PI compared to the respective control group (Figure 4.9). In this experiment, blocking the MB increased the PI of fed flies to the level of starved flies, making the behaviors of both groups statistically indistinguishable. This result demonstrates that the MB dependent aversive CO_2 signal is not only necessary for a normal behavior in the context of starvation but also in the context of food odor. The MB dependent pathway is thus integrating at least two context related stimuli with the aversive CO_2 signal. Furthermore, it is interesting to note that not only starvation is able to change necessity of the two CO_2 pathways but also the presence of a food odor.

Since blocking the MB could also influence vinegar behavior and thus present a different explanation for the aforementioned results, I conducted the same experiment without CO_2. However, none of the treatments had a significant impact on vinegar attraction compared to the respective control (Figure 4.9).

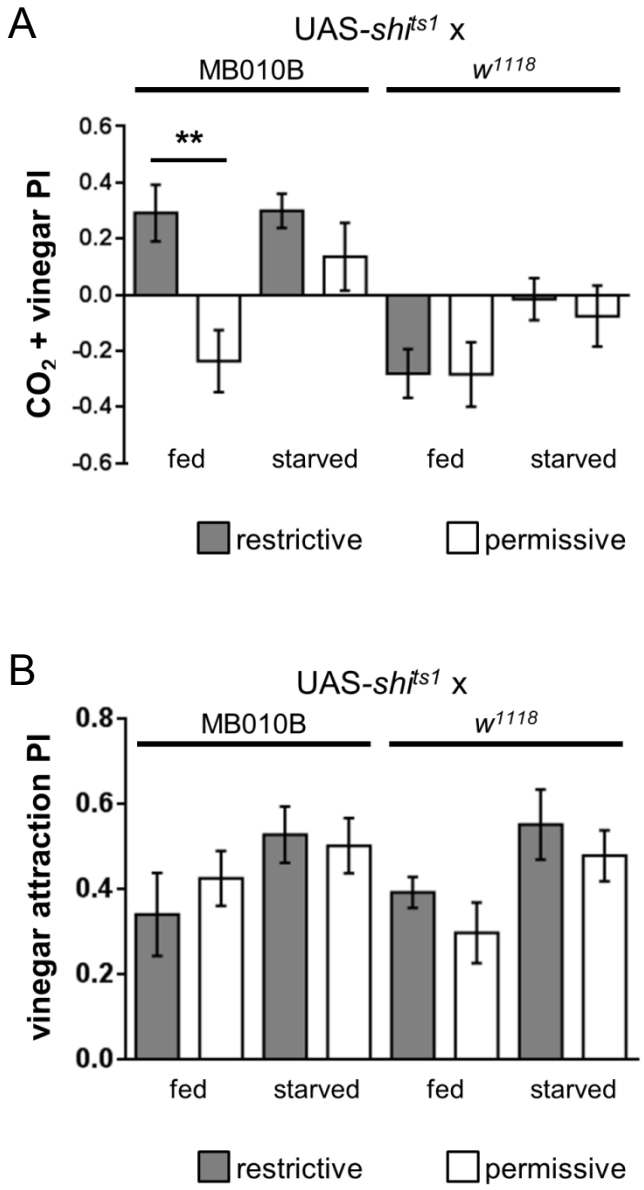

Figure 4.9: The presence of vinegar changes mushroom body dependent processing of CO_2 avoidance

(A) Behavioral reaction to a combination of vinegar and CO_2 tested versus air. Flies expressed UAS-*shi*^{ts1} under control of a GAL4 driver that covers all KC subsets. Animals were either starved 42 hours prior to experiments (starved) or kept on food (fed). Blocking the mushroom body in fed flies altered behavior. Error bars represent SEM (n = 8). **p < 0.005 (ANOVA, Bonferroni's multiple comparison test). **(B)** Vinegar attraction of flies that expressed UAS-*shi*^{ts1} under control of a GAL4 driver which covers all KC subsets. Flies were either starved 42 hr prior to experiments (starved) or kept on food (fed). Error bars indicate s.e.m. (*n*=8). No significant difference was detected (ANOVA, Bonferroni's multiple comparison test). Figure adapted from Bräcker et al. 2013 with permission.

4.3 Imaging the mushroom body after CO_2 stimulation

In my behavioral analysis, I showed that CO_2 processing is MB dependent in the presence of additional external and internal signals. To further collect evidence that the MB itself receives the CO_2 signal, imaging experiments were performed in collaboration with Siju K. Purayil. To visualize Ca^{2+} influx into KCs, the effector GCaMP5.0 (Akerboom et al. 2012) was expressed via different driver lines. Ca^{2+} influx serves as a proxy for firing of neurons, since it is triggered before release of synaptic vesicles at the chemical synapse. Upon binding of calcium, GCaMP5.0 increases its baseline fluorescent intensity and serves as a read out for cellular calcium levels. A suitable preparation gives light microscopic access to the brain while leaving most of the head and its olfactory appendages intact. With this technique, in vivo imaging of the MB reaction to olfactory stimulation is possible. Using this method, imaging of the MB after stimulation with different concentrations of CO_2 was performed. CO_2 was presented to the fly using a custom made odor stimulation set up. The same driver lines as in the behavioral experiments were utilized to distinguish between KC subsets: MB010B to image from the whole MB and MB186B to specifically address α'/β' lobes. In addition to these lines, MB247- and D52H-GAL4 were tested. Stimulating flies causes significant increases of fluorescence levels in the MB (Figure 4.10). Fluorescent signals increased with increased concentrations of CO_2 as it is expected from an odor signal.

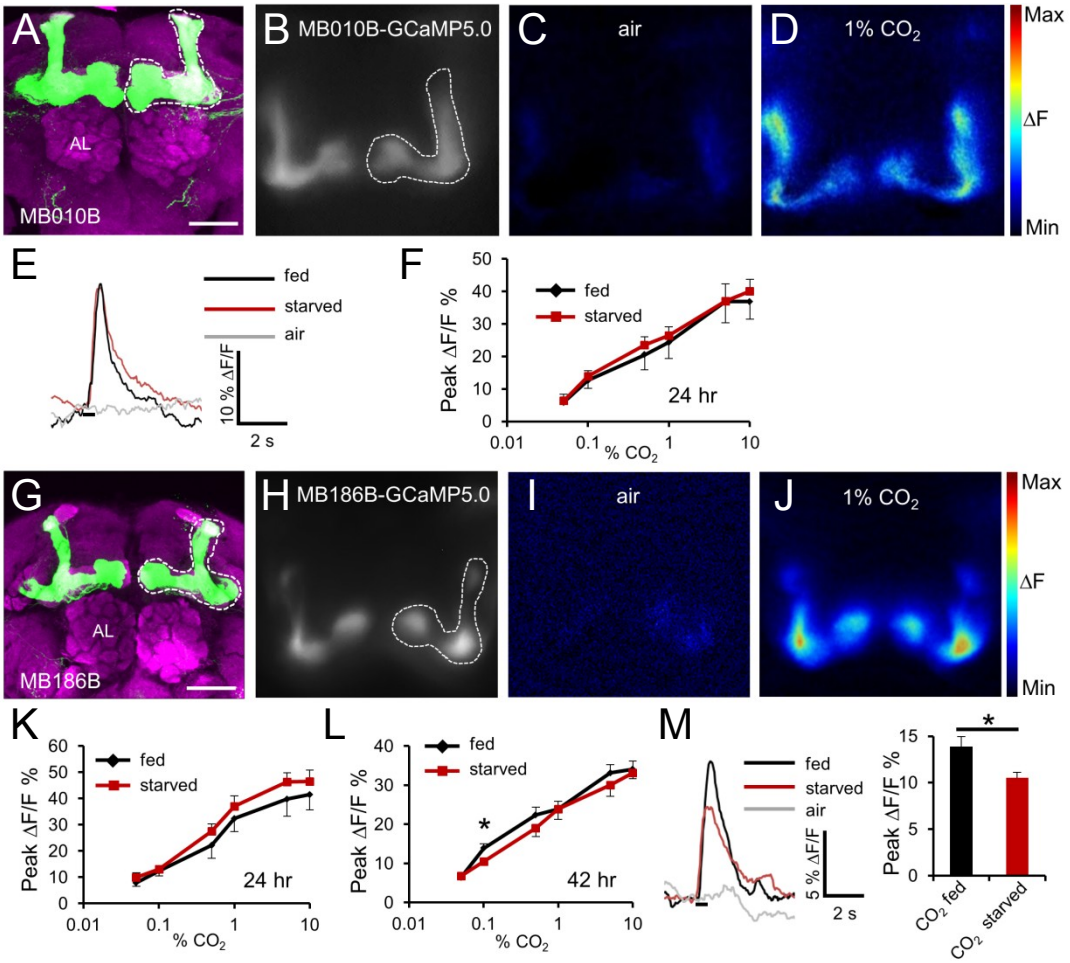

Figure 4.10: CO_2 activates the mushroom body

(A) Confocal image showing the expression pattern of MB010B-GAL4, visualized by anti-GFP (green) and anti-discs large (magenta) immunostaining. **(B)** Grayscale image showing a dorsal view of the mushroom body lobes in vivo. The region of interest for the fluorescence intensity measurement is marked with dotted lines. **(C and D)** Representative pseudo color images, showing the response to air and 1% CO_2, respectively. **(E)** Averaged time course of fluorescence intensity change plotted for stimulation with air or 1% CO_2 (fed and starved). The black bar indicates stimulus delivery. **(F)** Peak fluorescence intensity after stimulation with CO_2. **(G)** Confocal image showing the expression pattern of MB186B-GAL4, visualized by anti-GFP and anti-discs large immunostaining. **(H)** Grayscale image showing a dorsal view of the mushroom body lobes in vivo. The region of interest for the fluorescence intensity measurement is marked with dotted lines. **(I and J)** Representative pseudo color images, showing the response to air and 1% CO_2, respectively. **(K and L)** Peak fluorescence intensity after stimulation with CO_2 for 24 and 42 hours starved and fed flies. **(M)** Averaged time course of fluorescence intensity change plotted for stimulation with air or 0.1% CO_2 (fed and starved). The black bar indicates stimulus delivery. Peak fluorescence intensity after stimulation with 0.1% CO_2 for 42 hours starved and fed flies is also shown. AL, antennal lobe. Error bars represent s.e.m. (n = 5 in F; n = 8 in K; n = 8 in L and M). *p < 0.05, (Unpaired t test). Scale bars represent 50 μm. Figure adapted from Bräcker et al. 2013 with permission.

Imaging exclusively from α'/β' lobes revealed a slight tendency for signals from starved flies to be lower than the respective signals from fed animals. A significant difference between the two fluorescent intensity levels was found at 0.1% CO_2. The same concentration was used for behavioral experiments. Comparing the fluorescent signals of starved and fed flies did not yield any significant differences in MB010B. An increase of fluorescence intensity level after CO_2 stimulation was also observable across α/β and γ subsets utilizing MB247-GAL4 and D52H-GAL4. However, signal levels obtained from α'/β' KCs were larger in intensity then those measured from α/β and γ KCs combined (Figure 4.11).Taken together, these results show that KCs fire upon receiving CO_2 input, as it would be expected for a population of neurons that integrate CO_2 signals into a broader context.

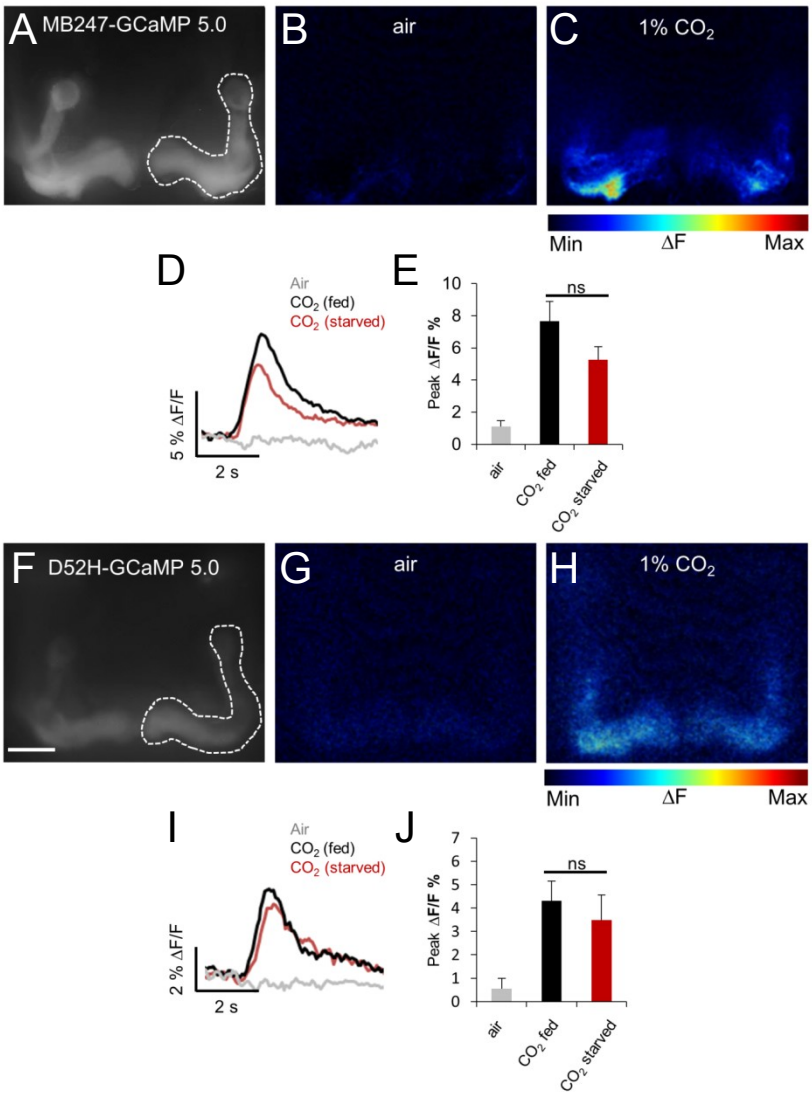

Figure 4.11: CO_2 activates α/β and γ Kenyon cells

(A) Grayscale image showing the dorsal *in vivo* view of the mushroom body lobes expressing GCaMP5.0 under the control of MB247-GAL4. **(B and C)** Representative pseudo color images showing the response to air and CO_2, respectively. **(D)** Averaged time course of fluorescence intensity change plotted for stimulation with air or CO_2 (fed and starved). **(E)** Peak fluorescence intensity after stimulation with air or CO_2. **(F)** Grayscale image showing the dorsal *in vivo* view of the mushroom body lobes expressing GCaMP5.0 under the control of D52H-GAL4. **(G and H)** Representative pseudo color images showing the response to air and CO_2, respectively. **(I)** Averaged time course of fluorescence intensity change plotted for stimulation with air or CO_2 (fed and starved). **(J)** Peak fluorescence intensity after stimulation with air or CO_2. Error bars indicate s.e.m. (*n*=8). ns, non-significant (Unpaired t test). Scale bars = 25 µm. Figure adapted from Bräcker et al. 2013 with permission.

4.4 A novel CO_2 projection neuron

Previously described neuronal pathways cannot explain how the CO_2 sensory signal reaches the MB. All sensory information from CO_2 receptor neurons arrives in the V-glomerulus of the AL, where it is presumably picked up by PNs. Only one PN has been described previously, which connects the V-glomerulus to the LH (Sachse et al. 2007).

To search for possible PNs that connect the V-glomerulus to the MB, the photoactivatable GFP (PA-GFP) method was employed (Patterson & Lippincott-Schwartz 2002). This technique allows for an unbiased discovery of novel neuronal pathways, since it does not rely on restrictive expression patterns, which would rule out any neurons not covered in a particular driver line (Datta et al. 2008). This method utilizes an engineered form of GFP, which increases its baseline fluorescence permanently after light stimulation with a specific wave length. Such stimulation can be directed to any areal of interest within the fly brain via two-photon laser scanning microscopy. After all PA-GFP in the stimulated area has been converted to its higher fluorescent state, it is allowed to diffuse within the respective cells. This causes it to label processes as well as cell bodies of all neurons that innervate the stimulated site. To discover novel pathways that transfer CO_2 information to higher brain centers, this method was used to label neurons innervating the V-glomerulus. These experiments were carried out in collaboration with Nélia Varela, in the lab of Maria Luísa Vasconcelos.

Stimulation of the V-glomerulus was performed on flies that expressed PA-GFP via the GAL4/UAS system in all neurons using the Nsyb-GAL4 driver line. Converting PA-GFP in the region of the V-glomerulus labeled a number

of neurons including LNs. In addition to these, four PN processes per brain hemisphere were consistently labeled (Figure 4.12). Two of these innervated only the LH. The other two processes bifurcated and innervated both the MB and LH. These processes thus might belong to a novel class of CO_2 PN.

A search based on the anatomy of these processes led to the identification of R53A05-GAL4 (biVPN-GAL4) in the FlyLight expression pattern database (http://flweb.janelia.org/cgi-bin/flew.cgi) (Jenett et al. 2012). This GAL4 driver line covers the novel CO_2 PN. To elucidate the anatomy of these neurons in detail, flippase based recombination clones were generated from the biVPN-GAL4 driver line (Bohm et al. 2010). This technique allows for a more detailed analysis of expression patterns, since random recombination events restrict the number of GAL4 expressing cells. These experiments were carried out in collaboration with Siju K. Purayil. Clonal analysis allowed for a subsequent reconstruction of the novel CO_2 PN, which was named biVPN. One biVPN per brain hemisphere has its cell body located in the SOG and then extends a process into the V-glomeruli of the ipsi- and contralateral AL (Figure 4.12). From each AL one axon is projected dorsally which then bifurcates to innervate the LH and the MB calyx of the respective ipsilateral brain hemisphere. Each biVPN extends one additional neurite exclusively in the respective ipsilateral AL.

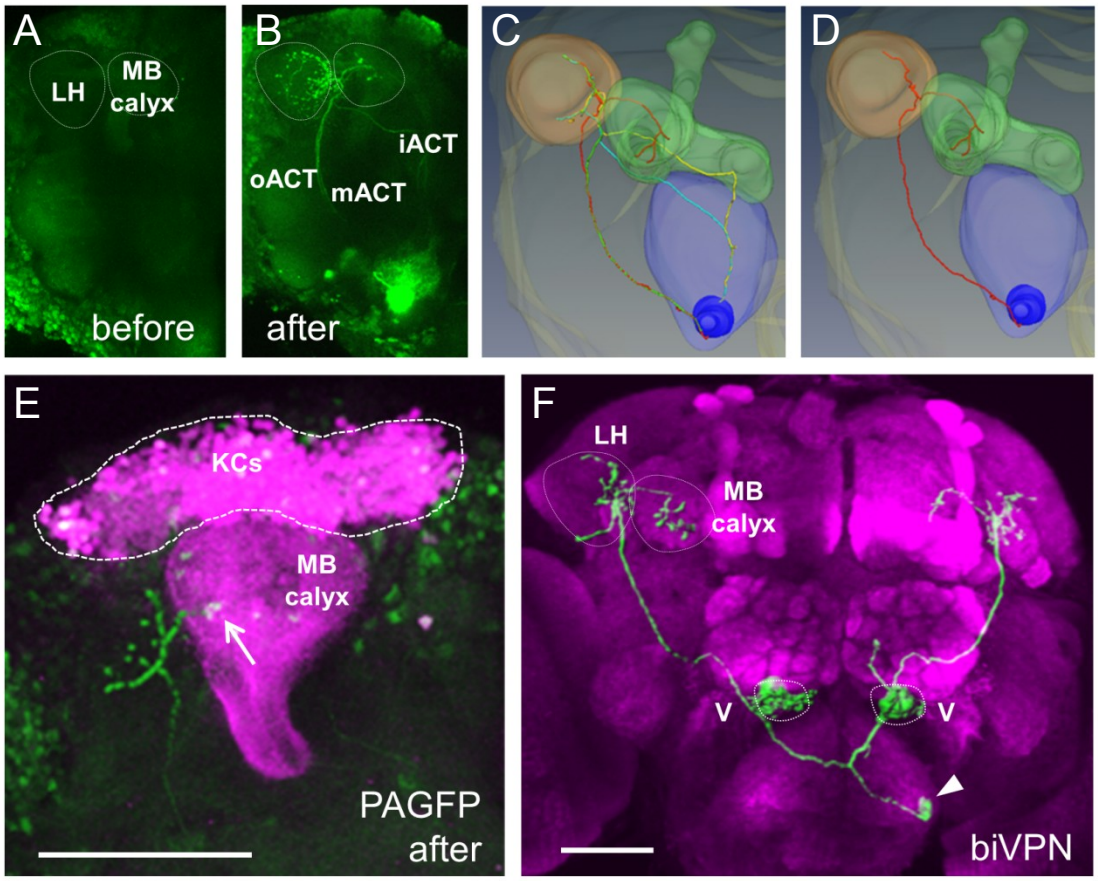

Figure 4.12: A novel CO_2 projection neuron type

(A,B) Z projections of two-photon laser scanning microscope imaging of a live *Drosophila* brain expressing UAS-C3PA-GFP under the control of the Nsyb-GAL4 driver before (A) and after (B) fluorophore photoconversion. Analysis reveals four projections connecting the V-glomerulus to higher brain centers. Two of these projections arborize in the lateral horn (LH), and the remaining two arborize both in the LH and the mushroom body (MB) calyx. **(C,D)** Amira three-dimensional reconstruction of the *Drosophila* fly brain shown in (B). All PNs (C) or only the PN that innervates both the LH and the MB calyx (D) are shown. Note: the shape of arborization within the LH may not be accurate in (D). **(E)** Detailed view of PN arborization pattern in the MB calyx (arrow). (F) Three-dimensional reconstruction of the biVPN (green), obtained from a heat shock Flp clone superimposed on the brain neuropil stained with anti-discs large (magenta). Arrowhead points to cell body locations. LH, lateral horn; MB, mushroom body; iACT, inner antennocerebral tract; mACT, medial antennocerebral tract; oACT, outer antennocerebral tract; V, V-glomerulus. Scale bars represent 50 μm. Figure adapted from Bräcker et al. 2013 with permission.

Imaging experiments were carried out to demonstrate that the biVPN is indeed a VPN and responds to CO_2 stimulation. These experiments were performed in collaboration with Siju K. Purayil. A modified in vivo preparation was utilized, by which the cell bodies of the biVPN and the V-glomerulus could be accessed for imaging through a ventral window in the anterior side of the head. Experimental flies expressed the Ca^{2+} sensor GCaMP5.0 under control of the biVPN-GAL4. Stimulating these flies with CO_2 evoked a fluorescent signal both in the biVPN cell bodies as well as in the V-glomerulus (Figure 4.13). This signal increased with increasing concentrations of CO_2.

Comparing imaging data from fed and starved animals did not indicate any differences in fluorescent intensity levels when imaging from the biVPN cell bodies. On the level of the V-glomerulus, signals from starved animals showed a trend to be smaller than those obtained from fed animals. However, this trend did not lead to a significant difference in signal intensities between both groups. Part of this can be attributed to properties of this specific preparation because it is difficult to obtain the same imaging focus on the level of the AL across animals. Interestingly, the observed trend in signal levels was similar to that observed for MB imaging: In both cases starvation lowered the response signal to CO_2 stimulation.

Finally, to show the relevance of the biVPN in CO_2 behavior, I silenced these neurons via the biVPN-GAL4 driver and the effector line UAS-*shibire*^{ts1}. I tested fed and starved flies for their CO_2 avoidance behavior in the T-maze assay. Blocking these neurons in fed flies did not impair CO_2 behavior (Figure 4.14). However, repeating the experiment with flies that were starved for 24 or 42 hours resulted in a complete abolishment of CO_2 avoidance.

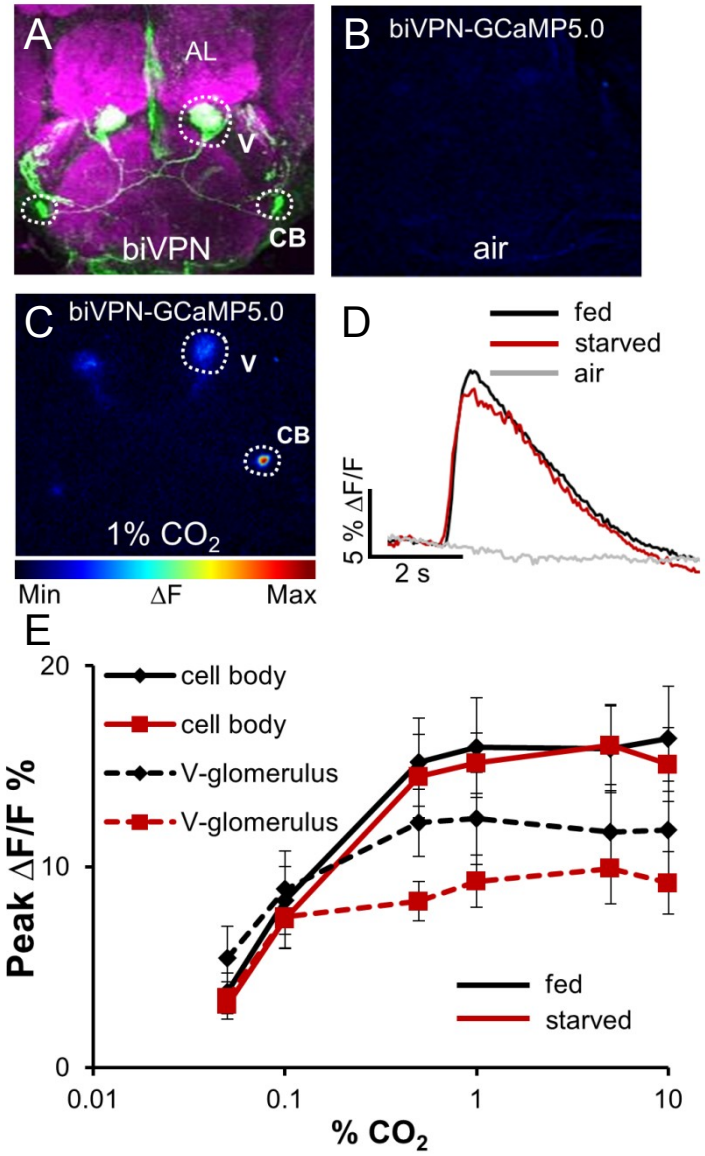

Figure 4.13: biVPN neurons respond to CO_2

(A) Confocal image of a heat shock Flp clone of biVPN-GAL4, showing the biVPNs with anti-GFP (green) and anti-discs large (magenta) immunostaining. **(B and C)** Representative pseudo color images of in vivo preparation of biVPN-GCaMP5.0, showing the response to air and 1% CO_2, respectively. **(D)** Averaged time course of fluorescence intensity change plotted for stimulation with air or CO_2 (fed and starved) from the biVPN cell body. **(E)** Peak fluorescence intensity from the cell body and V-glomerulus after stimulation with different concentrations of CO_2. Error bars represent SEM (n = 9). $p > 0.05$ for all points. (Unpaired t test). AL, antennal lobe; CB, cell body; V, V-glomerulus. Figure adapted from Bräcker et al. 2013 with permission.

Thus, blocking neurons within the biVPN-GAL4 led to similar results as blocking the MB. In both cases, CO_2 behavior was only affected after a period starvation. The starvation time needed to switch the requirement of a circuit part from independent to dependent was different for the biVPNs compared to KCs (Figure 4.14). After 24 hours of starvation, flies with silenced KCs still showed a residual CO_2 avoidance while flies with silenced biVPNs did not show any avoidance. This result indicates that the observed switch in circuit requirements between starved and fed flies might use different mechanisms at the level of the biVPNs compared to the level of the MB.

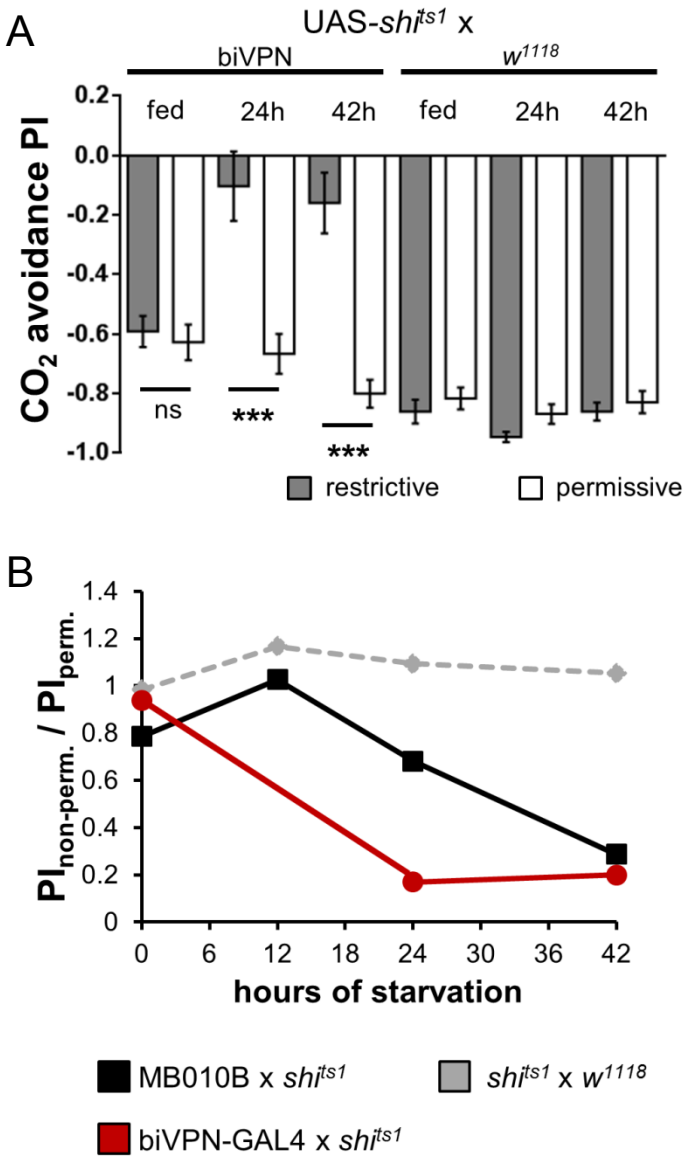

Figure 4.14: Blocking biVPN output abolishes CO_2 avoidance in starved flies

(A) CO_2 avoidance by flies that expressed UAS-*shi*^{ts1} under control of biVPN-GAL4. Animals were either starved 24 hours (24h) or 42 hours (42h) before the experiments or kept on food (fed). Error bars represent SEM (n = 9). ***p < 0.001 (ANOVA, Bonferroni's multiple comparison test). **(B)** CO_2 avoidance performance index (PI) after blocking neuronal output of all KCs (MB010B, black line) or biVPNs (biVPN-GAL4, red line). At 24 hours starvation, blocking the biVPN leads to a complete abolishment of CO_2 avoidance, while MB output-impaired flies still display a residual behavior. Figure adapted from Bräcker et al. 2013 with permission.

4.5 Dopamine and hunger signaling

Having shown that the neuronal circuit underlying CO_2 behavior is influenced by starvation, I next investigated how the starvation signal is actually integrated in the circuit. One circuit that has been implicated in starvation dependent olfactory behaviors is the dopaminergic system (Krashes et al. 2009).

To address this question, I tested the CO_2 avoidance of flies in a T-maze while blocking or activating dopaminergic neurons via TH-GAL4 driven expression of two effectors. Using two different effectors allowed me to test whether dopamine is required in an on or off state. I employed Shibire^{ts1} to block neuronal output (Kitamoto 2001). To activate neurons, I utilized the effector dTRPA1, which continuously depolarizes neurons at 32°C (Pulver, Pashkovski, Hornstein, Garrity, & Griffith 2009). Both experiments were conducted with the same protocol: Flies of each genotype were either fed or starved before the experiment and one group of flies was shifted to high temperature while another group was tested at low temperature to serve as a control.

Activating dopaminergic neurons covered by TH-GAL4 led to no effect in starved flies (Figure 4.15). In fed flies however, activation at high temperature significantly decreased CO_2 avoidance compared to control flies tested at low temperature. Consistent with this result, blocking neurons that express TH-GAL4 significantly increased avoidance in starved flies (Figure 4.15). Blocking dopaminergic neurons in fed flies had no effect. Taken together, these results show that dopamine can modify CO_2 behavior based on starvation state. An increased level of dopamine leads to a reduced avoidance in CO_2, which

resembles the starved state. Decreasing dopaminergic levels within the fly brain increased avoidance which seems to resemble the fed state. While the presented results are consistent, the genetic background within the experimental crosses might have interfered with CO_2 avoidance also in the low temperature control groups. For example, avoidance levels of fed TH-GAL4/UAS-*dTRPA1* flies at low temperature are higher than those of starved ones at low temperature. Despite this finding, neither the GAL4- nor the UAS-element alone in w^{1118} background showed abnormal CO_2 avoidance behavior under the experimental conditions (Figure 4.15). Thus, further experiments are necessary to elucidate these findings.

To complement these results, imaging experiments were carried out in collaboration with Siju K. Purayil. MB activity was imaged using MB186B as a driver to express GCaMP5.0. Before stimulating these flies with CO_2, dopamine levels in the brain were artificially increased by applying dopamine to the bath solution. Signal levels recorded this way were compared to control stimulation of the same individual carried out before dopamine application. This treatment significantly reduced fluorescent signals in fed flies but had no effect in flies that were starved before the experiment (Figure 4.16). A treatment with just saline but no dopamine did not change fluorescent signal intensity before and after treatment. This result is consistent with the findings obtained in the behavioral experiments using TH-GAL4. Increasing dopamine levels in the brain decreases the response of the MB to CO_2. This decrease lowers the response to a level found in starved flies. These results provide additional evidence that dopamine triggers a lowering of CO_2 aversion with increased starvation levels. Such a decrease might not be apparent under

natural conditions since the experiments which are presented here use methods to increase the levels of dopamine drastically. However, it might manifest as a modified CO_2 behavior which can be overcome in favor of appetitive behavior.

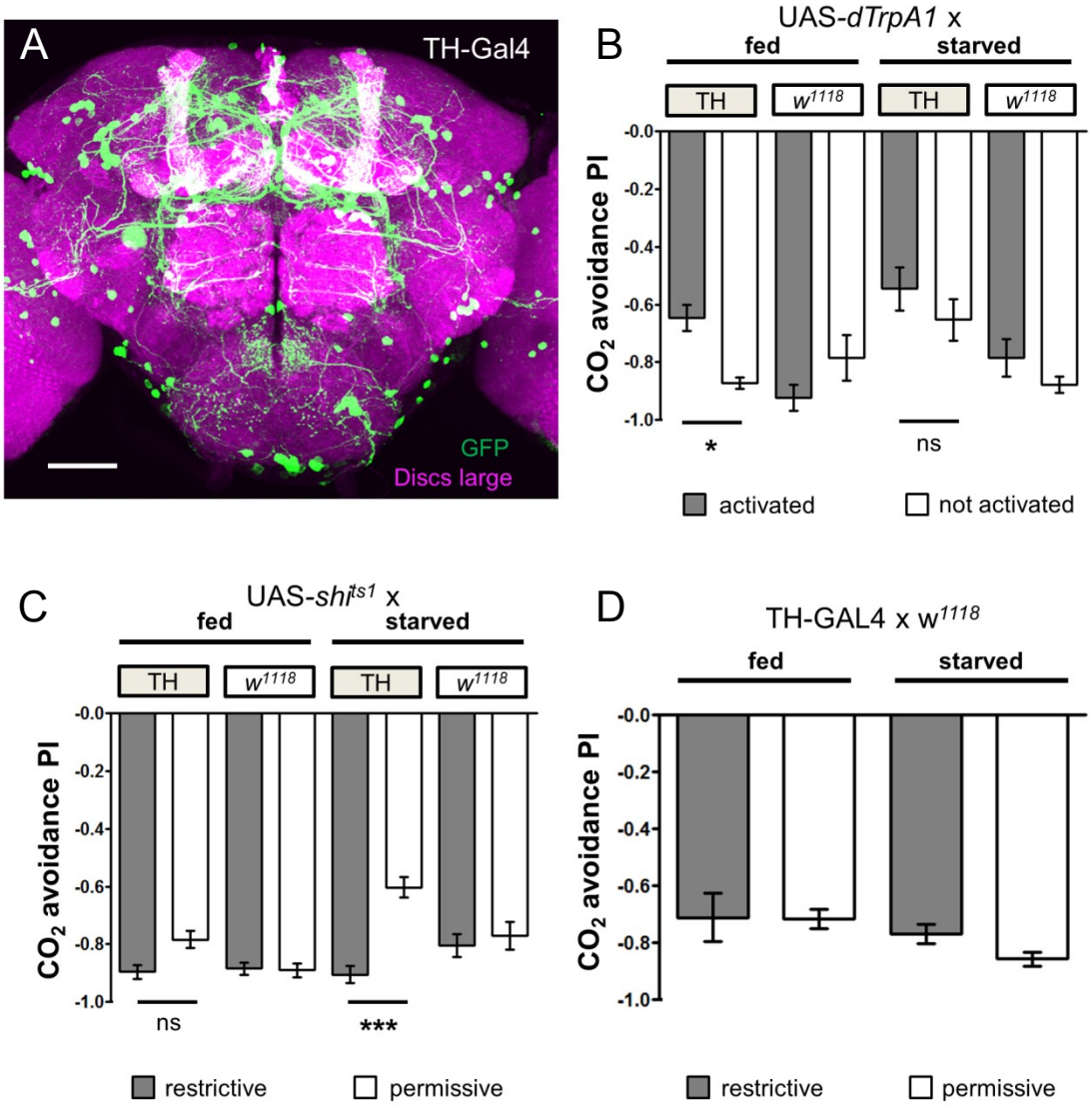

Figure 4.15: Dopamine modifies CO_2 behavior

(A) Expression pattern of TH-GAL4. Expression was visualized by UAS-*mCD8-GFP* and anti-Discs large immunostaining. **(B-C)** CO_2 avoidance of flies after activating TH-GAL4 neurons via dTRPA1 (B) or after blocking dopaminergic output of TH-GAL4 neurons via Shibire^{ts1} (C). Flies were either starved 42 hours prior to the experiment (starved) or kept on food (fed). Error bars indicate s.e.m. (n = 9). *p<0.05, ***p<0.001 (ANOVA, Bonferroni's multiple comparison test). **(D)** CO_2 avoidance of TH-GAL4/w^{1118} control flies that were either starved 42 hours prior to the experiment (starved) or kept on food (fed). The temperature shift does not influence their CO_2 avoidance. Error bars indicate s.e.m. (n = 8). (ANOVA, Bonferroni's multiple comparison test). Scale bar represents 50 μm. Figure adapted from Siju, Bräcker, & Grunwald Kadow 2014 with permission.

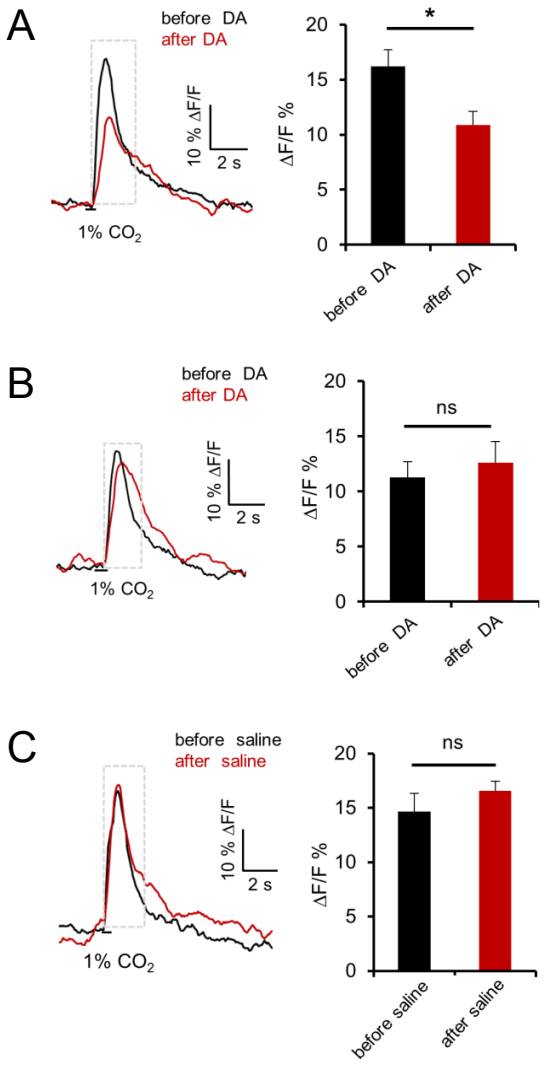

Figure 4.16: Dopamine modifies the CO_2 response of the mushroom body

(A) Averaged time course of fluorescent intensity change in α'/β' Kenyon cells of flies expressing GCaMP5.0 under control of MB186B (fed) to 1% CO_2 stimulation before and after treatment with dopamine (DA). (*n*=9). *p<0.05 (Paired t test). **(B)** Averaged time course of fluorescent intensity change in α'/β' Kenyon cells of starved flies expressing GCaMP5.0 under control of MB186B (42 hours starvation) to 1% CO_2 stimulation before and after treatment with dopamine (DA). (*n*=9). (Paired t test) **(C)** Averaged time course of fluorescent intensity change in α'/β' Kenyon cells of flies expressing GCaMP5.0 under control of MB186B (fed) to 1% CO_2 stimulation before and after treatment with imaging saline as control. (*n*=6). ns, not significant (Paired t test). Averaged peak fluorescence intensity is calculated over a time window (dotted box on the time course trace). Error bars indicate s.e.m. Raw data published in (Siju et al. 2014).

5 Discussion

My experiments demonstrate that the innately aversive cue CO_2 is processed differently in the fly brain dependent on the metabolic state of the animal. Similarly to the innate odor response to 3-octanol, fed flies process CO_2 independent of MB output. Starved flies however, rely on neural output of the MB when reacting to a CO_2 stimulus. Thus, the internal state of the fly influences how different pathways of the same neural circuit are utilized. Furthermore, these results demonstrate that the MB is not only involved in olfactory learning and memory, but also in context-dependent innate olfactory behavior.

5.1 A specialized neural circuit is dedicated to CO_2 processing

The neural circuit dedicated to CO_2 perception has been known to differ from classical pathways of other odors, because CO_2 sensory neurons use GRs to detect CO_2, their receptor downstream signaling utilizes $G\alpha_q$ (Yao & Carlson 2010), they innervate the AL unilaterally and are connected to a highly unusual type of bilateral PN. Further differences to the processing of other odors have been described. For instance, CO_2 activates a single glomerulus at all concentrations, while other odors including 3-octanol and vinegar activate different glomeruli in a concentration-dependent manner (Hallem & Carlson 2006; Semmelhack & Wang 2009). The broader glomerular activation pattern of normal odors is based on two mechanisms: First, one chemical compound can bind and activate multiple ORs with different specificity

(Hallem & Carlson 2006). Second, excitatory lateral connections recruit other glomeruli upon activation of a specific one (Yaksi & Wilson 2010). Both mechanisms seem to exclude the V-glomerulus and thus underline the notion that CO_2 processing is performed by an isolated and dedicated circuit unit in the olfactory system. A similar separation of the V-glomerulus from other glomeruli can also be found for lateral inhibitory connections. CO_2 receptor neurons, unlike all other ORNs, do not co-express $GABA_B$ receptors for presynaptic gain control (Root et al. 2008). This lack of inhibition might ensure the detection of even small changes in CO_2 concentrations within the presence of other odors. Such changes are difficult to detect, because the atmospheric level of CO_2 provides a relatively high background compared to regular odors. Taken together, the CO_2 processing pathway seems to provide a dedicated sensory channel within the olfactory system, which can detect this aversive stimulus reliably and independent of the context of other olfactory input. The finding that the MB is involved in CO_2 processing shows that also the requirements of higher brain centers differ from those of other aversive odors, as has been demonstrated by my experiments with 3-octanol aversion. Thus, the specialized CO_2 processing circuit also extends to the level of higher brain centers.

An interaction of CO_2 with other odors has only been shown on the level of the CO_2 receptors (Turner & Ray 2009) but not on the circuit level. The results presented in this thesis now demonstrate that an integration of the CO_2 signal with other olfactory signals occurs at the level of the MB. This integration step depends on the context in which the CO_2 stimulus is encountered by the fly. Since the MB receives massive olfactory input as well as input from various

other sensory sources, it provides an optimal center for integration of other stimuli within the neural circuit that processes CO_2 stimuli.

I was able to show that CO_2 avoidance behavior requires MB output in starved flies but not in fed ones. Thus, the CO_2 processing circuit also consists of a MB independent processing pathway. Based on the anatomy of VPNs and the functional redundancy of the biVPN under fed conditions, I propose that the non MB-dependent pathway utilizes the LH and the previously described VPN (Sachse et al. 2007) (Figure 5.1). Thus, starvation related modulation of this circuit might occur at the level of the LH or its output, since this pathway is not sufficient for CO_2 avoidance in starved flies. However, research on this part of the circuit remains difficult, since genetic tools that specifically target this structure are not yet available. Future research should aim at further characterizing the circuit by identifying the postsynaptic partner of the biVPN on the level of the LH as well as the MBEN that receives MB output. Furthermore, discovering more information about these two pathways might also elucidate their interaction points. One possibility could be that the starvation signal blocks the LH pathway.

Taken together, the unique characteristics of the neural circuit underlying CO_2 processing emphasize how specific this subunit of the olfactory system is. It is atypical and composed of at least two different parallel pathways. These two pathways are distinct in their use of PNs, higher brain centers and their requirement of different inner states of the animal.

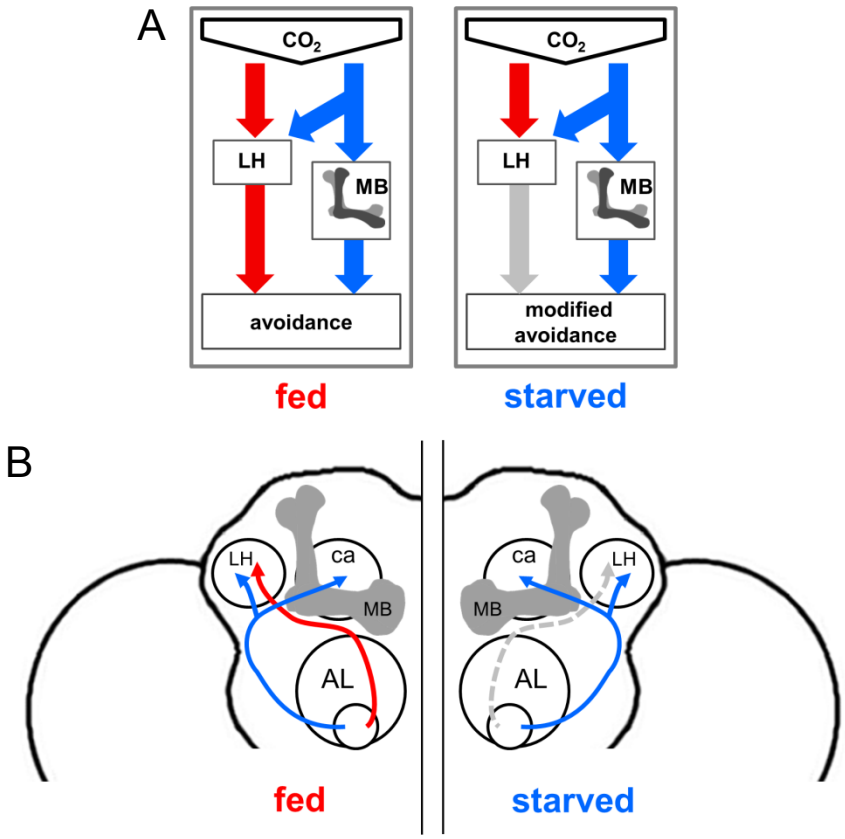

Figure 5.1: A model for the processing of CO_2 behavior in the fly brain

(A) In this model**,** two parallel circuits process CO_2 behavior in the fly brain. Under fed conditions, the lateral horn dependent circuit is sufficient for avoidance behavior, while the mushroom body dependent circuit is redundant. Under starved conditions, the mushroom body dependent circuit becomes necessary for avoidance behavior, while the lateral horn dependent circuit is no longer sufficient. **(B)** The two parallel CO_2 circuits diverge on the level of the V-glomerulus. One pathway likely utilizes a VPN that connects the V-glomerulus directly to the lateral horn and the other pathway utilizes the biVPN. The latter one becomes necessary under starved conditions. Figure adapted from Siju, Bräcker, & Grunwald Kadow 2014 with permission.

5.2 A novel function of the mushroom body in innate olfactory behavior

The MB has been studied in the context of many different behaviors, with a focus on its role in learning and memory. In fact, it is believed that the MB is dispensable for innate olfactory behaviors, since MB ablation did not affect choice behavior to certain odors such as benzaldehyde (Belle & Heisenberg 1994). My data on 3-octanol avoidance recapitulates this, since 3-octanol

avoidance is not influenced by MB silencing. The involvement of the MB in CO_2 behavior now demonstrates a novel function of this neuropil in an innate olfactory behavior. MB output becomes essential for CO_2 avoidance processing only when the fly is starved. I showed that this necessity is gradually increasing based on starvation time. Starvation periods of 24 hours and more switch CO_2 processing from MB-independent to MB–dependent.

While my data suggests that α'/β' KCs are essential for context dependent CO_2 avoidance, imaging data revealed that also other KC subtypes undergo CO_2 dependent Ca^{2+} influx, and thus receive CO_2 related input. Currently, we can only speculate why other KCs receive CO_2 input. Thus, future research should aim to identify the specific roles of different MB subunits in this behavior.

5.3 An atypical projection neuron connects CO_2 sensory input to the mushroom body calyx

Olfactory input from the antennae and maxillary palps arrives first in the AL, where it is picked up by different types of olfactory PNs. A previous study described a VPN that bypasses the MB calyx and projects to the LH but not to the MB (Sachse et al. 2007). However, imaging experiments demonstrated that the MB reacts to CO_2 stimulation and that the obtained fluorescence signals were largest in α'/β' lobes, which is consistent with the results obtained in behavioral experiments. Based on these results, the MB likely receives direct CO_2 related input to generate avoidance behavior. Hence, I aimed at identifying a candidate PN for bringing CO_2 sensation from the V-

glomerulus in the AL to the MB calyx. An unbiased approach using PA-GFP resulted in consistent labeling of three types of neurites in each hemisphere. From these, only one type appeared to connect to the LH as well as to the MB calyx. Reconstructing the neuron with this type of innervation revealed that it is indeed a VPN like neuron. However, several characteristics distinguish it from regular PNs. The position of its cell body is located lateral to the suboesophagial ganglion (SOG), which is the gustatory center of the fly brain. This cell body location is unusual compared to the location of other olfactory PN cell bodies, which are located either in a dorsal or lateral cluster around the AL. Furthermore, in contrast to regular PNs, this VPN bifurcates and innervates the V-glomeruli bilaterally before it extends a projection to both the LH and the MB calyx. Taken together, the biVPN has a highly distinct anatomy based on cell body location, innervation of both V-glomeruli and innervation of both brain hemispheres. It is interesting to note that, as stated above, CO_2 sensory neurons are also an exception to regular ORNs in that they innervate the AL only ipsilaterally and not ipsi- and contralaterally in *Drosophila*. Future research should be aimed at further characterizing the biVPN. This includes the need to find a definitive proof for synapses with KCs. Furthermore, additional data for the locations of input regions is needed. The most likely input regions are the V-glomeruli. In addition to the innervations of the V-glomeruli, each of the biVPNs extends at least one more process in the ipsilateral AL which is not found in its innervation of the contralateral AL. Thus, it needs to be determined which of these processes serve as input our output regions. Finally, it is intriguing to speculate about the cell body location, since it is not only different from the majority of other PNs, but also because it

is situated in a gustatory center of the fly. Here, further possibilities for modulation or gustatory input to these neurons could arise.

5.4 Dopamine release is involved in starvation dependent processing of CO_2

Dopaminergic signaling has been shown to play a role in motivation related processes in mammals, such as the regulation of feeding behavior in mice (Szczypka et al. 1999). Research in the fly indicates that this neuromodulator fulfills similar roles in invertebrates as it does in humans (Van Swinderen & Andretic 2011; Waddell 2010). For example, dopamine plays a vital role in feeding behavior in the fly. One dopaminergic neuron in the SOG regulates feeding related proboscis extension behavior (Marella, Mann, & Scott 2012). Artificially activating this neuron triggers proboscis extension in satiated flies, which would otherwise not display this behavior. This suggests that dopamine release correlates with the internal state of starvation in this system.

Dopaminergic neurons are grouped in eight clusters within the fly brain. These include the protocerebral anterior medial (PAM) and protocerebral posterior lateral (PPL) cluster (Mao & Davis 2009b). Neurons of these clusters innervate the lobes of the MB and are required for olfactory conditioning of flies with shock or sugar reinforcements (Ito et al. 2010; C. Liu et al. 2012). Sugar conditioning is gated by the metabolic state of the fly. Only a hungry fly is motivated to associate a sugar with an odor and retrieve this memory later on (Gruber et al. 2013). PPL cluster neurons that are TH-GAL4 positive have been shown to regulate starvation-dependent memory execution. Blocking six

of these neurons released memory in fed flies suggesting that dopamine gates this starvation dependent behavior (Krashes et al. 2009).

I found that TH-GAL4 positive neurons are also involved in modification of CO_2 avoidance behavior. Blocking output of dopaminergic neurons via TH-GAL4 increased CO_2 avoidance in starved flies but had no effect in satiated flies. Complementary to this finding, activation of these neurons blocked CO_2 avoidance in satiated flies to a level that is comparable to that of starved flies. Taken together, these results not only complement each other but also suggest that dopamine gates starvation dependent changes in CO_2 processing. However, it remains unknown whether dopaminergic neurons signal directly onto the MB. The imaging data suggest that release of dopamine reduces CO_2-stimulated Ca^{2+} influx into α'/β' neurons and that dopamine thus directly or indirectly influences processing of the CO_2 signal in the MB. These findings are a first step into elucidating the role of dopamine and how the starvation signal is implemented into context dependent CO_2 behavior. Future research will have to test the population of dopaminergic neurons for individual candidate neurons that carry the starvation signal. Knowledge about these neurons will also reveal where the starvation signal is integrated into the CO_2 circuit. As stated before, this could occur both in the MB dependent as well as the MB independent part of the circuit. While dopaminergic neurons might only be one part of the starvation related signaling pathway, they might lead to the discovery of other parts. Thus, both the starvation sensing neurons in the upstream part as well as the neurons that relay the signal onto KCs might be identified. In addition to dopaminergic signaling, research focusing on the role of neuropeptides could reveal further

signaling steps in this circuit. Previous studies have connected dopaminergic hunger signaling in MB dependent behavior to neuropeptide F (NPF, a homolog of the mammalian neuropeptide Y) (Krashes et al. 2009). Testing the involvement of different neuropeptide signaling systems in CO_2 avoidance might also give rise to novel insights into the relationship of starvation and innate olfactory behavior.

5.5 CO_2 avoidance behavior as a paradigm to study decision making

The behavioral experiments presented in this thesis, reveal interesting new insights into how the model organism of *Drosophila* computes information during a decision making process. This is especially true for the CO_2 plus vinegar combinatorial experiments and their interpretation within the framework of value based decision making (Rangel et al. 2008).

As stated in the introduction, the basis of every decision is the formation of an appropriate representation of the problem. In the case of the CO_2 plus vinegar experiment, this representation consists of the external olfactory stimuli CO_2 and vinegar odor. The exclusion of other external stimuli in this paradigm, such as light, benefits the analysis of the decision making process. The representation of this decision problem also incorporates the internal state of the fly by evaluating the hunger level of the animal. I was able to show that this evaluation process most likely determines the energy level of the animal in a gradual fashion. Such a gradual shift in hunger level is reflected in the finding, that the requirement of the MB for CO_2 behavior differs at different starvation times, and increases gradually. Finally, based on these external

and internal states, the representation of the problem within the fly brain incorporates a set of possible actions to choose from. Considering the assay of the T-maze, only two of these actions were measured in all experiments: approaching the odor source or avoiding it. While the T-maze assay does not detect other behavioral actions, its population approach makes it a powerful tool for the purpose of investigating decision making. On the single fly level, only a binary decision outcome is measured in the form of avoidance or approach of the odor mixture. By measuring large groups of flies, the resulting PI reflects the probabilistic basis of each individual's decision making process.

How the fly brain generates a behavioral decision in the CO_2 plus vinegar paradigm depends on the internal sensory signals. I found that after prolonged starvation, the approach of food sources is prioritized over CO_2 avoidance. Without starvation, flies always avoided CO_2 in my experiments. These findings provide insight into the valuation step of this decision making process, which is based on the aforementioned representation of the problem. On a primary level, the decision making process in a CO_2 plus vinegar combinatorial experiment has characteristics of a goal directed valuation system. The two possible actions of approach or avoidance are valued based on their outcomes: avoiding danger or feeding on a potential food source. Feeding has a different value for the fly, depending on whether the animal is hungry or satiated. In a satiated fly, finding additional food has a lower beneficial effect than avoiding the potential danger signal CO_2, and thus the decision is made to avoid the odor mixture. A starved fly however, values the beneficial effect of acquiring food higher than that of avoiding CO_2, because it is more important for survival. Thus, the behavioral results obtained from wild

type flies suggest a goal directed valuation system, which drives this particular decision process (Figure 4.1). Both a Pavlovian and a habitual valuation system would lead to different results in the same choice situation. Based on the characteristic, that these systems do not change their valuation based on the outcome of an action, flies would always value each action similarly. Thus, they would always choose to either avoid or approach the odor mixture, independent of starvation, because the relation of the value given to CO_2 avoidance versus food approach is always constant.

But does the fly really display goal driven valuation in this choice situation? Alternatively, the decision in a CO_2 plus vinegar experiment could be generated by starvation dependent switching between two Pavlovian valuation systems. For a true goal directed decision, the brain needs to store and process all possible action to outcome and outcome to value connections at the time of the decision, in order to compute appropriate value to action connections. This gives rise to a level of computing, which resembles the process of active planning.

5.6 The mushroom body as a center for value based decision making

The results obtained in my circuit mapping experiments point to the existence of a goal directed valuation system within this paradigm. I propose the hypothesis, that the two parts of the CO_2 circuit cover two different valuation systems: one goal directed which is connected to the MB dependent pathway, and one Pavlovian which is connected to the MB independent pathway of CO_2 processing. Extensive studies on its role in learning and memory (Qiu & Davis

1993; Hitier et al. 1998; Zars et al. 2000; Josh Dubnau et al. 2001; Fiala 2007), have established the MB as a center for habitual value based decision making. Evidence for the existence of a goal directed valuation system in the MB, comes from the experiment, in which I blocked KC output and then tested the reaction to a combinatorial stimulus of both CO_2 and vinegar (Figure 4.9). This experiment demonstrates that MB output is necessary for the computation of this decision process, even without the context of starvation. CO_2 stimuli that occur in the context of specific external and internal feeding related stimuli are processed in the MB. Utilizing this integration center, might make a more complicated goal directed valuation possible. As stated before, the MB receives input from various sensory systems and is known to integrate these in the process of learning. For example, during the formation of appetitive memory through sugar reward driven conditioning, a representation of the situation is processed in the MB. A fly will only connect a stimulus with the presence of sugar if it is motivated by starvation (Gruber et al. 2013; Krashes et al. 2009). Such a form of learning related motivation might be similar to the motivation that is required to overcome CO_2 avoidance and approach a food stimulus. Further evidence for this hypothesis comes from the imaging experiments presented in this thesis. The data collected from Ca^{2+}-imaging of the MB clearly shows, that CO_2 stimulation leads to KC activity both in starved and satiated flies. This supports the notion, that the MB always receives CO_2 information, in order to process it in upcoming context driven decisions. Strong support for this hypothesis also comes from the fact, that the MB is necessary for certain saliency based decisions during flight. When the fly encounters a dilemma, in which it has to choose one of two

stimuli parameters to follow, it needs the MB to form novel decisions (Zhang, Guo, Peng, Xi, & Guo 2007). The dilemma was generated through preceding training periods with a specific parameter combination, and then reversing this combination in the test. The results of this study demonstrate that the MB is necessary to form novel decisions. Taken together, I thus want to extend my previous hypothesis with the following statement: The MB is a center for computing complex context based problems, in order to provide optimal decisions through a goal directed valuation system. Interestingly, MB output is not necessary in fed flies that have to avoid only CO_2 (Figure 4.5). Thus, this relatively easy computation might be processed by a Pavlovian system located in the MB independent CO_2 pathway. This pathway might perform a simple stimulus based computation, were the strength of the stimulus determines the value of a reaction to it, and thus the overall choice probability.

Finding conclusive evidence for this hypothesis will not be a trivial task. This is partially due to a lack of robust definitions, which describe and categorize the processes that underlie decision making. Does value based decision making require dedicated neurons, which reflect the strength of a value signal in their activity? In the case of habitual valuation systems, the activity of specific MBEN has been related to a punishment or reward signal (Ito et al. 2010; C. Liu et al. 2012; Rolls 2011; Séjourné et al. 2011; Thum, Jenett, Ito, Heisenberg, & Tanimoto 2007). It has been shown, that neurons, which normally respond to punishment, can alter their response profile after a training period with a combination of odor and punishment stimuli (Riemensperger et al. 2005). After the training, the punishment neuron also displays a prolonged response to the trained odor without the stimulus of

punishment, and thus transferred the value of avoiding the punishment to avoiding this odor. A comparison with the choice paradigm of CO_2 plus vinegar raises the question whether such a dedicated valuation signaling neuron also exists for innate olfactory behavior. Identifying candidate neurons for this task could be the first step in validating the aforementioned hypothesis. In *Drosophila*, conducting a behavioral and imaging based screen is possible, and might lead to the identification of neurons that possess a value specific activity profile.

Further investigation of the neuronal correlate which underlies starvation signaling in this particular behavior presents an alternative approach to gain new insights into how the CO_2 plus vinegar decision is computed. My results on the dopaminergic system of *Drosophila* suggest that this neurotransmitter system is part of a circuit, which is necessary to adjust the values of different outcomes to the state of starvation. Knowing the detailed connectivity of individual neurons in this circuit might also reveal in turn the neurons that carry the value specific signal, since these are likely connected in some form.

It might also be possible, that the correlate for value signaling in innate CO_2 behavior does not exist in the form of dedicated neurons. As an alternative, values could be coded on a different structural level within the circuit. Valuation could be in the form of synaptic strength or temporal response profiles or neurons. This might already take place on the level of primary or secondary neurons within the sensory systems. In the olfactory system for example, hunger related sNPF signaling triggers presynaptic facilitation in ORNs that are activated by food related odors (Root et al. 2011). This mechanism then increases the sensitivity of this ORN type and thus promotes

food searching behavior. Facilitation of sensory signals might be a mechanism that is part of a simple perception based decision making system, but it might also be a first step in increasing the value of specific actions which are connected to the goal of locating food sources. Similar peptidergic signaling might play a role during valuation in MB dependent decision making. Indeed, in a learning and memory focused study, NPF signaling was shown to represent the motivation of hunger within the process of appetitive conditioning (Krashes et al. 2009). With only a limited number of available neurons in the brain of *Drosophila*, global value related signaling acting on many levels of a decision making circuit simultaneously, might have presented evolution with a tool to incorporate more complicated computations without increasing the number of neurons or connections within this circuit. Despite the restrictions of the fly's brain in terms of complexity, it still houses several distinct circuits for processing the innate stimulus of CO_2. Future research on the neurobiological basis of decision making will have to find a more precise set of definitions to categorize the underlying processing steps. It is likely, that invertebrates use several decision making systems simultaneously, so they can tackle more complicated problems. Similar to humans, these systems might not always agree and thus give rise to behavioral variation (Rangel et al. 2008).

5.7 The ecological significance of CO_2 processing

CO_2 avoidance can be inhibited by fruit related odors directly on the level of the odorant receptors (Turner & Ray 2009). Processing of CO_2 by the MB during starvation periods provides an additional level of integration of CO_2

aversion into a general context, which includes food and other sensory stimuli as well as the inner state of the animal. During evolution, enabling an adjustable behavior rather than a hardwired response to the ubiquitous odor CO_2 might have given flies an advantage in survival. This might have been essential for the survival of starved flies, since CO_2 is present in the context of food related stimuli. Thus, processing it differentially based on the current feeding state of the animal instead of triggering a hardwired avoidance reaction, enabled the individual fly to overcome danger signals and acquire food. This is supported by the fact that fruits, one of the natural habitats of this fly, produce varying amounts of CO_2 that must be evaluated based on the general context as well as the inner state of the fly. Notably, mosquitoes also adjust their CO_2 induced behavior to context and inner state. After a blood meal, females prefer odors required for locating oviposition sites over CO_2, lactic acids and other animal and human host odors (Siju et al. 2010; Takken & Knols 1999). It will be interesting to understand whether higher brain centers like the MB contribute to this change in behavior, and whether manipulation of the MB or environmental context might open possibilities for fighting insects and the vector-borne diseases which are associated with them.

6 Acknowledgements

I would like to express my gratitude to Ilona for having me in her lab and providing the topic for my thesis. Thanks for the trust in me during setting up behavioral paradigms in the lab. Thanks for the time and freedom I needed to pursue the experiments which eventually led to be a major part of this thesis.

I want to thank Alexander Borst for being my doctor father and for all the helpful feedback during my thesis committees.

Further I want to thank André Fiala for being on my thesis committee and commenting on the direction of my thesis.

I want to thank Hiromu Tanimoto for introducing me to the field of neurobiology. His support continued during my thesis committee meetings and the screen.

I want to thank Siju for working with me on this project. Thanks for all the nice conversations and discussions (and the fish curry). Thanks for enduring the publication process and the constant flood of new imaging experiments.

I want to thank Chrissi, Verena, Julia and Christiane for working with me during the large primary screen, both for support in planning as well as in the laborious preparatory part. Thanks also for all the nice conversations that eased up the time in front of the box.

I want to thank all the members of the Kadow lab, past and present. Thanks for the nice times in the lab and the office. Along these lines I want to thank

my office mates Daniel, Juhi and Christina for all the nice chatting about the life of a PhD student. Further I want to thank all the people I came across in the institute, the nice visits on the Wiesn and all the other occasions.

Zum Schluss möchte ich meinen Eltern danken, ohne die ich nicht da stehen würde wo ich jetzt bin. Ebenfalls Danke an alle anderen Freunde die mich durch diese Zeit begleitet haben, besonders Marcel, Max, Florian und Stefan.

7 Literature

Abuin, L., Bargeton, B., Ulbrich, M. H., Isacoff, E. Y., Kellenberger, S., & Benton, R. (2011). Functional architecture of olfactory ionotropic glutamate receptors. *Neuron*, *69*(1), 44–60. doi:10.1016/j.neuron.2010.11.042

Akerboom, J., Chen, T.-W., Wardill, T. J., Tian, L., Marvin, J. S., Mutlu, S., … Looger, L. L. (2012). Optimization of a GCaMP calcium indicator for neural activity imaging. *The Journal of neuroscience : the official journal of the Society for Neuroscience*, *32*(40), 13819–40. doi:10.1523/JNEUROSCI.2601-12.2012

Aso, Y., Grübel, K., Busch, S., Friedrich, A. B., Siwanowicz, I., & Tanimoto, H. (2009). The mushroom body of adult Drosophila characterized by GAL4 drivers. *Journal of neurogenetics*, *23*(1-2), 156–72. doi:10.1080/01677060802471718

Belle, J. S. De, & Heisenberg, M. (1994). Associative odor learning in Drosophila abolished by chemical ablation of mushroom bodies. *Science-AAAS-Weekly Paper …*, *263*(4), 692–695. Retrieved from http://faculty.unlv.edu/debelle/lab/pdfs/debelle94.pdf

Benton, R., Sachse, S., Michnick, S., & Vosshall, L. (2006). Atypical membrane topology and heteromeric function of Drosophila odorant receptors in vivo. *PLoS biology*, *4*(2). doi:10.1371/journal.pbio.0040020

Benton, R., Vannice, K. S., Gomez-Diaz, C., & Vosshall, L. B. (2009). Variant ionotropic glutamate receptors as chemosensory receptors in Drosophila. *Cell*, *136*(1), 149–62. doi:10.1016/j.cell.2008.12.001

Benzer, S. (1967). Behavioral mutants of Drosophila isolated by countercurrent distribution. *Proceedings of the National Academy of Sciences of the United States of America*, *58*(3), 1112–9. Retrieved from http://www.pubmedcentral.nih.gov/articlerender.fcgi?artid=335755&tool=pmcentrez&rendertype=abstract

Bohm, R., Welch, W., Goodnight, L., Cox, L., Henry, L., Gunter, T., … Zhang, B. (2010). A genetic mosaic approach for neural circuit mapping in Drosophila. *Proceedings of the …*, *107*(37), 16378–16383. doi:10.1073/pnas.1004669107/-/DCSupplemental.www.pnas.org/cgi/doi/10.1073/pnas.1004669107

Bowen, M. F. (1991). The sensory physiology of host-seeking behavior in mosquitoes. *Annual review of entomology*, *36*, 139–58. doi:10.1146/annurev.en.36.010191.001035

Bräcker, L. B., Siju, K. P., Varela, N., Aso, Y., Zhang, M., Hein, I., … Grunwald Kadow, I. C. (2013). Essential Role of the Mushroom Body in Context-Dependent CO2 Avoidance in Drosophila. *Current biology : CB*, *23*(13), 1228–34. doi:10.1016/j.cub.2013.05.029

Brand, a H., & Perrimon, N. (1993). Targeted gene expression as a means of altering cell fates and generating dominant phenotypes. *Development (Cambridge, England)*, *118*(2), 401–15. Retrieved from http://www.ncbi.nlm.nih.gov/pubmed/8223268

Chou, Y.-H., Spletter, M. L., Yaksi, E., Leong, J. C. S., Wilson, R. I., & Luo, L. (2010). Diversity and wiring variability of olfactory local interneurons in the Drosophila antennal lobe. *Nature neuroscience*, *13*(4), 439–49. doi:10.1038/nn.2489

Clyne, P. J., Warr, C. G., Freeman, M. R., Lessing, D., Kim, J., & Carlson, J. R. (1999). A novel family of divergent seven-transmembrane proteins: candidate odorant receptors in Drosophila. *Neuron*, *22*(2), 327–38. Retrieved from http://www.ncbi.nlm.nih.gov/pubmed/10069338

Couto, A., Alenius, M., & Dickson, B. J. (2005). Molecular, anatomical, and functional organization of the Drosophila olfactory system. *Current biology : CB*, *15*(17), 1535–47. doi:10.1016/j.cub.2005.07.034

Das, A., Chiang, A., Davla, S., Priya, R., Reichert, H., Vijayraghavan, K., & Rodrigues, V. (2011). Identification and analysis of a glutamatergic local interneuron lineage in the adult Drosophila olfactory system. *Neural systems & circuits*, *1*(1), 4. doi:10.1186/2042-1001-1-4

Datta, S. R., Vasconcelos, M. L., Ruta, V., Luo, S., Wong, A., Demir, E., … Axel, R. (2008). The Drosophila pheromone cVA activates a sexually dimorphic neural circuit. *Nature*, *452*(7186), 473–7. doi:10.1038/nature06808

Dubnau, J., Grady, L., Kitamoto, T., & Tully, T. (2001). Disruption of neurotransmission in Drosophila mushroom body blocks retrieval but not acquisition of memory. *Nature*, *411*(6836), 476–80. doi:10.1038/35078077

Faucher, C., Forstreuter, M., Hilker, M., & De Bruyne, M. (2006). Behavioral responses of Drosophila to biogenic levels of carbon dioxide depend on life-stage, sex and olfactory context. *The Journal of experimental biology*, *209*(Pt 14), 2739–48. doi:10.1242/jeb.02297

Fiala, A. (2007). Olfaction and olfactory learning in Drosophila: recent progress. *Current opinion in neurobiology*, *17*(6), 720–6. doi:10.1016/j.conb.2007.11.009

Fiala, A., & Spall, T. (2003). In vivo calcium imaging of brain activity in Drosophila by transgenic cameleon expression. *Science's STKE : signal*

transduction knowledge environment, *2003*(174), PL6. doi:10.1126/stke.2003.174.pl6

Gong, Z., Liu, J., Guo, C., Zhou, Y., Teng, Y., & Liu, L. (2010). Two pairs of neurons in the central brain control Drosophila innate light preference. *Science (New York, N.Y.)*, *330*(6003), 499–502. doi:10.1126/science.1195993

Goyret, J., Markwell, P. M., & Raguso, R. a. (2008). Context- and scale-dependent effects of floral CO2 on nectar foraging by Manduca sexta. *Proceedings of the National Academy of Sciences of the United States of America*, *105*(12), 4565–70. doi:10.1073/pnas.0708629105

Gruber, F., Knapek, S., Fujita, M., Matsuo, K., Bräcker, L., Shinzato, N., … Tanimoto, H. (2013). Suppression of conditioned odor approach by feeding is independent of taste and nutritional value in Drosophila. *Current biology : CB*, *23*(6), 507–14. doi:10.1016/j.cub.2013.02.010

Guerenstein, P. G., & Hildebrand, J. G. (2008). Roles and effects of environmental carbon dioxide in insect life. *Annual review of entomology*, *53*, 161–78. doi:10.1146/annurev.ento.53.103106.093402

Gupta, N., & Stopfer, M. (2012). Functional analysis of a higher olfactory center, the lateral horn. *The Journal of neuroscience : the official journal of the Society for Neuroscience*, *32*(24), 8138–48. doi:10.1523/JNEUROSCI.1066-12.2012

Hallem, E. a, & Carlson, J. R. (2006). Coding of odors by a receptor repertoire. *Cell*, *125*(1), 143–60. doi:10.1016/j.cell.2006.01.050

Hallem, E. a, & Sternberg, P. W. (2008). Acute carbon dioxide avoidance in Caenorhabditis elegans. *Proceedings of the National Academy of Sciences of the United States of America*, *105*(23), 8038–43. doi:10.1073/pnas.0707469105

Hartl, M., Loschek, L. F., Stephan, D., Siju, K. P., Knappmeyer, C., & Kadow, I. C. G. (2011). A new Prospero and microRNA-279 pathway restricts CO2 receptor neuron formation. *The Journal of neuroscience : the official journal of the Society for Neuroscience*, *31*(44), 15660–73. doi:10.1523/JNEUROSCI.2592-11.2011

Hayashi, S., Ito, K., Sado, Y., Taniguchi, M., Akimoto, A., Takeuchi, H., … Goto, S. (2002). GETDB, a database compiling expression patterns and molecular locations of a collection of Gal4 enhancer traps. *Genesis (New York, N.Y. : 2000)*, *34*(1-2), 58–61. doi:10.1002/gene.10137

Heisenberg, M., Borst, A., Wagner, S., & Byers, D. (1985). Drosophila mushroom body mutants are deficient in olfactory learning. *Journal of neurogenetics*, *2*(1), 1–30. Retrieved from http://www.ncbi.nlm.nih.gov/pubmed/4020527

Hitier, R., Heisenberg, C. A. M., & Préat, T. (1998). Abnormal mushroom body plasticity in the Drosophila memory, *9*(12), 2717–2719.

Ito, K., Aso, Y., Siwanowicz, I., Bräcker, L., Kitamoto, T., & Tanimoto, H. (2010). Specific dopaminergic neurons for the formation of labile aversive memory. *Current biology : CB*, *20*(16), 1445–51. doi:10.1016/j.cub.2010.06.048

Jefferis, G. S. X. E., Potter, C. J., Chan, A. M., Marin, E. C., Rohlfing, T., Maurer, C. R., & Luo, L. (2007). Comprehensive maps of Drosophila higher olfactory centers: spatially segregated fruit and pheromone representation. *Cell*, *128*(6), 1187–203. doi:10.1016/j.cell.2007.01.040

Jenett, A., Rubin, G. M., Ngo, T.-T. B., Shepherd, D., Murphy, C., Dionne, H., … Zugates, C. T. (2012). A GAL4-driver line resource for Drosophila neurobiology. *Cell reports*, *2*(4), 991–1001. doi:10.1016/j.celrep.2012.09.011

Joiner, W. J., Crocker, A., White, B. H., & Sehgal, A. (2006). Sleep in Drosophila is regulated by adult mushroom bodies. *Nature*, *441*(7094), 757–60. doi:10.1038/nature04811

Jones, W. D., Cayirlioglu, P., Kadow, I. G., & Vosshall, L. B. (2007). Two chemosensory receptors together mediate carbon dioxide detection in Drosophila. *Nature*, *445*(7123), 86–90. doi:10.1038/nature05466

Joseph, R. M., Devineni, A. V, King, I. F. G., & Heberlein, U. (2009). Oviposition preference for and positional avoidance of acetic acid provide a model for competing behavioral drives in Drosophila. *Proceedings of the National Academy of Sciences of the United States of America*, *106*(27), 11352–7. doi:10.1073/pnas.0901419106

Kitamoto, T. (2001). Conditional modification of behavior in Drosophila by targeted expression of a temperature-sensitive shibire allele in defined neurons. *Journal of neurobiology*, *47*(2), 81–92. Retrieved from http://onlinelibrary.wiley.com/doi/10.1002/neu.1018/full

Krashes, M. J., DasGupta, S., Vreede, A., White, B., Armstrong, J. D., & Waddell, S. (2009). A neural circuit mechanism integrating motivational state with memory expression in Drosophila. *Cell*, *139*(2), 416–27. doi:10.1016/j.cell.2009.08.035

Krashes, M. J., Keene, A. C., Leung, B., Armstrong, J. D., & Waddell, S. (2007). Sequential use of mushroom body neuron subsets during drosophila odor memory processing. *Neuron*, *53*(1), 103–15. doi:10.1016/j.neuron.2006.11.021

Kremer, M. C., Christiansen, F., Leiss, F., Paehler, M., Knapek, S., Andlauer, T. F. M., … Tavosanis, G. (2010). Structural long-term changes at

mushroom body input synapses. *Current biology : CB*, *20*(21), 1938–44. doi:10.1016/j.cub.2010.09.060

Larsson, M. C., Domingos, A. I., Jones, W. D., Chiappe, M. E., Amrein, H., & Vosshall, L. B. (2004). Or83b encodes a broadly expressed odorant receptor essential for Drosophila olfaction. *Neuron*, *43*(5), 703–14. doi:10.1016/j.neuron.2004.08.019

Leopold, P., & Perrimon, N. (2007). Drosophila and the genetics of the internal milieu. *Nature*, *450*(7167), 186–8. doi:10.1038/nature06286

Lin, C. H. A., Tomioka, M., Pereira, S., Sellings, L., Iino, Y., & Van der Kooy, D. (2010). Insulin signaling plays a dual role in Caenorhabditis elegans memory acquisition and memory retrieval. *The Journal of neuroscience : the official journal of the Society for Neuroscience*, *30*(23), 8001–11. doi:10.1523/JNEUROSCI.4636-09.2010

Liu, C., Plaçais, P.-Y., Yamagata, N., Pfeiffer, B. D., Aso, Y., Friedrich, A. B., … Tanimoto, H. (2012). A subset of dopamine neurons signals reward for odour memory in Drosophila. *Nature*, *488*(7412), 512–516. doi:10.1038/nature11304

Liu, L., Wolf, R., Ernst, R., & Heisenberg, M. (1999). Context generalization in Drosophila visual learning requires the mushroom bodies. *Nature*, *400*(6746), 753–6. doi:10.1038/23456

Luan, H., Peabody, N. C., Vinson, C. R., & White, B. H. (2006). Refined spatial manipulation of neuronal function by combinatorial restriction of transgene expression. *Neuron*, *52*(3), 425–36. doi:10.1016/j.neuron.2006.08.028

Maisak, M. S., Haag, J., Ammer, G., Serbe, E., Meier, M., Leonhardt, A., … Borst, A. (2013). A directional tuning map of Drosophila elementary motion detectors. *Nature*, *500*(7461), 212–6. doi:10.1038/nature12320

Mao, Z., & Davis, R. L. (2009a). Eight different types of dopaminergic neurons innervate the Drosophila mushroom body neuropil: anatomical and physiological heterogeneity. *Frontiers in neural circuits*, *3*(July), 5. doi:10.3389/neuro.04.005.2009

Mao, Z., & Davis, R. L. (2009b). Eight different types of dopaminergic neurons innervate the Drosophila mushroom body neuropil : anatomical and physiological heterogeneity MATERIALS AND METHODS. *Frontiers: A Journal of Women Studies*, *3*(July), 1–17. doi:10.3389/neuro.04.005.2009

Marella, S., Mann, K., & Scott, K. (2012). Dopaminergic modulation of sucrose acceptance behavior in Drosophila. *Neuron*, *73*(5), 941–50. doi:10.1016/j.neuron.2011.12.032

Masse, N. Y., Turner, G. C., & Jefferis, G. S. X. E. (2009). Olfactory information processing in Drosophila. *Current biology : CB*, *19*(16), R700–13. doi:10.1016/j.cub.2009.06.026

McBride, S. M., Giuliani, G., Choi, C., Krause, P., Correale, D., Watson, K., … Siwicki, K. K. (1999). Mushroom body ablation impairs short-term memory and long-term memory of courtship conditioning in Drosophila melanogaster. *Neuron*, *24*(4), 967–77. Retrieved from http://www.ncbi.nlm.nih.gov/pubmed/10624959

Min, S., Ai, M., Shin, S. a, & Suh, G. S. B. (2013). Dedicated olfactory neurons mediating attraction behavior to ammonia and amines in Drosophila. *Proceedings of the National Academy of Sciences of the United States of America*, *110*(14), E1321–9. doi:10.1073/pnas.1215680110

Miyamoto, T., Slone, J., Song, X., & Amrein, H. (2012). A fructose receptor functions as a nutrient sensor in the Drosophila brain. *Cell*, *151*(5), 1113–25. doi:10.1016/j.cell.2012.10.024

Moss, C. F., & Dethier, V. G. (1983). Central nervous system regulation of finicky feeding by the blowfly. *Behavioral neuroscience*, *97*(4), 541–8. Retrieved from http://www.ncbi.nlm.nih.gov/pubmed/6615630

Murthy, M., Fiete, I., & Laurent, G. (2008). Testing odor response stereotypy in the Drosophila mushroom body. *Neuron*, *59*(6), 1009–23. doi:10.1016/j.neuron.2008.07.040

Nässel, D. R., & Winther, A. M. E. (2010). Drosophila neuropeptides in regulation of physiology and behavior. *Progress in neurobiology*, *92*(1), 42–104. doi:10.1016/j.pneurobio.2010.04.010

Navarrete-Palacios, E., Hudson, R., Reyes-Guerrero, G., & Guevara-Guzmán, R. (2003). Lower olfactory threshold during the ovulatory phase of the menstrual cycle. *Biological Psychology*, *63*(3), 269–279. doi:10.1016/S0301-0511(03)00076-0

Neuhaus, E. M., Gisselmann, G., Zhang, W., Dooley, R., Störtkuhl, K., & Hatt, H. (2005). Odorant receptor heterodimerization in the olfactory system of Drosophila melanogaster. *Nature neuroscience*, *8*(1), 15–7. doi:10.1038/nn1371

Patterson, G. H., & Lippincott-Schwartz, J. (2002). A photoactivatable GFP for selective photolabeling of proteins and cells. *Science (New York, N.Y.)*, *297*(5588), 1873–7. doi:10.1126/science.1074952

Pulver, S. R., Pashkovski, S. L., Hornstein, N. J., Garrity, P. a, & Griffith, L. C. (2009). Temporal dynamics of neuronal activation by Channelrhodopsin-2 and TRPA1 determine behavioral output in Drosophila larvae. *Journal of neurophysiology*, *101*(6), 3075–88. doi:10.1152/jn.00071.2009

Qin, H., Cressy, M., Li, W., Coravos, J. S., Izzi, S. a, & Dubnau, J. (2012). Gamma neurons mediate dopaminergic input during aversive olfactory memory formation in Drosophila. *Current biology : CB*, *22*(7), 608–14. doi:10.1016/j.cub.2012.02.014

Qiu, Y., & Davis, R. L. (1993). Genetic dissection of the learning/memory gene dunce of Drosophila melanogaster. *Genes & Development*, *7*(7b), 1447–1458. doi:10.1101/gad.7.7b.1447

Rangel, A., Camerer, C., & Montague, P. R. (2008). A framework for studying the neurobiology of value-based decision making. *Nature reviews. Neuroscience*, *9*(7), 545–56. doi:10.1038/nrn2357

Rein, K., Zöckler, M., Mader, M. T., Grübel, C., & Heisenberg, M. (2002). The Drosophila standard brain. *Current biology : CB*, *12*(3), 227–31. Retrieved from http://www.ncbi.nlm.nih.gov/pubmed/11839276

Riemensperger, T., Völler, T., Stock, P., Buchner, E., & Fiala, A. (2005). Punishment prediction by dopaminergic neurons in Drosophila. *Current biology : CB*, *15*(21), 1953–60. doi:10.1016/j.cub.2005.09.042

Rolls, E. T. (2007). Sensory processing in the brain related to the control of food intake. *The Proceedings of the Nutrition Society*, *66*(1), 96–112. doi:10.1017/S0029665107005332

Rolls, E. T. (2011). Taste, olfactory and food texture reward processing in the brain and obesity. *International journal of obesity (2005)*, *35*(4), 550–61. doi:10.1038/ijo.2010.155

Root, C. M., Ko, K. I., Jafari, A., & Wang, J. W. (2011). Presynaptic facilitation by neuropeptide signaling mediates odor-driven food search. *Cell*, *145*(1), 133–44. doi:10.1016/j.cell.2011.02.008

Root, C. M., Masuyama, K., Green, D. S., Enell, L. E., Nässel, D. R., Lee, C.-H., & Wang, J. W. (2008). A presynaptic gain control mechanism fine-tunes olfactory behavior. *Neuron*, *59*(2), 311–21. doi:10.1016/j.neuron.2008.07.003

Sachse, S., Rueckert, E., Keller, A., Okada, R., Tanaka, N. K., Ito, K., & Vosshall, L. B. (2007). Activity-dependent plasticity in an olfactory circuit. *Neuron*, *56*(5), 838–50. doi:10.1016/j.neuron.2007.10.035

Sato, K., Pellegrino, M., Nakagawa, T. T., Vosshall, L. B., & Touhara, K. (2008). Insect olfactory receptors are heteromeric ligand-gated ion channels. *Nature*, *452*(7190), 1002–6. doi:10.1038/nature06850

Schloegl, H., Percik, R., Horstmann, A., Villringer, A., Stumvoll, M., & 1. (2011). Peptide hormones regulating appetite – focus on neuroimaging studies in humans. *Diabetes/metabolism research and reviews*, *27*(2), 104–112. doi:10.1002/dmrr

Séjourné, J., Plaçais, P.-Y., Aso, Y., Siwanowicz, I., Trannoy, S., Thoma, V., … Preat, T. (2011). Mushroom body efferent neurons responsible for aversive olfactory memory retrieval in Drosophila. *Nature neuroscience*, *14*(7), 903–910. doi:10.1038/nn.2846

Semmelhack, J. L., & Wang, J. W. (2009). Select Drosophila glomeruli mediate innate olfactory attraction and aversion. *Nature*, *459*(7244), 218–23. doi:10.1038/nature07983

Shih, H.-W., & Chiang, A.-S. (2011). Anatomical characterization of thermosensory AC neurons in the adult Drosophila brain. *Journal of neurogenetics*, *25*(1-2), 1–6. doi:10.3109/01677063.2011.571323

Siju, K. P., Bräcker, L. B., & Grunwald Kadow, I. C. (2014). Neural mechanisms of context-dependent modification of CO2 avoidance behavior in fruit flies. *Fly*, *8*(2).

Siju, K. P., Hill, S. R., Hansson, B. S., & Ignell, R. (2010). Influence of blood meal on the responsiveness of olfactory receptor neurons in antennal sensilla trichodea of the yellow fever mosquito, Aedes aegypti. *Journal of insect physiology*, *56*(6), 659–65. doi:10.1016/j.jinsphys.2010.02.002

Sitaraman, D., Zars, M., Laferriere, H., Chen, Y.-C., Sable-Smith, A., Kitamoto, T., … Zars, T. (2008). Serotonin is necessary for place memory in Drosophila. *Proceedings of the National Academy of Sciences of the United States of America*, *105*(14), 5579–84. doi:10.1073/pnas.0710168105

Smith, D. P. (2007). Odor and pheromone detection in Drosophila melanogaster. *Pflügers Archiv : European journal of physiology*, *454*(5), 749–58. doi:10.1007/s00424-006-0190-2

Stocker, R. F. (1994). The organization of the chemosensory system in Drosophila melanogaster : a rewiew. *Cell and Tissue Research*, *275*(1), 3–26.

Su, C.-Y., Menuz, K., & Carlson, J. R. (2009). Olfactory perception: receptors, cells, and circuits. *Cell*, *139*(1), 45–59. doi:10.1016/j.cell.2009.09.015

Sugrue, L. P., Corrado, G. S., & Newsome, W. T. (2005). Choosing the greater of two goods: neural currencies for valuation and decision making. *Nature reviews. Neuroscience*, *6*(5), 363–75. doi:10.1038/nrn1666

Suh, G. S. B., Ben-Tabou de Leon, S., Tanimoto, H., Fiala, A., Benzer, S., Anderson, D. J., & Leon, S. B. De. (2007). Light activation of an innate olfactory avoidance response in Drosophila. *Current biology : CB*, *17*(10), 905–8. doi:10.1016/j.cub.2007.04.046

Suh, G. S. B., Wong, A. M., Hergarden, A. C., Wang, J. W., Simon, A. F., Benzer, S., … Anderson, D. J. (2004). A single population of olfactory sensory neurons mediates an innate avoidance behaviour in Drosophila. *Nature*, *431*(7010), 854–9. doi:10.1038/nature02980

Szczypka, M. S., Rainey, M. a, Kim, D. S., Alaynick, W. a, Marck, B. T., Matsumoto, a M., & Palmiter, R. D. (1999). Feeding behavior in dopamine-deficient mice. *Proceedings of the National Academy of Sciences of the United States of America*, *96*(21), 12138–43. Retrieved from http://www.pubmedcentral.nih.gov/articlerender.fcgi?artid=18425&tool=pmcentrez&rendertype=abstract

Takken, W., & Knols, B. G. (1999). Odor-mediated behavior of Afrotropical malaria mosquitoes. *Annual review of entomology*, *44*, 131–57. doi:10.1146/annurev.ento.44.1.131

Tanaka, N. K., Endo, K., & Ito, K. (2012). Organization of antennal lobe-associated neurons in adult Drosophila melanogaster brain. *The Journal of comparative neurology*, *520*(18), 4067–130. doi:10.1002/cne.23142

Tanaka, N. K., Tanimoto, H., & Ito, K. (2008). Neuronal assemblies of the Drosophila mushroom body. *The Journal of comparative neurology*, *508*(5), 711–55. doi:10.1002/cne.21692

Tang, S., & Guo, a. (2001). Choice behavior of Drosophila facing contradictory visual cues. *Science (New York, N.Y.)*, *294*(5546), 1543–7. doi:10.1126/science.1058237

Thum, A. S., Jenett, A., Ito, K., Heisenberg, M., & Tanimoto, H. (2007). Multiple memory traces for olfactory reward learning in Drosophila. *The Journal of neuroscience : the official journal of the Society for Neuroscience*, *27*(41), 11132–8. doi:10.1523/JNEUROSCI.2712-07.2007

Tully, T., & Quinn, W. G. (1985). Classical conditioning and retention in normal and mutant Drosophila melanogaster. *Journal of comparative physiology. A, Sensory, neural, and behavioral physiology*, *157*(2), 263–77. Retrieved from http://www.ncbi.nlm.nih.gov/pubmed/3939242

Turner, S. L., & Ray, A. (2009). Modification of CO2 avoidance behaviour in Drosophila by inhibitory odorants. *Nature*, *461*(7261), 277–81. doi:10.1038/nature08295

Van Swinderen, B., & Andretic, R. (2011). Dopamine in Drosophila: setting arousal thresholds in a miniature brain. *Proceedings. Biological sciences / The Royal Society*, *278*(1707), 906–13. doi:10.1098/rspb.2010.2564

Vosshall, L. B., & Stocker, R. F. (2007). Molecular architecture of smell and taste in Drosophila. *Annual review of neuroscience*, *30*, 505–33. doi:10.1146/annurev.neuro.30.051606.094306

Waddell, S. (2010). Dopamine reveals neural circuit mechanisms of fly memory. *Trends in neurosciences*, *33*(10), 457–64. doi:10.1016/j.tins.2010.07.001

Wang, Y., Pu, Y., & Shen, P. (2013). Neuropeptide-gated perception of appetitive olfactory inputs in Drosophila larvae. *Cell reports*, *3*(3), 820–30. doi:10.1016/j.celrep.2013.02.003

Wang, Y. Y., Chang, R. B., & Liman, E. R. (2010). TRPA1 is a component of the nociceptive response to CO2. *The Journal of neuroscience : the official journal of the Society for Neuroscience*, *30*(39), 12958–63. doi:10.1523/JNEUROSCI.2715-10.2010

Wehner, R., & Gering, W. (1995). *Zoologie* (23rd ed., pp. 429–430). Georg Thieme Verlag.

Xu, P., Atkinson, R., Jones, D. N. M., & Smith, D. P. (2005). Drosophila OBP LUSH is required for activity of pheromone-sensitive neurons. *Neuron*, *45*(2), 193–200. doi:10.1016/j.neuron.2004.12.031

Yaksi, E., & Wilson, R. I. (2010). Electrical coupling between olfactory glomeruli. *Neuron*, *67*(6), 1034–47. doi:10.1016/j.neuron.2010.08.041

Yao, C. A., & Carlson, J. R. (2010). Role of G-proteins in odor-sensing and CO2-sensing neurons in Drosophila. *The Journal of neuroscience : the official journal of the Society for Neuroscience*, *30*(13), 4562–72. doi:10.1523/JNEUROSCI.6357-09.2010

Zars, T., Fischer, M., Schulz, R., & Heisenberg, M. (2000). Localization of a Short-Term Memory in Drosophila. *Science*, *288*(5466), 672–675. doi:10.1126/science.288.5466.672

Zhang, K., Guo, J. Z., Peng, Y., Xi, W., & Guo, A. (2007). Dopamine-mushroom body circuit regulates saliency-based decision-making in Drosophila. *Science (New York, N.Y.)*, *316*(5833), 1901–4. doi:10.1126/science.1137357

Zhu, Y., Nern, A., Zipursky, S. L., & Frye, M. a. (2009). Peripheral visual circuits functionally segregate motion and phototaxis behaviors in the fly. *Current biology : CB*, *19*(7), 613–9. doi:10.1016/j.cub.2009.02.053

8 Copyright clearance

All previously published figures in this thesis were reproduced with the agreement of the respective publisher. For individual permissions, which were issued via the *RightsLink* © service, please see the references below.

Article Title	Publication	Type Of Use	Order Status	Order Number
The organization of the chemosensory system in Drosophila melanogaster: a rewiew	Cell and Tissue Research	Thesis/Dissertation	Completed	3296471226976
Essential Role of the Mushroom Body in Context-Dependent CO2Avoidance in *Drosophila*	Current Biology	reuse in a thesis/dissertation	Completed	3294951066368
Refined Spatial Manipulation of Neuronal Function by Combinatorial Restriction of Transgene Expression	Neuron	reuse in a thesis/dissertation	Completed	3294950744945
The *Drosophila* Standard Brain	Current Biology	reuse in a thesis/dissertation	Completed	3294940373100
Two chemosensory receptors together mediate carbon dioxide detection in Drosophila	Nature	reuse in a dissertation / thesis	Completed	3294940090805

Article Title	Publication	Type Of Use	Order Status	Order Number
Neuronal assemblies of the Drosophila mushroom body	Journal of Comparative Neurology	Dissertation/Thesis	Completed	3294931319222
Olfactory Perception: Receptors, Cells, and Circuits	Cell	reuse in a thesis/dissertation	Completed	3294930879149
Molecular, Anatomical, and Functional Organization of the *Drosophila* Olfactory System	Current Biology	reuse in a thesis/dissertation	Completed	3294930720042
Olfaction in *Drosophila*	Current Opinion in Neurobiology	reuse in a thesis/dissertation	Completed	3294930462637
Odor and pheromone detection in Drosophila melanogaster	Pflügers Archiv European Journal of Physiology	Thesis/Dissertation	Completed	3294430019451
Insect olfactory receptors are heteromeric ligand-gated ion channels	Nature	reuse in a dissertation / thesis	Completed	3294401484704
Neural mechanisms of context-dependent modification of CO2 avoidance behavior in fruit flies.	Fly	Thesis/Dissertation	Free license for reuse by authors	